REGULATION OF IS*492* TRANSPOSITION IN *PSEUDOALTEROMONAS ATLANTICA*

by

BRIAN PATRICK HIGGINS

(Under the Direction of Anna C. Karls)

ABSTRACT

A variety of specialized DNA recombination systems create genetic diversity and regulate gene expression in prokaryotes and eukaryotes. The goal of this research was to characterize the regulation of an unusual specialized recombination system, reversible insertion and excision of the insertion sequence IS*492*. Transposition of IS*492*, which is mediated by the transposase MooV, controls the production of peripheral extracellular polysaccharide (^{P}EPS) in the Gram-negative marine organism *Pseudoalteromonas atlantica*. ^{P}EPS production is necessary for the switch from a planktonic existence in ocean water columns to biofilm formation on solid surfaces and in sediment. This work demonstrates that the on/off phase variation of ^{p}EPS is controlled by insertion and precise excision of IS*492* from a single site within *epsG*, a glycosyl transferase gene that is essential for ^{p}EPS production. In a novel application of real time polymerase chain reaction (qPCR) technology, the frequency of IS*492* precise excision from *epsG* was measured and found to be as high as 10^{-2} per cell per generation, which is unprecedented for a IS element. This high frequency precise excision is dependent on the chromosomal context of IS*492* and on environmental factors. Analysis of the relevance of the chromosomal context for IS*492* indicates that transcription through the element from an external promoter increases the level of transpose-encoding transcripts. Thus, a regulator *epsG* transcription would control excision of IS*492;* the best candidate for this regulator, based ^{p}EPS

phase variation and IS*492* excision frequency assays under various growth conditions, is the primary building block of ^{p}EPS, galactose.

INDEX WORDS: transposition, mobile genetic elements, recombination, insertion sequence, *Pseudoalteromonas*, IS*492*, regulation, marine bacterium, quorum sensing

REGULATION OF IS*492* TRANSPOSITION IN *PSEUDOALTEROMONAS ATLANTICA*

by

BRIAN PATRICK HIGGINS

B.S., University of Maryland, College Park, 2000

A Dissertation Submitted to the Graduate Faculty of The University of Georgia in Partial Fulfillment of the Requirements for the Degree

DOCTOR OF PHILOSOPHY

ATHENS, GEORGIA

2006

REGULATION OF IS*492* TRANSPOSITION IN *PSEUDOALTEROMONAS ATLANTICA*

by

BRIAN PATRICK HIGGINS

Major Professor: Anna Karls

Committee: Janet Westpheling
Sidney Kushner
Larry Shimkets
Tim Hoover

Electronic Version Approved:

Maureen Grasso
Dean of the Graduate School
The University of Georgia
August 2006

DEDICATION

To Mom.

ACKNOWLEDGEMENTS

Thanks to Dr. Anna Karls, without whom this work would have been impossible in every conceivable way.

TABLE OF CONTENTS

Page

LIST OF TABLES

Page

LIST OF FIGURES

Page

CHAPTER 1

INTRODUCTION

A. Specialized Recombination Systems

DNA recombination events involve the exchange, integration, excision, deletion, and inversion of DNA segments. The recombination of DNA segments is an essential tool for generating genetic diversity. The effects of DNA recombination events on an organism vary significantly, as some may be phenotypically silent while others deleterious to an organism. Insight into DNA recombination events has been gained by genetically and biochemically characterizing a few model recombination systems such that now the interactions between DNA segments and recombination machinery in these systems are well understood.

DNA recombination can be divided into two categories: general recombination and specialized recombination. General recombination is the exchange of DNA between two genetic loci on the same DNA molecule or loci on separate DNA molecules. Although general recombination is not sequence-specific, it does require significant stretches of sequence homology between the recombining DNA segments. Much of the research in the field of general recombination stems from the discovery of the *recA* gene (2, 3).

Specialized recombination refers to recombination reactions that take place between regions of DNA with little or no sequence homology. There are two categories of specialized DNA recombination; site-specific recombination and transposition. Specialized DNA recombination systems are responsible for controlling a variety of cellular processes, from the variation of surface antigens on bacterial pathogens (6-8) to immunoglobulin diversity in humans (9).

The theory that recombination could occur at specific sites on the bacterial chromosome was put forth in 1962 (10) and was based on studies investigating the insertion and incorporation of bacteriophage lambda into the *E. coli* chromosome, first described by Esther Lederberg (11, 12). In the years since this research, many systems that facilitate the physical rearrangement of DNA at a specific site have been discovered. These site-specific recombination (SSR) reactions are catalyzed by members of the tyrosine and serine recombinase families and involve the rearrangement of DNA at a defined target site (13). With the exception of the DNA exchange, the reactions catalyzed by site-specific recombinases are biochemically similar to those catalyzed by DNA topoisomerases, which are responsible for regulating levels of DNA supercoiling (14). Unlike general recombination, SSR reactions commonly occur within a very short yet specific DNA segment called a recombination site. These sites are small (~30 bp) relative to those required for general recombination and often exhibit a dyad symmetry that is recognized by the multimers of the recombinase (15, 16).

Examples of tyrosine site-specific recombinases include the Xer protein, which is responsible for bacterial chromosome segregation after replication (17), λ integrase, which mediates the insertion and excision of bacteriophage lambda into/out of the *E. coli* chromosome (10), FimB/FimE, which regulate type I fimbriae production in *E. coli* (18), and FLP, which maintains plasmid copy number in the yeast *Saccharomyces cerevisiae* (19). Two well-studied examples of the serine site-specific recombinase family are the Hin (*H* segment *in*version) and Tn*3* resolvase. The Hin invertase controls flagellar gene expression in *Salmonella* by inverting a segment of DNA containing an active promoter upstream of the flagellar subunit-encoding gene *fljB* and transcriptional repressor gene (*fljA*) for the second flagellar gene *fljC* (6, 20). The resolvase of Tn*3* is responsible for the resolution of cointegrates, which involves recombination

between two *res* sites on directly repeated transposon copies within the same DNA molecule (21, 22).

The grouping of the tyrosine and serine recombinase families is based upon the catalytic tyrosine or serine residue, respectively, involved in the recombination reaction. In addition, there are other residues that are conserved among members of the family. Members of the tyrosine recombinase family share a conserved Arg-His-Arg-His-Lys/His motif (23) while those of the serine recombinase family share several conserved key active residues, Arg-Arg-Arg-Gln-Asp (24, 25). The SSR reactions catalyzed by both tyrosine and serine recombinases share similarities not only in the reactions catalyzed by their respective members, but also in the reaction mechanisms themselves. SSR reactions are conservative, thus there is no net gain or loss of any DNA involved in the recombination reaction. This conservative rearrangement of DNA molecule(s) does not require host replication or repair functions for completion of the recombination reaction, as the breaking and re-joining of DNA molecules is performed by the site-specific recombinase. The energy present in the phosphodiester bonds of the recombining DNA molecules is conserved in a covalent recombinase-DNA intermediate, thus circumventing the requirement for high energy cofactors such as ATP.

SSR reactions begin with the site-specific recombinase binding to the core recombination sites and forming a synaptic complex in which these sites are brought close together. Formation of this higher-ordered nucleoprotein complex often involves accessory proteins, such as IHF (*i*ntegration *h*ost *f*actor) and FIS (*f*actor for *i*nversion *s*timulation), which facilitate the interaction of the recombinase-bound sites in the synaptic orientation for deletion, inversion, or integration. After the synaptic complex is formed, the DNA phosphodiester backbone is broken by the nucleophilic attack of a hydroxyl group on the conserved catalytic tyrosine or serine residue,

resulting in a DNA-protein intermediate in which the DNA is covalently linked to the conserved catalytic residue (16, 26, 27). A second transesterification then occurs in which the hydroxyl of the exchanging strand breaks the protein-DNA linkage and restores the phosphodiester backbone of the exchanged strand.

In addition to the conserved catalytic residue, a distinguishing feature between the serine and tyrosine recombinases is the order of strand cleavage and exchange for each strand of the recombination sites. For the tyrosine recombinases, only one pair of homologous DNA molecules are broken, exchanged, and rejoined at a time (**Fig. 1.1**). The result is a Holliday junction intermediate (16), which is then resolved by the breaking, exchange, and rejoining of the other pair of DNA molecules. The serine recombinases break, exchange, and rejoin all four DNA strands of the recombination sites concertedly (**Fig. 1.2**). As mentioned above, there is no net gain or loss of DNA at the recombination site through either mechanism.

Another form of specialized recombination is transposition, which is defined as the movement or copying of a mobile genetic element from a donor DNA site to a target DNA site with no requirement for DNA homology. The movement of these discrete DNA segments can occur in an intermolecular or intramolecular manner. Transposition events play an important role in genome composition (28), as evidenced by the fact that >40% of the human, mouse, and rice genomes are composed of transposon-derived DNA elements (1, 29-31). The movement of a transposable element (TE) can activate or inactivate gene expression, cause DNA inversions, deletions, or replicon fusions (32). Depending on where transposition occurs, the effect of this movement can range from phenotypically silent to cell death. The ability to translocate genes has made transposable elements effective agents of horizontal gene transfer. For example, TEs contribute greatly to the spread of antibiotic resistance among bacteria (16). TEs have also

evolved to play a critical role in genome structure and gene expression, which is seen in telomere maintenance (33, 34), V(*D*)J rearrangements (35), and nuclear intron splicing (36).

A transposition event is catalyzed by an enzyme called a transposase (Tnp). The movement of a transposable element usually requires three DNA sites: the two ends of the transposable element and the target DNA site. The term transposable element encompasses a large group of mobile genetic elements with a wide variety of capabilities that are usually self-encoded. In prokaryotes, simple transposable elements encoding only those genes required to mediate movement are called insertion sequences (IS). More complex transposons encode additional information, such as antibiotic resistance genes (Tn*10,* Tn*5*), regulatory genes (Tn*7*), or phage genes (bacteriophage Mu). The movement of a TE can be mediated by a single protein or several proteins, and many TEs encode their own accessory factors (37).

There are five protein families that have been shown to mediate transposition: DDE transposases, tyrosine (Y) transposases, serine (S) transposases, Y2 or rolling circle (RC) transposases, and target-primed transposases (TP) (32). Each Tnp enzyme must perform essentially the same task: excise the TE from a donor DNA site through the breaking of DNA phosphodiester bonds and insert it into a new nonhomologous target DNA site through rejoining.

The best characterized Tnp family includes the DDE-motif transposases. It was a member of this family that McClintock originally described in her pioneering work in the field of recombination while studying mutable loci in maize (38, 39). This protein family is defined by the presence of three invariant amino acid residues, Asp, Asp, and Glu. The role of these amino acids is to coordinate one or two divalent metal cations within the catalytic pocket (40). The catalytic pocket is the region where the two TE ends are brought together in a synaptic complex (41), often called a transpososome, after which these ends undergo two subsequent chemical

reactions catalyzed by the DDE Tnp. The first reaction is a hydrolysis reaction in which a Tnp-activated water molecule, acting as a nucleophile, attacks the ends of the element and generates a free 3'OH on each end of the TE (**Fig. 1.3A**) (42). From this step, there are several mechanisms that DDE transposases have evolved to excise the TE completely from the donor site and insert it into a new target DNA site (43).

One well characterized approach is that utilized by bacteriophage Mu, in which the free 3'OH ends of the TE are joined directly to the target DNA via a 1-step transesterification reaction (44). The attack of each strand of the double-stranded target DNA by Mu ends is staggered by 5 bp (45); this stagger is unique to each TE and is generally 2-9 bp. The result of this strand transfer reaction is the generation of free 3'OH ends in the flanking target DNA and a fusion of the target and donor DNA to form a Shapiro intermediate (46). Replication proceeds from the 3'OH ends through the Mu sequence and results in a cointegrate molecule, in which the donor and target molecules are joined at each of their ends by a copy of the TE. This replication also fills in the gaps created by the initial staggered cleavage, thus giving direct repeats, flanking the TE; this is a defining characteristic of DDE Tnp-mediated transposition. This mechanism of transposition is often referred to as replicative, as resolution of the cointegrate results in a copy of the TE being carried by the donor and target DNA molecules.

A subset of the DDE transposases create a hairpin structure, either at the end of the element or in the flanking DNA, to excise the element from a donor DNA molecule. Bacterial IS elements IS*10* and IS*50* coordinate the attack of their 5'ends by the free 3'OH (generated in the initial hydrolysis described above), resulting in a hairpin intermediate structure where the 3' end of one IS element strand is linked to the 5' end of the complementary strand (47, 48). In essence, this reaction is the same strand transfer reaction described above, except in this case the target

DNA site is the complementary strand of the IS element. The formation of a hairpin intermediate serves to free the TE from the donor DNA. Resolution of the hairpin is achieved through another Tnp-mediated hydrolysis reaction, which generates another set of free 3'OH ends on the TE. These ends then participate in strand transfer into a new target DNA site. The plant transposable elements *Ac/Ds* and *Tam3* excise from their donor DNA site by catalyzing the formation of a hairpin structure in the DNA flanking the donor site (49). The recombination-activating gene (RAG) 1, which is responsible for V(*D*)J immunoglobulin rearrangements, contains a DDE motif and utilizes a mechanism involving hairpin formation in flanking DNA to excise the signal sequences bridging coding joints in immunoglobulin genes (9, 50).

Tn*7* is a well-studied TE that has evolved a unique mechanism for excision from donor DNA. The TnsB protein of Tn*7* is a DDE Tnp and, after a synaptic complex is formed, nicks at the 3' end of the element to generate free 3'OH ends (51). Instead of utilizing strand transfer/replication or hairpin formation to excise its 5' end, Tn*7* utilizes an element-encoded type II restriction endonuclease, TnsA, to cleave the element at its 5' ends (51, 52). The excised transposon is now capable of insertion into a new target site.

Members of the IS*3* family of insertion sequences transpose from a donor DNA site to a target site utilizing a mechanism that requires host DNA replication functions. The first step in this mechanism is a Tnp-mediated nick (via hydrolysis) at just one 3' end of the element. The newly generated 3'OH then acts as a nucleophile and attacks just outside (2-3 bp) the 5'end of the same strand. Strand transfer (via transesterification) generates a figure-eight structure where only one strand of the element is still attached to the donor DNA (53). DNA replication then proceeds from the nick at the element-host junction, resulting in a circularized form of the

element (bridged by 2-3 bp flanking sequence), which can then be linearized (via nicking at each end of the element) and inserted into a new target site (54).

The Y and S families of transposases are both structurally and mechanistically similar to the Y and S recombinases that catalyze site-specific recombination reactions. Y and S transposases catalyze reactions that utilize a conserved active site nucleophile for initial strand breaking (tyrosine and serine, respectively) and involve a covalent DNA-protein intermediate. In the Y and S transposition reactions, TEs are transposed to nonhomologous DNA target sites, and it is this ability to transpose into nonhomologous target sites that separates the Y and S transposases from their site-specific recombination counterparts. Int of Tn*916* is a well-studied member of the Y-Tnp family (55, 56).

Utilizing the catalytic tyrosine residue, Int excises Tn*916* precisely via sequential cleavage and transfer steps at nonhomologous coupling sequences that flank the Tn*916* insertion. This reaction generates a circular intermediate with a heteroduplex region from the paired flanking sequences and a heteroduplex relegated donor site. DNA replication resolves the heteroduplex region in the excised molecules. The circular intermediate of Tn*916* inserts into a target site, again generating the coupling sequences instead of the target site duplication generated by the DDE transposases (**Fig. 1.3B**) (57). Many members of the Y-Tnp family encode genes that allow an excised transposon to be transferred from one bacterium to another before insertion into a new target site, and for this reason they are known as conjugative transposons. Members of the S-Tnp family catalyze reactions very similar to those of the Y-Tnps, with the major differences being 1) the utilization of a serine residue to generate strand cleavage and 2) a 4-strand cleavage event to excise the transposon (**Fig 1.3C**) (58).

Y2-Tnp family elements, such as IS*91*, share DNA and protein sequence similarities with RC-plasmids and phage (59, 60). The defining characteristic of the Y2-Tnp is the conservation of two tyrosine residues that are required for the catalysis of transposition (**Fig. 1.3D**) (60). Members of the Y2-Tnp family are also called RC-Tnps due to the similarity of transposition intermediates to those seen in RC replication, which is often used by bacterial plasmids and bacteriophage (61).

Members of the TP-Tnp family catalyze a recombination reaction known as retrotransposition. The movement of retrotransposable elements requires a Tnp and a full length RNA molecule generated from the TE. Tnps of the TP family generally encode a reverse transcriptase (RT) and an endonuclease. One well characterized member of the TP-Tnp family catalyzes the movement of the most abundant and active retrotransposon in the human genome, the long interspersed nuclear element (LINE-1) (62). The first step in a retrotransposition reaction is the generation of a TE-derived RNA molecule. In the case of the LINE-1 elements, this reaction is performed by the host RNA polymerase. The annealing and reverse transcribing of this RNA into a target site is shown in **Figure 1.3E**. In the case of the Group II introns, a group of mobile and autocatalytic introns, the TE RNA splices itself out of a pre-mRNA molecule (62, 63). This RNA molecule bound by the element-encoded endonuclease and RT reverse splices into the sense strand of the target site. The endonuclease cleaves the antisense strand of the target site, resulting in a free 3'OH, which is then used as a primer for reverse transcription of the TE RNA. The term **t**arget **p**rimed (TP) transposition is derived from this step in the reaction. The retrotransposition process is completed by a sequence of events in which the RNA-containing DNA strand is nicked and the RNA is replaced by DNA (64, 65). The newly inserted TE is flanked by a target site duplication due to the staggered nature of the 2nd strand

nick (**Fig. 1.3E**). Interestingly, repeated transposition of two retrotransposons in *Drosophila* creates a telomere structure required for maintenance of chromosome ends (66). While this is different from most studied eukaryotic telomere mechanisms, telomerases are in fact related to the RT of the TP-Tnp family (67).

B. Regulation of Specialized Recombination

Specialized recombination reactions have the ability to alter an organism's genetic context and gene expression. Therefore, the recombination levels in a cell are often kept at a low basal level to reduce the possibility of recombination-induced deleterious effects such as the deletion or disruption of essential genes. Due to the complexity and diversity of the specialized recombination systems, no consensus for defining a favorable environment for recombination exists. As a result, many diverse regulatory mechanisms have evolved to control specialized recombination reactions. In many SSR systems, activity at the recombination sites is maintained at a constitutive low basal level to pre-adapt a sub-population of cells for changes in the environment, affecting genes involved in receptor specificity (68) , pilin expression (8), flagellar antigen type (6). The regulatory mechanisms controlling the transposition of TEs also maintain low basal levels of activity. However, due to the ability of a TE to target nonhomologous sequences, the regulation of transposition has evolved in many cases to modulate activity (frequency) ***and/or*** target specificity in order to maintain the fitness of the host.

There are many conditions which put a bacterial cell under stress, such as nutrient starvation or changes in osmolarity, pH, or temperature. If the cell fails to address these stresses correctly, it may die. In the case of certain TE's, the response to host cell stress is an increase in transposition events, which may result in a mutation that allows for the survival of the host or for the movement of the element to a new host with a greater chance of survival. The integrative

and conjugative element (ICE) ICE*Bs1* of *Bacillus subtilis* exhibits an increase in transfer from a donor cell to a new target cell when the donor cell's SOS response is induced by a DNA damaging agent (69), thus escaping a host under stress. A similar strategy is utilized by the bacterial transposon Tn*4652*. Transcription from the promoter for Tn*4652* Tnp is controlled by the stationary phase sigma factor σ^S, resulting in increased transposition frequencies when the cells enter stationary phase (70). Both of these systems exemplify regulation mechanisms that increase transposition when the host's fitness is threatened.

Most TEs have evolved mechanisms to control the frequency of transposition to prevent deleterious genome rearrangements (71). A wide variety of strategies are utilized to maintain low level transposition, acting at different steps in the transposition process. In particular, the Tnp enzyme is often the target of these regulation mechanisms because it is the generally the only element-encoded protein required for the movement of a TE. From transcription to translation to protein stability, the levels of transposase gene (*tnp*) transcript and gene product are precisely controlled.

The initiation of *tnp* transcription in Tn*10* and Tn*5* is controlled by DAM (**D**NA **a**denine **m**ethylase) methylation sites that overlap the *tnp* promoter region (**Fig. 1.4B**). These promoters are inefficient when fully methylated, so transposase is only transcribed efficiently after the passage of a replication fork (72, 73). This strategy ensures the host chromosome region that encodes the mobile element is replicated before transposition occurs. This is important because cut and paste transposition can result in a double-stranded break in the donor site.

TEs such as IS*911*, IS*30*, and Tn*10* maintain low *tnp* transcript levels by utilizing weak internal promoters to drive transcription of the *tnp* gene (74-76). IS*911* forms a circular intermediate upon excision; the nonreplicating circular element is lost if it does not reinsert. Due

to weak transcription from the internal promoter, there is very little Tnp to carry out the reinsertion of the TE. IS*911* solves this problem by encoding an inwardly-directed -10 sequence at its left end and an outwardly-directed -35 sequence at its right end (**Fig 1.5**). Upon formation of the circular element, the left and right ends are brought together and form a strong promoter called P_{JUNC}, which drives the expression of *tnp* and increases the likelihood of a reinsertion event (77). Tnp binding to the circular intermediate disassembles P_{JUNC} and reduces *tnp* expression levels so that subsequent high-frequency transposition events are unlikely.

Without the proper regulation, the insertion of a TE downstream of a strong promoter could be deleterious or lethal due to increased levels of the transposase. Several mechanisms have been described for TEs that address this issue at the transcriptional and/or translational level. In the case of bacteriophage Mu, transcription through the ends of the element prevent stable binding of the Tnp, MuA, to its recognition site and element end, thus counteracting the increasing levels of transposase (78). Tn*5* and Tn*10* encode sequences near the ends of the elements that form secondary structure in externally-derived *tnp* transcript which sequesters the translation initiation signal of the Tnp (**Fig. 1.4C**) (79, 80). These initiation signals are only accessible when the *tnp* transcript is generated by the element's own promoter. In addition, the outwardly-directed promoter present at the 5' end of Tn*10* (pOUT) has stronger activity than the internal transposase promoter (pIN) (76, 79). The RNA transcript generated by pOUT, which begins ~ 40 bp downstream of pIN transcript, shares homology with the 5' end of the transposase transcript and is able to anneal to translation initiation signals, thus blocking ribosome binding (**Fig. 1.4D**) (76). A similar system of antisense RNA regulation has been proposed for IS*30* (81). In this system, the antisense RNA anneals tightly to the middle of the transposase RNA transcript and impedes the passage of a translating ribosome (81).

A very effective method of controlling transposase levels has been observed for members of the IS*1* and IS*3* families, which encode two ORFs, A and B, that are required for transposition. The downstream ORF (OrfB) is read in a -1 phase relative to the upstream ORF (OrfA); a functional transposase (OrfAB) is generated only when there is a -1 translational frameshift (**Fig. 1.5A**) (82). This frameshift occurs when a translating ribosome "slips" one base upstream and resumes translation in the -1 phase. The frequency of frameshifting, which in the case of of IS*911* is ~ 15%, determines the amount of transposase translated. The individual ORFs may or may not play a role on the transposition of the TE. For example, the OrfA protein of IS*911* modulates the activity and specificity of OrfAB Tnp, while no role has been discovered for the OrfB protein alone (83).

The bacterial IS element IS*903* utilizes several mechanisms to control transposition. The translational start codon for the IS*903* Tnp is GUG, which does not initiate translation as efficiently as the preferred *E. coli* start codon AUG (**Fig. 1.6**) (84). In addition to the presence of an atypical start codon, IS*903* controls the initation of translation by sequestering this start codon in a stem loop structure. In this structure, the start codon basepairs with mRNA 32 nucletides downstream (84). A class of mutations which allowed for increased Tnp expression all mapped to the region within this stem-loop and were found to 1) alter the start codon to AUG or 2) destabilize the stem loop structure (84). Once functional Tnp is produced, it is efficiently degraded by the Lon protease (85). This protein instability has two consequences for IS*903* transposition. First, transposition will occur at low levels because of the quick turnover of functional Tnp. Second, activity of the Tnp will only occur near the site of Tnp synthesis (*cis*-acting preference), as it is degraded before it can venture to another site on the chromosome and stimulate the transposition of another IS*903* copy. *Trans* activity of IS*903* Tnp is restored to *cis*

levels when 1) amino acid substitutions are introduced which stabilize the protein in the presence of Lon (84) or 2) the element is placed in a *lon* strain of *E. coli* (85).

Many TEs have evolved target preferences which prevent or reduce insertion into essential host genes. In the case of Tn*7*, the target site is a very specific nucleotide sequence in the *E. coli* genome (attTn*7*) that is located directly downstream of the *glmS* gene (86-88). While this target specificity at the nucleotide sequence level is rarely observed for TEs, a number of TEs have been found to target "hotspots" for insertion. These hotspots represent small regions of DNA where the insertions of a TE will cluster in a nonrandom fashion. The bacterial TE IS*256* targets 11 different sites in the *icaC* gene of *Staphylococcus epidermidis* (89, 90). IS*256* insertions are found elsewhere in the *ica* operon and the *S. epidermidis* genome, but this clustering of insertion sites is unique to the *icaC* gene. Efforts to discern a consensus sequence for TEs that target hotspots have not been very successful. While there are TEs that appear to target sequences homologous to their own ends, such as IS*911* (91) and IS*30* (92), and palindromic repeats in extragenic regions, such as IS*1397* (93), no criteria exist which clearly define a hotspot for each element in terms of nucleotide sequence. Instead, recent studies suggest that the transposition machinery recognizes and targets a particular DNA topology that is unique for each element. The target preference of the eukaryotic TEs *P* element and *Sleeping Beauty* were both initially characterized by consensus nucleotide sequence until it was discovered that the insertion sites all shared common topological characteristics which defined the bendability, *A*-philicity, GC content, and deformability of DNA at a preferred insertion site (94, 95). Regions of DNA which are easily accessed by the transposition machinery are more likely to act as targets for insertion of *P* element and *Sleeping Beauty* (94, 95).

A study of Mu insertion sites in the *E. coli* genome suggests that the efficiency of transcription in a given area and the local chromosome structure play a greater role in target site selection than nucleotide sequence (96). Regions of the chromosome that were poorly transcribed were transposition hotspots whereas highly transcribed regions served as poor target sites (96). The use of DNA topology, instead of strict nucleotide sequence, in choosing an insertion site may explain why most TEs have no consensus nucleotide target sequence; multiple variations of DNA sequence may give rise to comparable DNA structural motifs and variable sites within the chromosome can share structural motifs with the nucleoid.

The target choice of a TE in a host cell is a key regulatory aspect of transposition. Essential genes and regulatory regions must be avoided as targets if the host's fitness is to be maintained. Multiple insertions in a single region are also problematic due to the possibility of increased transposition resulting from higher transposase levels in a localized region. Bacteriophage Mu and Tn*7* employ target immunity mechanisms to carefully limit proximal insertion sites. In addition to the transposase enzyme Mu and Tn*7* encode proteins which aid in target selection, MuB and TnsD or E, respectively (**Fig. 1.7**). These targeting proteins bind target DNA and recruit the TE-bound transposase. Interactions with the transposase cause the targeting proteins to then dissociate from the target DNA (97-99). The presence of transposase bound to TE ends causes the continued dissociation of the targeting proteins in neighboring DNA at a range up to several kilobases (100, 101). As a result, neither Tn*7* nor bacteriophage Mu will target regions where a copy of the element already resides. While target immunity appears to decrease with distance from the TE ends (102), it is still an effective mechanism for controlling the target preference of an element and, once a threshold of elements has been achieved, inhibiting further insertion or replicative transposition of the element in the host genome

(crowding effect). Target immunity is taken to another level, the host cell level, by ICE*Bs1*. An intracellular signaling peptide produced by all ICE*Bs1* elements, PhrI, inhibits excision of the element when present at a critical concentration (69). This inhibition is observed when an ICE*Bs1*-bearing cell is surrounded by other cells containing the element, resulting in a build-up of inhibitor peptide (69). This strategy eliminates element crowding in a single host cell and encourages the spread of the TE in a population of cells that do not contain the TE.

Insertion of an IS element into the regulatory region or open reading frame of a gene controlling a phenotypic trait will disrupt expression of that gene, and therefore cause a change in the phenotypic appearance. If the IS element is able to excise precisely from this insertion site and restore the original nucleotide sequence, expression of the phenotypic trait is restored. This process of on-and-off switching is called phase variation and, as mentioned above, is commonly controlled by site-specific recombinases (6, 68, 103, 104); only a few insertion sequences have been shown to cause phase variation by reversible insertion. The reversible insertion of IS*256* into the *ica* operon in *S. epidermidis* mediates the bacterium's ability to produce an adhesin required for biofilm formation (89). The sialylation of lipopolysaccharide in *Neisseria meningitidis* is controlled by the reversible insertion of IS*1301* at the *sia* locus (7, 105). The frequency of IS element-mediated on-off phase variation (insertion) for IS*256* is ~ 1.9×10^{-5} per cell per generation (89), while for IS*1301* the on-off frequency of sialylation is $\leq 10^{-8}$ (7). The frequencies of off-to-on switching for the *ica* and *sia* loci are $\leq 10^{-8}$ and 10^{-4} per cell per generation, respectively. In these studies PCR analysis was used to show that the original gene sequence was restored. In neither system, however, was it shown that the excision of the IS element was Tnp-dependent. Generally the precise excision of a bacterial IS element is Tnp-independent and occurs at a low frequency (106, 107) .

While investigating the genetic regulation of polysaccharide synthesis in the marine bacterium *Pseudoalteromonas atlantica*, Bartlett and colleagues (108) determined the switching frequency for EPS^+ to EPS^- to be less than 10^{-5} per cell per generation. However, switching from EPS^- to EPS^+ occurred at a variable frequency ranging from 0.5 to 10^{-5} per cell per generation depending on colony density; lower colony density resulted in a higher frequency of reversion to the EPS^+ phenotype. Southern blot analysis of chromosomal DNA isolated from phase variant colonies showed that insertion and excision of a 1.2 kb element correlated with the phase variation of EPS production (**Fig. 1.8B**). A cosmid library, prepared from the chromosomal DNA of an EPS^+ variant, was used to complement for the EPS^- defect in crenated colonies (**Fig. 1.8A**). The complementing cosmid (pDB200) was then used to probe a cosmid library derived from a crenated colony, identifying the cosmid containing the *eps* sequence with the 1.2 kb insertion (pDB440) (108). DNA sequencing of subclones from pDB200 and pDB440 identified the insertion sequence IS*492* and its target sequence in the *eps* locus (109). The *eps* locus targeted by IS*492* for insertion has been shown to be essential for EPS production and other mutations in this region cause a non-reversible EPS^- phenotype (108).

C. A New Family of Recombinase Enzymes

The Tnp of IS*492* has been placed in a group of recombinase enzymes, the Piv/MooV family, that does not fit into any of the established classification systems described above. The recombinases of this family are grouped together because they share conserved amino acid motifs that have been shown to be essential for Piv/MooV recombinase activity, while at the same time members of this family lack similarity to the conserved amino acid motifs of the well characterized recombinases (103, 110). Piv/MooV members are able to mediate either DNA

inversion reactions or the transposition of bacterial IS elements. This ability to mediate both SSR and transposition reactions makes the Piv/MooV family a novel group of recombinases that could shed new light on our understanding of DNA recombination.

The Tnps of the Piv/MooV recombinase family facilitate the movement of bacterial IS elements belonging to the IS*110*/IS*492* family. IS elements of the IS*110*/IS*492* family have been identified in a variety of gram positive and gram negative bacteria, including species of *Neisseria* (111), *Coxiella* (112), *Enterobacter (113), Leptospira* (114), *Mycobacterium* (115-120), *Streptomyces* (121, 122), *Thermus* (123), *Yersinia* (124, 125), and *Pseudoalteromonas* (126). The IS elements of this family are unique among bacterial IS elements in that they have no or very small (< 7 bp) inverted repeats and many IS*110*/*492* elements do not generate target site duplications upon insertion. (103). These elements range from 1.1 to 1.6 kb in length and contain a single long orf encoding the Tnp. The Tnps of this family do not contain the catalytic DDE motif shared by most DNA transposases. Instead, Tnps of the IS*110*/IS*492* family share several completely conserved amino acid motifs with the novel site-specific invertase Piv (pilin inversion) from *Moraxella lacunata*. These unusual characteristics make IS*110*/IS*492* family members likely candidates to reveal new insights into DNA recombination.

The novel characteristics of IS*492* and ease of genetics in its native host *P. atlantica* and a naïve host, *E. coli*, make it an excellent candidate to shed new light on our understanding of transposition. The high frequency phase variation mediated by IS*492* is significantly higher than those reported in other IS-element mediated phase variation systems. High frequency precise excision of bacterial IS elements is a very rare occurrence, thus determining what factors, either at the molecular level or in response to environmental factors such as colony density, influence transposition will possibly reveal a novel regulatory system in transposition. The fact that IS*492*

is the only bacterial IS element whose precise excision has been shown to be Tnp-dependent (126) lends further credence to the argument that it is important to characterize the transposition of IS*492*. The insertion of IS*492* appears to target a particular region in the *eps* locus, although the Southern blot used in this analysis could only narrow down the point of insertion to +/- 50 bp (108). Coupled with its homology to a site-specific recombinase, this target specificity may be the result of a novel transposition mechanism.

This thesis presents the results of my analysis of IS*492* precise excision, site-specific insertion, and the environmental factors that influence these processes. In the conclusion I discuss what this work has revealed about the novel reaction of IS*492* transposition and how this work influences future directions for the study of the regulation of IS*110*IS*492* elements and the biochemistry of the insertion and excision reactions mediated by MooV.

REFERENCES

1. Lander, E. S., Linton, L. M., Birren, B., Nusbaum, C., Zody, M. C., Baldwin, J., Devon, K., Dewar, K., Doyle, M., FitzHugh, W., Funke, R., Gage, D., Harris, K., Heaford, A., Howland, J., Kann, L., Lehoczky, J., LeVine, R., McEwan, P., McKernan, K., Meldrim, J., Mesirov, J. P., Miranda, C., Morris, W., Naylor, J., Raymond, C., Rosetti, M., Santos, R., Sheridan, A., Sougnez, C., Stange-Thomann, N., Stojanovic, N., Subramanian, A., Wyman, D., Rogers, J., Sulston, J., Ainscough, R., Beck, S., Bentley, D., Burton, J., Clee, C., Carter, N., Coulson, A., Deadman, R., Deloukas, P., Dunham, A., Dunham, I., Durbin, R., French, L., Grafham, D., Gregory, S., Hubbard, T., Humphray, S., Hunt, A., Jones, M., Lloyd, C., McMurray, A., Matthews, L., Mercer, S., Milne, S., Mullikin, J. C., Mungall, A., Plumb, R., Ross, M., Shownkeen, R., Sims, S., Waterston, R. H., Wilson, R. K., Hillier, L. W., McPherson, J. D., Marra, M. A., Mardis, E. R., Fulton, L. A., Chinwalla, A. T., Pepin, K. H., Gish, W. R., Chissoe, S. L., Wendl, M. C., Delehaunty, K. D., Miner, T. L., Delehaunty, A., Kramer, J. B., Cook, L. L., Fulton, R. S., Johnson, D. L., Minx, P. J., Clifton, S. W., Hawkins, T., Branscomb, E., Predki, P., Richardson, P., Wenning, S., Slezak, T., Doggett, N., Cheng, J. F., Olsen, A., Lucas, S., Elkin, C., Uberbacher, E., Frazier, M., et al. (2001) *Nature* **409,** 860-921.
2. Clark, A. J. & Margulies, A. D. (1965) *Proc Natl Acad Sci U S A* **53,** 451-9.
3. Howard-Flanders, P. & Theriot, L. (1966) *Genetics* **53,** 1137-50.
4. Ogawa, T., Yu, X., Shinohara, A. & Egelman, E. H. (1993) *Science* **259,** 1896-9.
5. Shinohara, A., Ogawa, H., Matsuda, Y., Ushio, N., Ikeo, K. & Ogawa, T. (1993) *Nat Genet* **4,** 239-43.
6. Zieg, J., Silverman, M., Hilmen, M. & Simon, M. (1977) *Science* **196,** 170-2.

7. Hammerschmidt, S., Hilse, R., van Putten, J. P., Gerardy-Schahn, R., Unkmeir, A. & Frosch, M. (1996) *Embo J* **15,** 192-8.

8. Tobiason, D. M., Lenich, A. G. & Glasgow, A. C. (1999) *J Biol Chem* **274,** 9698-706.

9. Roth, D. B. & Craig, N. L. (1998) *Cell* **94,** 411-4.

10. Campbell, A. M. (1962) *Advances in Genetics Incorporating Molecular Genetic Medicine* **11,** 101-145.

11. Lederberg, E. M. & Lederberg, J. (1953) *Genetics* **38,** 51-64.

12. Lederberg, E. M. (1951) *Genetics* **36,** 560-560.

13. Sadowski, P. D. (1993) *Faseb Journal* **7,** 760-767.

14. Wang, J. C. (1996) *Annu Rev Biochem* **65,** 635-92.

15. Stark, W. M., Boocock, M. R. & Sherratt, D. J. (1992) *Trends Genet* **8,** 432-9.

16. Hallet, B. & Sherratt, D. J. (1997) *FEMS Microbiol Rev* **21,** 157-78.

17. Hayes, F. & Sherratt, D. J. (1997) *Journal of Molecular Biology* **266,** 525-537.

18. McClain, M. S., Blomfield, I. C. & Eisenstein, B. I. (1991) *Journal of Bacteriology* **173,** 5308-5314.

19. Futcher, A. B. (1986) *Journal of Theoretical Biology* **119,** 197-204.

20. Nanassy, O. Z. & Hughes, K. T. (1998) *Genetics* **149,** 1649-63.

21. Krasnow, M. A. & Cozzarelli, N. R. (1983) *Cell* **32,** 1313-24.

22. Stark, W. M., Boocock, M. R. & Sherratt, D. J. (1989) *Trends Genet* **5,** 304-9.

23. Chen, Y. & Rice, P. A. (2003) *Annu Rev Biophys Biomol Struct* **32,** 135-59.

24. Hughes, R. E., Hatfull, G. F., Rice, P., Steitz, T. A. & Grindley, N. D. (1990) *Cell* **63,** 1331-8.

25. Yang, W. & Steitz, T. A. (1995) *Cell* **82,** 193-207.

26. Pargellis, C. A., Nunesduby, S. E., Devargas, L. M. & Landy, A. (1988) *Journal of Biological Chemistry* **263,** 7678-7685.

27. Smith, M. C. M. & Thorpe, H. M. (2002) *Molecular Microbiology* **44,** 299-307.

28. Shapiro, J. A. (1993) *Curr Opin Genet Dev* **3,** 845-8.

29. Waterston, R. H., Lindblad-Toh, K., Birney, E., Rogers, J., Abril, J. F., Agarwal, P., Agarwala, R., Ainscough, R., Alexandersson, M., An, P., Antonarakis, S. E., Attwood, J., Baertsch, R., Bailey, J., Barlow, K., Beck, S., Berry, E., Birren, B., Bloom, T., Bork, P., Botcherby, M., Bray, N., Brent, M. R., Brown, D. G., Brown, S. D., Bult, C., Burton, J., Butler, J., Campbell, R. D., Carninci, P., Cawley, S., Chiaromonte, F., Chinwalla, A. T., Church, D. M., Clamp, M., Clee, C., Collins, F. S., Cook, L. L., Copley, R. R., Coulson, A., Couronne, O., Cuff, J., Curwen, V., Cutts, T., Daly, M., David, R., Davies, J., Delehaunty, K. D., Deri, J., Dermitzakis, E. T., Dewey, C., Dickens, N. J., Diekhans, M., Dodge, S., Dubchak, I., Dunn, D. M., Eddy, S. R., Elnitski, L., Emes, R. D., Eswara, P., Eyras, E., Felsenfeld, A., Fewell, G. A., Flicek, P., Foley, K., Frankel, W. N., Fulton, L. A., Fulton, R. S., Furey, T. S., Gage, D., Gibbs, R. A., Glusman, G., Gnerre, S., Goldman, N., Goodstadt, L., Grafham, D., Graves, T. A., Green, E. D., Gregory, S., Guigo, R., Guyer, M., Hardison, R. C., Haussler, D., Hayashizaki, Y., Hillier, L. W., Hinrichs, A., Hlavina, W., Holzer, T., Hsu, F., Hua, A., Hubbard, T., Hunt, A., Jackson, I., Jaffe, D. B., Johnson, L. S., Jones, M., Jones, T. A., Joy, A., Kamal, M., Karlsson, E. K., et al. (2002) *Nature* **420,** 520-62.

30. Yu, J., Hu, S., Wang, J., Wong, G. K., Li, S., Liu, B., Deng, Y., Dai, L., Zhou, Y., Zhang, X., Cao, M., Liu, J., Sun, J., Tang, J., Chen, Y., Huang, X., Lin, W., Ye, C., Tong, W., Cong, L., Geng, J., Han, Y., Li, L., Li, W., Hu, G., Huang, X., Li, W., Li, J., Liu, Z., Li,

L., Liu, J., Qi, Q., Liu, J., Li, L., Li, T., Wang, X., Lu, H., Wu, T., Zhu, M., Ni, P., Han, H., Dong, W., Ren, X., Feng, X., Cui, P., Li, X., Wang, H., Xu, X., Zhai, W., Xu, Z., Zhang, J., He, S., Zhang, J., Xu, J., Zhang, K., Zheng, X., Dong, J., Zeng, W., Tao, L., Ye, J., Tan, J., Ren, X., Chen, X., He, J., Liu, D., Tian, W., Tian, C., Xia, H., Bao, Q., Li, G., Gao, H., Cao, T., Wang, J., Zhao, W., Li, P., Chen, W., Wang, X., Zhang, Y., Hu, J., Wang, J., Liu, S., Yang, J., Zhang, G., Xiong, Y., Li, Z., Mao, L., Zhou, C., Zhu, Z., Chen, R., Hao, B., Zheng, W., Chen, S., Guo, W., Li, G., Liu, S., Tao, M., Wang, J., Zhu, L., Yuan, L. & Yang, H. (2002) *Science* **296,** 79-92.

31. Goff, S. A., Ricke, D., Lan, T. H., Presting, G., Wang, R., Dunn, M., Glazebrook, J., Sessions, A., Oeller, P., Varma, H., Hadley, D., Hutchison, D., Martin, C., Katagiri, F., Lange, B. M., Moughamer, T., Xia, Y., Budworth, P., Zhong, J., Miguel, T., Paszkowski, U., Zhang, S., Colbert, M., Sun, W. L., Chen, L., Cooper, B., Park, S., Wood, T. C., Mao, L., Quail, P., Wing, R., Dean, R., Yu, Y., Zharkikh, A., Shen, R., Sahasrabudhe, S., Thomas, A., Cannings, R., Gutin, A., Pruss, D., Reid, J., Tavtigian, S., Mitchell, J., Eldredge, G., Scholl, T., Miller, R. M., Bhatnagar, S., Adey, N., Rubano, T., Tusneem, N., Robinson, R., Feldhaus, J., Macalma, T., Oliphant, A. & Briggs, S. (2002) *Science* **296,** 92-100.

32. Curcio, M. J. & Derbyshire, K. M. (2003) *Nat Rev Mol Cell Biol* **4,** 865-77.

33. Eickbush, T. H. (1997) *Science* **277,** 911-2.

34. Nakamura, T. M. & Cech, T. R. (1998) *Cell* **92,** 587-90.

35. Agrawal, A., Eastman, Q. M. & Schatz, D. G. (1998) *Nature* **394,** 744-51.

36. Sharp, P. A. (1991) *Science* **254,** 663.

37. Craig, N. L. (1996) in *Escherichia coli and Salmonella typhimurium: Cellular and Molecular Biologu*, ed. Neidhardt et al, F. C. (American Society for Microbiology, Washington, D.C.), pp. 2339-2362.

38. Mc, C. B. (1950) *Proc Natl Acad Sci U S A* **36,** 344-55.

39. McClintock, B. (1948) *Mutable loci in maize* (Carnegie Institute Washingotn Year Book.

40. Davies, D. R., Goryshin, I. Y., Reznikoff, W. S. & Rayment, I. (2000) *Science* **289,** 77-85.

41. Mizuuchi, M., Baker, T. A. & Mizuuchi, K. (1992) *Cell* **70,** 303-11.

42. Vink, C., Yeheskiely, E., van der Marel, G. A., van Boom, J. H. & Plasterk, R. H. (1991) *Nucleic Acids Res* **19,** 6691-8.

43. Turlan, C. & Chandler, M. (2000) *Trends Microbiol* **8,** 268-74.

44. Craigie, R. & Mizuuchi, K. (1985) *Cell* **41,** 867-76.

45. Allet, B. (1979) *Cell* **16,** 123-9.

46. Shapiro, J. A. (1979) *Proc Natl Acad Sci U S A* **76,** 1933-7.

47. Bhasin, A., Goryshin, I. Y. & Reznikoff, W. S. (1999) *J Biol Chem* **274,** 37021-9.

48. Kennedy, A. K., Guhathakurta, A., Kleckner, N. & Haniford, D. B. (1998) *Cell* **95,** 125-34.

49. Kunze, R., Weil, C.F. (2002) in *Mobile DNA II*, ed. Craig, N. L., Craigie, R.J., Gellert, M., Lambowitz, A.M. (American Society for Microbiology, Washington, D.C.), pp. 565-610.

50. Gellert, M. (2002) in *Mobile DNA II*, ed. Craig, N. L., Craigie, R., Gellert, M., Lambowitz, A. (American Society for Microbiology, Washington, D.C.), pp. 705-729.

51. Biery, M. C., Stewart, F. J., Stellwagen, A. E., Raleigh, E. A. & Craig, N. L. (2000) *Nucleic Acids Res* **28,** 1067-77.

52. Biery, M. C., Lopata, M. & Craig, N. L. (2000) *J Mol Biol* **297,** 25-37.

53. Polard, P., Prere, M. F., Fayet, O. & Chandler, M. (1992) *Embo J* **11,** 5079-90.

54. Ton-Hoang, B., Polard, P. & Chandler, M. (1998) *Embo J* **17,** 1169-81.

55. Rudy, C., Taylor, K. L., Hinerfeld, D., Scott, J. R. & Churchward, G. (1997) *Nucleic Acids Research* **25,** 4061-4066.

56. Caparon, M. G. & Scott, J. R. (1989) *Cell* **59,** 1027-1034.

57. Churchward, G. (2002) in *Mobile DNA II*, eds. Craig, N. L., Craigie, R., Gellert, M. & Lambowitz, A. (American Society for Microbiology, Washington, D.C.), pp. 177-191.

58. Crellin, P. K. & Rood, J. I. (1997) *Journal of Bacteriology* **179,** 5148-5156.

59. Diazaroca, E., Delacruz, F., Zabala, J. C. & Ortiz, J. M. (1984) *Molecular & General Genetics* **193,** 493-499.

60. Garcillan-Barcia, M., Bernales, I., Mendiola,V., de la Cruz, F. (2002) in *Mobile DNA II*, eds. Craig, N. L., Craigie, R., Gellert, M. & Lambowitz, A. (American Society for Microbiology, Washington, D.C.), pp. 891-904.

61. Kahn, S. (2000) *Molecular Microbiology* **37,** 477-484.

62. Moran, J. V. & Gilbert, N. (2002) in *Mobile DNA II*, eds. Craig, N. L., Craigie, R., Gellert, M. & Lambowitz, A. (American Society for Microbiology, Washington, D.C.), pp. 836-869.

63. Cousineau, B., Lawrence, S., Smith, D. & Belfort, M. (2000) *Nature* **404,** 1018-21.

64. Symer, D. E., Connelly, C., Szak, S. T., Caputo, E. M., Cost, G. J., Parmigiani, G. & Boeke, J. D. (2002) *Cell* **110,** 327-38.

65. Martin, S. L. & Bushman, F. D. (2001) *Mol Cell Biol* **21,** 467-75.

66. Pardue, M., DeBaryshe, P. (2002) in *Mobile DNA II*, eds. Craig, N. L., Craigie, R., Gellert, M. & Lambowitz, A. (American Society for Microbiology, Washington, D.C.), pp. 870-887.

67. Nugent, C. I. & Lundblad, V. (1998) *Genes Dev* **12,** 1073-85.

68. Kahmann, R., Rudt, F., Koch, C. & Mertens, G. (1985) *Cell* **41,** 771-780.

69. Auchtung, J. M., Lee, C. A., Monson, R. E., Lehman, A. P. & Grossman, A. D. (2005) *Proc Natl Acad Sci U S A* **102,** 12554-9.

70. Ilves, H., Horak, R. & Kivisaar, M. (2001) *J Bacteriol* **183,** 5445-8.

71. Reznikoff, W. S. (2003) *Mol Microbiol* **47,** 1199-206.

72. Roberts, D., Hoopes, B. C., Mcclure, W. R. & Kleckner, N. (1985) *Cell* **43,** 117-130.

73. Yin, J. C., Krebs, M. P. & Reznikoff, W. S. (1988) *J Mol Biol* **199,** 35-45.

74. Dalrymple, B. & Arber, W. (1985) *Embo J* **4,** 2687-93.

75. Duval-Valentin, G., Normand, C., Khemici, V., Marty, B. & Chandler, M. (2001) *Embo J* **20,** 5802-11.

76. Simons, R. W. & Kleckner, N. (1983) *Cell* **34,** 683-91.

77. Ton-Hoang, B., Betermier, M., Polard, P. & Chandler, M. (1997) *Embo J* **16,** 3357-71.

78. Goosen, N. & van de Putte, P. (1986) *J Bacteriol* **167,** 503-7.

79. Davis, M. A., Simons, R. W. & Kleckner, N. (1985) *Cell* **43,** 379-87.

80. Krebs, M. P. & Reznikoff, W. S. (1986) *J Mol Biol* **192,** 781-91.

81. Arini, A., Keller, M. P. & Arber, W. (1997) *Biol Chem* **378,** 1421-31.

82. Chandler, M. & Fayet, O. (1993) *Mol Microbiol* **7,** 497-503.

83. Loot, C., Turlan, C., Rousseau, P., Ton-Hoang, B. & Chandler, M. (2002) *Embo J* **21,** 4172-82.

84. Derbyshire, K. M. & Grindley, N. D. F. (1996) *Molecular Microbiology* **21,** 1261-1272.

85. Derbyshire, K. M., Kramer, M. & Grindley, N. D. F. (1990) *Proceedings of the National Academy of Sciences of the United States of America* **87,** 4048-4052.

86. Gay, N. J., Tybulewicz, V. L. & Walker, J. E. (1986) *Biochem J* **234,** 111-7.

87. Lichtenstein, C. & Brenner, S. (1982) *Nature* **297,** 601-3.

88. DeBoy, R. T. & Craig, N. L. (2000) *J Bacteriol* **182,** 3310-3.

89. Ziebuhr, W., Krimmer, V., Rachid, S., Lossner, I., Gotz, F. & Hacker, J. (1999) *Mol Microbiol* **32,** 345-56.

90. Lyon, B. R., Gillespie, M. T. & Skurray, R. A. (1987) *J Gen Microbiol* **133,** 3031-8.

91. Polard, P., Seroude, L., Fayet, O., Prere, M. F. & Chandler, M. (1994) *J Bacteriol* **176,** 1192-6.

92. Olasz, F., Fischer, T., Szabo, M., Nagy, Z. & Kiss, J. (2003) *J Mol Biol* **334,** 967-78.

93. Clement, J. M., Wilde, C., Bachellier, S., Lambert, P. & Hofnung, M. (1999) *J Bacteriol* **181,** 6929-36.

94. Vigdal, T. J., Kaufman, C. D., Izsvak, Z., Voytas, D. F. & Ivics, Z. (2002) *J Mol Biol* **323,** 441-52.

95. Liao, G. C., Rehm, E. J. & Rubin, G. M. (2000) *Proc Natl Acad Sci U S A* **97,** 3347-51.

96. Manna, D., Breier, A. M. & Higgins, N. P. (2004) *Proc Natl Acad Sci U S A* **101,** 9780-5.

97. Greene, E. C. & Mizuuchi, K. (2002) *Mol Cell* **10,** 1367-78.

98. Greene, E. C. & Mizuuchi, K. (2002) *Mol Cell* **9,** 1079-89.

99. Stellwagen, A. E. & Craig, N. L. (1997) *Embo J* **16,** 6823-34.

100. Greene, E. C. & Mizuuchi, K. (2002) *Embo J* **21,** 1477-86.

101. Skelding, Z., Queen-Baker, J. & Craig, N. L. (2003) *Embo J* **22,** 5904-17.

102. Chaconas G., R. M. H. (2002) in *Mobile DNA II*, eds. Craig, N. L., Craigie, R. & Lambowitz, A. (American Society of Microbiology Press, Washington, D.C.), pp. 384-402.

103. Lenich, A. G. & Glasgow, A. C. (1994) *J Bacteriol* **176,** 4160-4.

104. Parsons, R. L., Prasad, P. V., Harshey, R. M. & Jayaram, M. (1988) *Molecular and Cellular Biology* **8,** 3303-3310.

105. Hilse, R., Hammerschmidt, S., Bautsch, W. & Frosch, M. (1996) *J Bacteriol* **178,** 2527-32.

106. Berg, D. E. (1989) in *Mobile DNA*, ed. Berg, D. E. a. H., M.M. (American Society for Microbiology Press, Washington, D.C.), pp. 185-210.

107. Kleckner, N. (1989) in *Mobile DNA*, eds. Berg, D. E. & Howe, M. M. (American Society for Microbiology Press, Washington, D.C.), pp. 227-268.

108. Bartlett, D. H., Wright, M. E. & Silverman, M. (1988) *Proceedings of the National Academy of Sciences of the United States of America* **85,** 3923-3927.

109. Bartlett, D. H. & Silverman, M. (1989) *J Bacteriol* **171,** 1763-6.

110. Buchner, J. M., Robertson, A. E., Poynter, D. J., Denniston, S. S. & Karls, A. C. (2005) *J Bacteriol* **187,** 3431-7.

111. Skaar, E. P., Lecuyer, B., Lenich, A. G., Lazio, M. P., Perkins-Balding, D., Seifert, H. S. & Karls, A. C. (2005) *J Bacteriol* **187,** 1276-86.

112. Hoover, T. A., Vodkin, M. H. & Williams, J. C. (1992) *J Bacteriol* **174,** 5540-8.

113. Thorsted, P. B., Macartney, D. P., Akhtar, P., Haines, A. S., Ali, N., Davidson, P., Stafford, T., Pocklington, M. J., Pansegrau, W., Wilkins, B. M., Lanka, E. & Thomas, C. M. (1998) *J Mol Biol* **282,** 969-90.

114. Zuerner, R. L. (1994) *Plasmid* **31,** 1-11.

115. Kunze, Z. M., Wall, S., Appelberg, R., Silva, M. T., Portaels, F. & McFadden, J. J. (1991) *Mol Microbiol* **5,** 2265-72.

116. Hernandez Perez, M., Fomukong, N. G., Hellyer, T., Brown, I. N. & Dale, J. W. (1994) *Mol Microbiol* **12,** 717-24.

117. Moss, M. T., Malik, Z. P., Tizard, M. L., Green, E. P., Sanderson, J. D. & Hermon-Taylor, J. (1992) *J Gen Microbiol* **138,** 139-45.

118. Green, E. P., Tizard, M. L., Moss, M. T., Thompson, J., Winterbourne, D. J., McFadden, J. J. & Hermon-Taylor, J. (1989) *Nucleic Acids Res* **17,** 9063-73.

119. Fang, Z., Doig, C., Morrison, N., Watt, B. & Forbes, K. J. (1999) *J Bacteriol* **181,** 1021-4.

120. Fang, Z., Doig, C., Kenna, D. T., Smittipat, N., Palittapongarnpim, P., Watt, B. & Forbes, K. J. (1999) *J Bacteriol* **181,** 1014-20.

121. Henderson, D. J., Lydiate, D. J. & Hopwood, D. A. (1989) *Mol Microbiol* **3,** 1307-18.

122. Bruton, C. J. & Chater, K. F. (1987) *Nucleic Acids Res* **15,** 7053-65.

123. Ashby, M. K. & Bergquist, P. L. (1990) *Plasmid* **24,** 1-11.

124. Rakin, A., Noelting, C., Schubert, S. & Heesemann, J. (1999) *Infect Immun* **67,** 5265-74.

125. Rakin, A. & Heesemann, J. (1995) *FEMS Microbiol Lett* **129,** 287-92.

126. Perkins-Balding, D., Duval-Valentin, G. & Glasgow, A. C. (1999) *J Bacteriol* **181,** 4937-48.

Figure 1.1. Site-specific recombination by the tyrosine recombinases. Following the formation of a synaptic complex, the sessile phosphodiester bonds of one strand within each paired recombination site (hatched line) is attacked (arrows) by the hydroxyl of the catalytic tyrosine of the activated recombinases (Y in red ovals) **(i)**. The cleaved DNA strands are exchanged within the homologous core of the recombination sites (black dots) **(ii)**. 5'OHs (open circles) of the exchanged strands attack the 3'-phosphotyrosyl linkages between the recombinases and the cleaved DNA strand, thus restoring the phosphodiester linkage and releasing inactive recombinase (Y in gray oval). This completes the first set of 2-step transesterification reactions and creates a Holliday junction **(iii)**. Isomerization of this Holliday junction activates the next pair of recombinases on opposing strands (solid lines) **(iv)**, leading to the second set of 2-steps transesterification reactions that result in the final recombination products **(v)**.

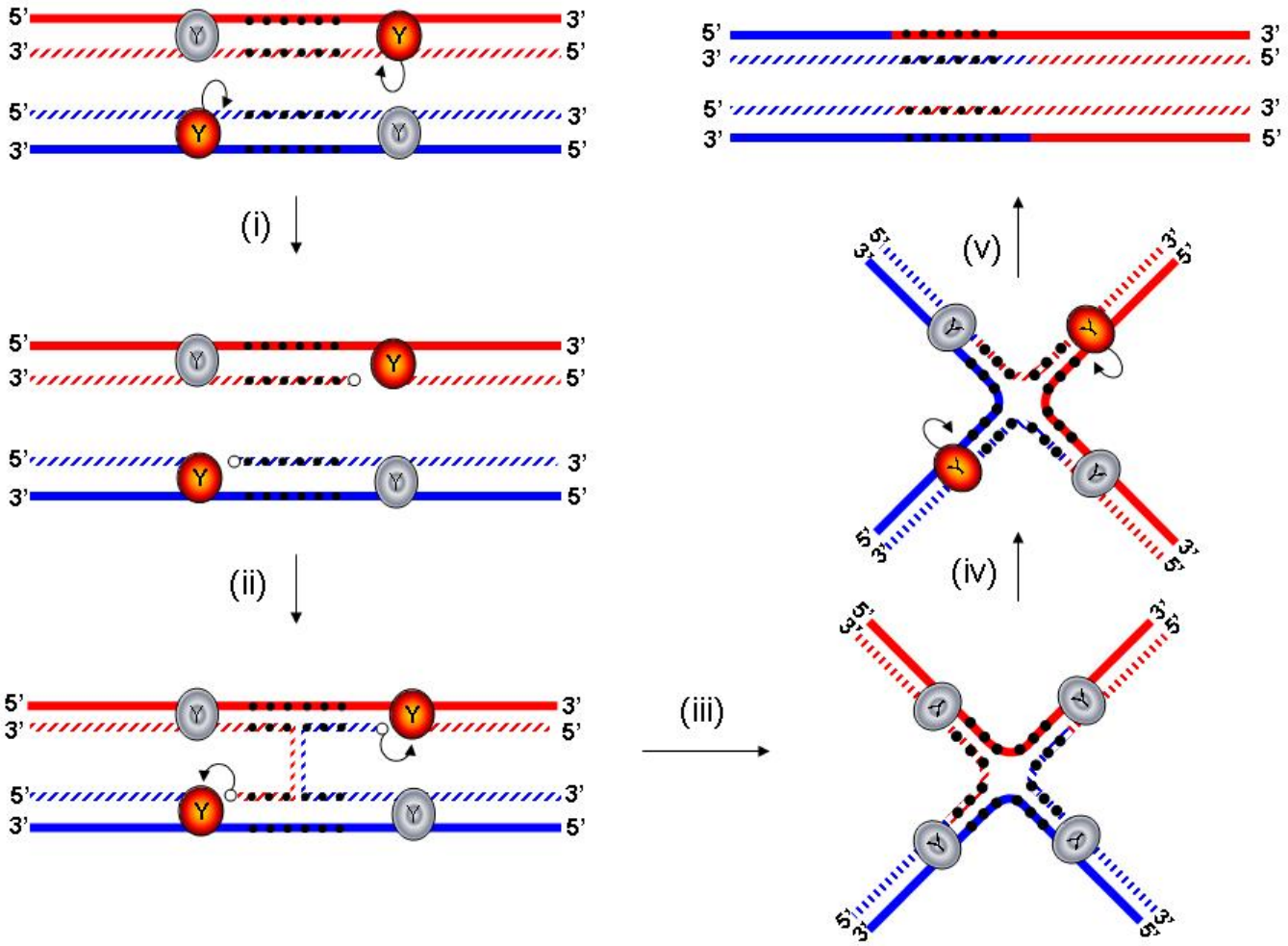
5'
3'
Y
(i)
(ii)
(iii)
(iv)
(V)

Figure 1.2. Site-specific recombination by the serine recombinases. Within the synaptic complex the serine recombinases concertedly cleave all the DNA strands at the core sequence of the recombination sites (arrows), covalently linking the catalytic serine to the 5' phosphate and exposing a 3'OH **(i)**. One pair of the recombinases that are linked to opposing cleaved strands rotate within the complex, thus exchanging strands **(ii)**. The 3'OHs (red or blue closed circles) of the cleaved DNA attack the phosphoseryl bonds, thus sealing the nicks in the exchanged DNA and releasing the recombinases **(iii)**.

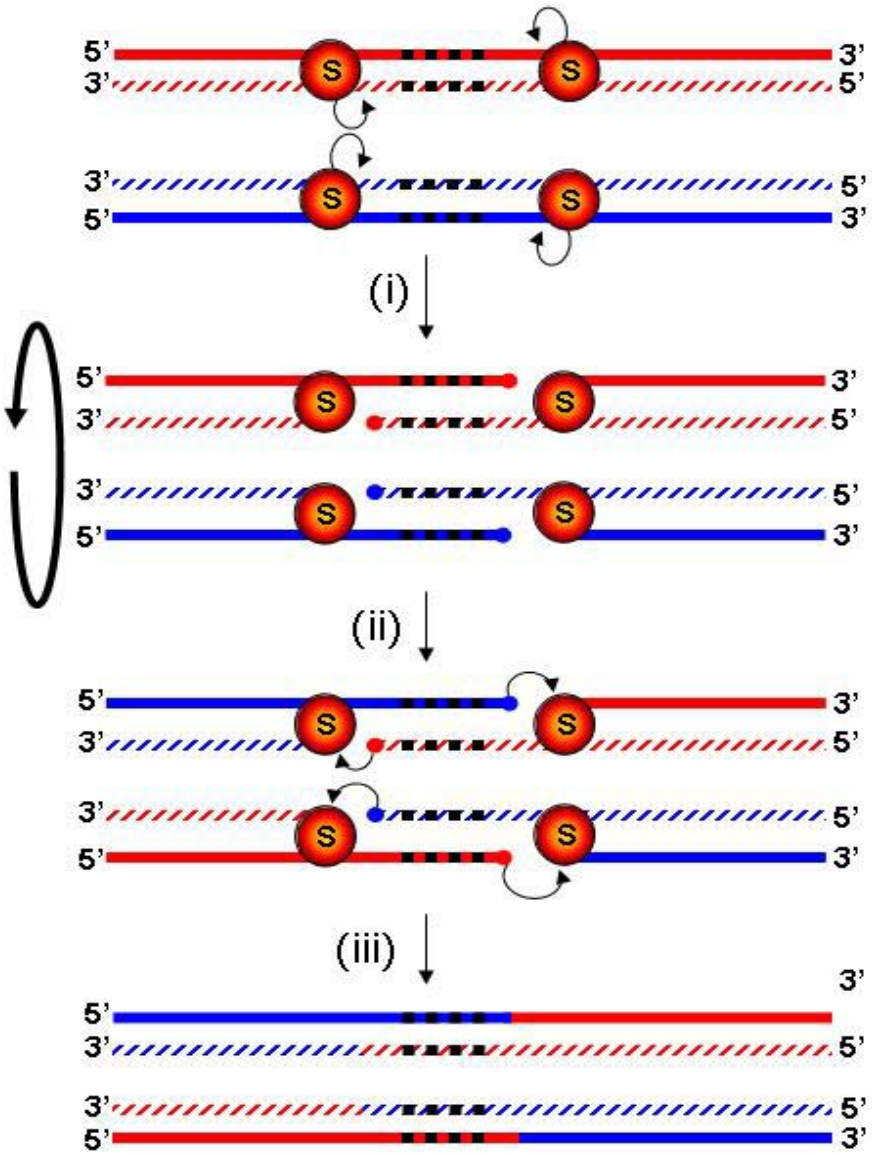
5'
3'
S
S
3'
5'
5'
3'
(i)
(ii)
(iii)

Figure 1.3. Pathways of transposition. **A**) Most DDE-Tnp excise the element (red lines) from donor DNA (green lines), generating a linear element and a double stranded break in the donor **(i)**. The DDE-Tnp directs the exposed 3' OHs (closed circles) at the ends of the element in strand transfer to the target site (blue line); nicking and transfer occurs at bases staggered by 2-9 bp on the complementary strands (hatched region) **(ii)**, thus leaving gaps in the target DNA **(iii)**. DNA repair fills the gaps so that the final insertion is flanked by target site duplications (hatched boxes) **(iv)**. **B**) Y-Tnp nick 5' of the flanking sequence at each end of the element on one DNA strand such that a short segment of flanking DNA is left attached to the 5' end of the element. Like with the site-specific Y recombinases the first step of the two-step trans-esterification reaction generates 3'-phosphotyrosine linkage (Y in circle) and 5'-OHs (hatched circles) **(i)**; the 5'-OHs attack the 3' phosphotyrosyl linkages at the opposing ends, resulting in circularization of the element strand and joining of the flanking DNA. This step is repeated on the bottom strand, resulting in joining of the flanking DNA and in a circular intermediate with the heterologous flanking DNA forming a coupling sequence that links the ends of the element **(ii)**. For insertion of the circular intermediate, the sequential steps of cleavage and joining is repeated after target capture **(iv).** The resulting insert has heterologous DNA flanking the 5'ends of the element; DNA replication of the target DNA resolves this intermediate to have the donor DNA on either the left or right side **(v)**. **C**) S-Tnp mediate concerted double-strand breaks at each transposon end, forming 5'-phosphoserine linkages (S in circle) and 3'-OHs **(i)**; nucleophilic attack by the 3'OHs of the linkages at the opposite end of each strand generates a circular intermediate and joins flanking DNA **(ii)**. Following target capture, the process is repeated **(iii)** to insert the transposon into a new target site. **D**) The Y2-Tnp cleaves one end of the transposon and forms a 5'-phosphotyrosine linkage (Y in circle) **(i)**; the resulting 3'-OH is used to prime replacement

strand synthesis (hatched red box) **(ii)**. Tnp-mediated cleavage of the displaced transposon strand at the 3' end releases the transposition intermediate which targets Tnp-cleaved target site **(iii)**. Nucleophilic attack by the exposed 3'-OHs of the phosphotyrosyl linkages inserts the single transposon strand into the target site **(iv).** DNA replication yields the final transposition product **(v)**. **E**) TP-Tnp, which is composed of a reverse transcriptase (RT) and endonuclease (EN), generates retrotransposon RNA (pink line), **(i)**. EN nicks target DNA and the resulting 3'OH is used to prime cDNA synthesis (light blue line) by RT using the RNA as template **(ii)**. EN then introduces a nick on the top strand of the target site and the newly synthesized cDNA anneals by microhomologies to the top strand and the exposed 3'OH primes second strand cDNA synthesis by RT **(iv)**. DNA ligase completes the insertion of the LINE element (light blue) **(v)**.

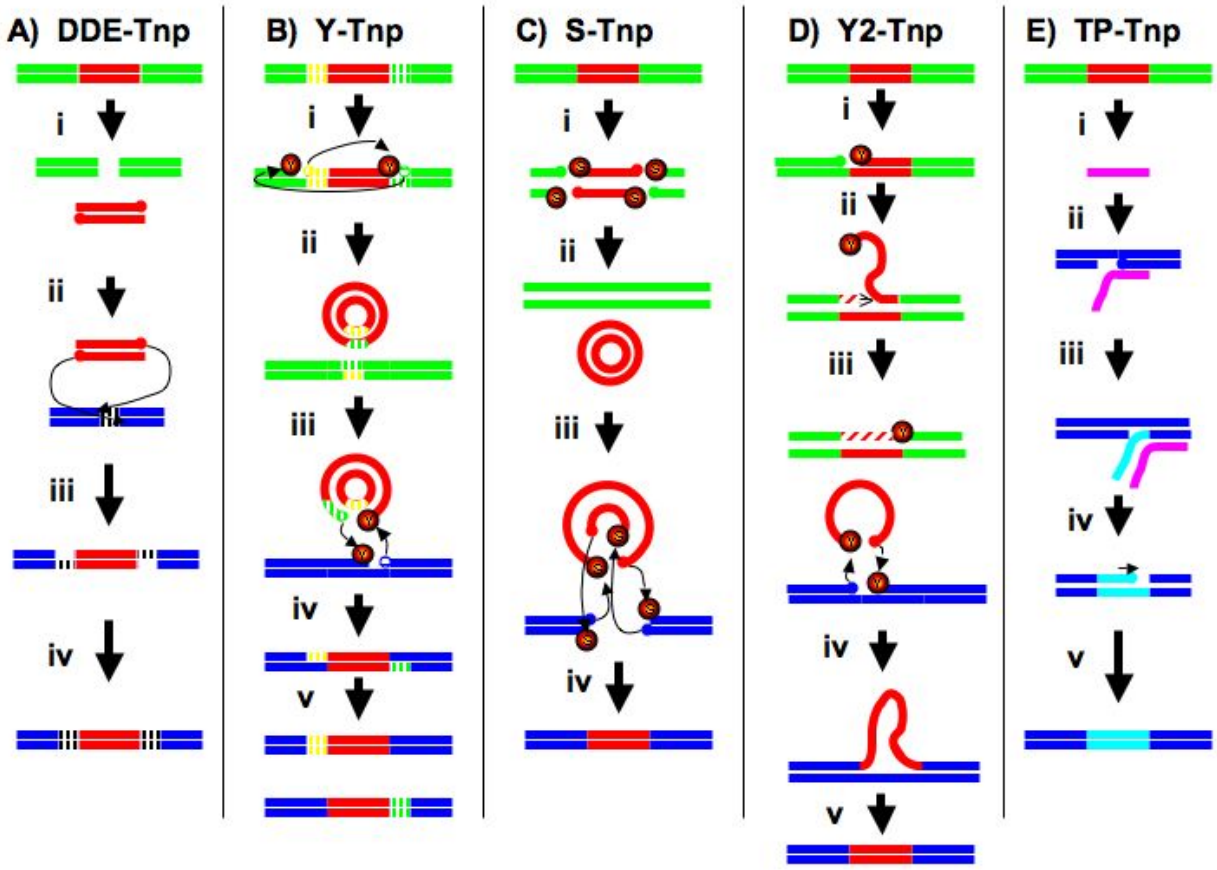
A) DDE-Tnp
i
ii
iii
iv
B) Y-Tnp
i
ii
iii
iv
v
C) S-Tnp
i
ii
iii
iv
D) Y2-Tnp
i
ii
iii
iv
v
E) TP-Tnp
i
ii
iii
iv
v

Figure 1.4. Regulation of Tn*10* transposition. A) *Tn*10 *structure*. Tn*10* transposon is a compound transposon consisting of two IS*10* elements (solid reds lines) and interveneing sequence encoding tetracycline resistance (broken red lines). IS10 right encodes the active transposase for Tn10; the pink arrow represents the *tnp* promoter and the light green arrow is a promoter within the flanking chromosomal DNA (green lines). B) *Role of methylation in tnp transcription initiation.* When the DAM methylation sequence within the *tnp* promoter is fully methylated (methyl groups represented by star), transcription initiation is inefficient. Following the passage of a replication fork, the *tnp* promoter is hemimethylated, resulting in a brief period of increased *tnp* transcript levels. C) *Sequestration of translation initiation signal*. When transcription of *tnp* is initiated from an external promoter, the Tn*10 tnp* mRNA (light green/pink line) forms secondary structures that result in sequestration of the *tnp* translation initiation codon (AUG) in a stem-loop structure **(i)**. However, the AUG initiation codon is fully accessible to the ribosome on the *tnp* mRNA that is initiated from the internal *tnp* promoter **(ii)**. D) *RNA interference.* The *tnp* promoter and resulting transcript are shown in pink. Transcript from an outwardly-directed promoter (pOUT) is shown in grey. Transcripts from these two promoters are complementary over a 35 bp region and will therefore anneal to each other, effectively decreasing the amount *tnp* transcript accessible to ribosomes for translation.

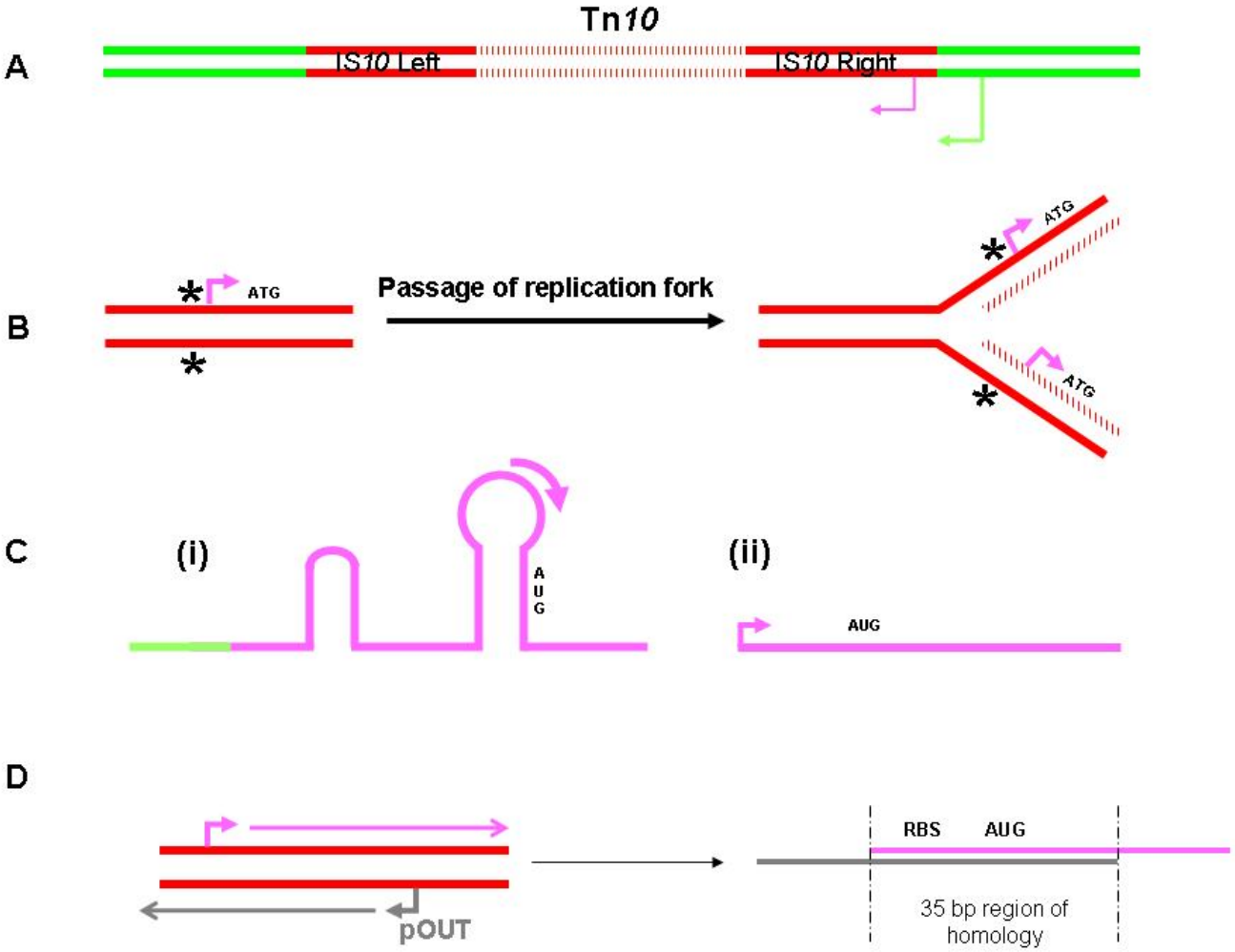
A
Tn10
IS10 Left
IS10 Right
B
ATG
Passage of replication fork
ATG
ATG
C
(i)
A
U
G
(ii)
AUG
D
pOUT
RBS
AUG
35 bp region of
homology

Figure 1.5. Regulation of IS*911* transposition. A) *Programmed translational frame shifting of IS*911. IS*911* encodes two open reading frames, *orfA* and *orfB*. *orfA* is read in the 0 phase, while *orfB* is read in the -1 phase. To generate a functional Tnp, a -1 frame shift occurs, resulting in production of the OrfAB Tnp (blue/brown circle). This frame shift occurs in ~ 15% of *orfA* translations. The terminal inverted repeats (TIR) at left and right ends are shown as gray and white arrowheads, respectively, and the internal IS*911* promoter is represented by pink arrow. B) *Formation of a strong promoter*. Following excision, IS*911* (red lines) forms a circular intermediate in which the left and right ends are bridged by 2-3 bp of flanking DNA (green line with black boxes). Focusing on the junction region shows that a -35 sequence is present in the right TIR and a -10 sequence is present in the left TIR; when spaced correctly in the circular form, these sequences form a very strong hybrid promoter (P_{JUNC}) upstream of the element's resident promoter. P_{JUNC} drives higher levels of transcription for *tnp* than that of the resident promoter.

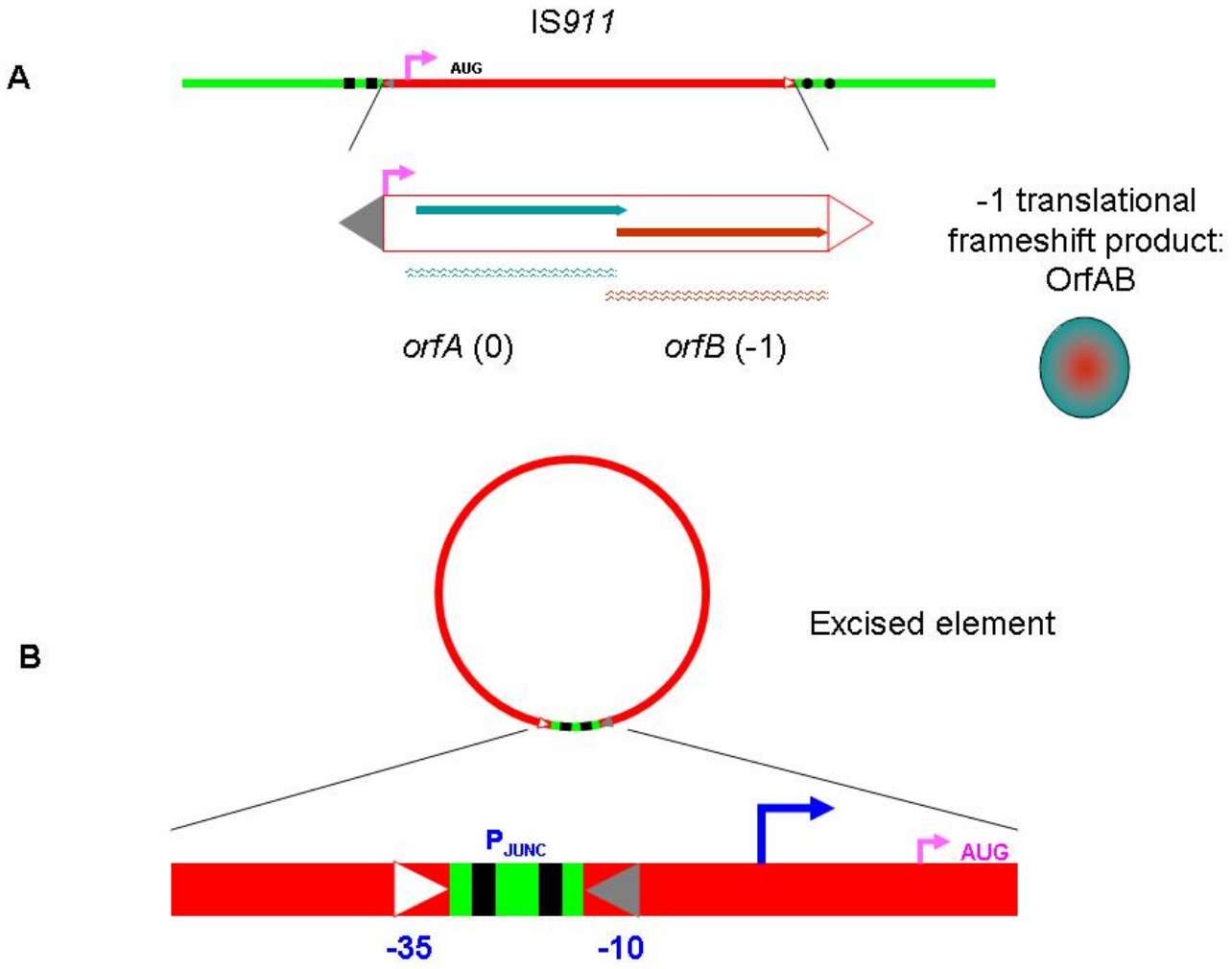
IS911
A
AUG
-1 translational
frameshift product:
OrfAB
orfA (0)
orfB (-1)
B
Excised element
P JUNC
AUG
-35
-10

Figure 1.6. Regulation of IS*903* transposition. IS*903* is a composite transposon; the red lines represent the IS element with the hatched area indicating the *tnp* coding sequence and the pink arrow showing the location of the *tnp* promoter. Regulation of IS*903* transposition is accomplished in part by the utilization of an atypical start codon, GUG, for translation initiation from the *tnp* transcript (pink line). The low levels of Tnp (red oval) result in lower levels of transposition. Further regulation occurs post-translationally by Lon recognition and degradation of Tnp. The low level of active Tnp available from the site of synthesis due to poor translation and degradation results in an apparent *cis*-preference of Tnp; i.e. the detectable activity of the Tnp drops precipitously with increasing distance from the site of its synthesis.

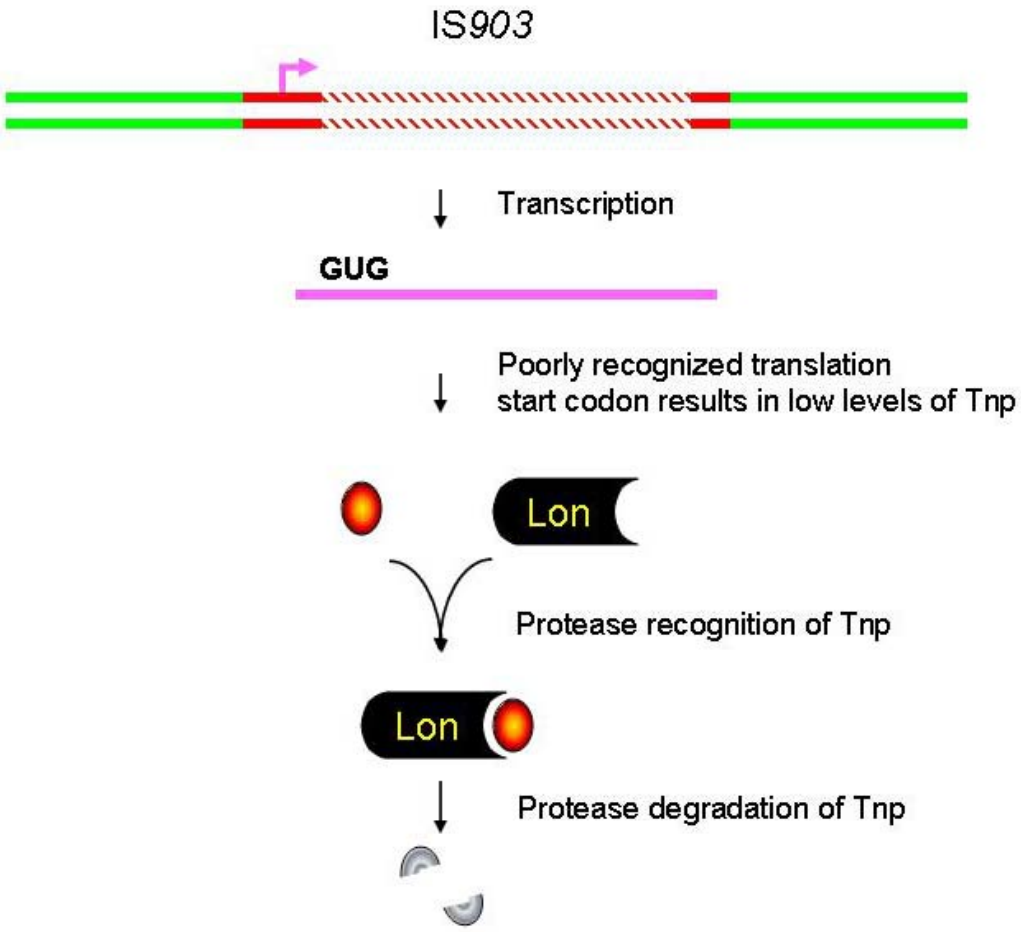
IS903
Transcription
GUG
Poorly recognized translation
start codon results in low levels of Tnp
Lon
Protease recognition of Tnp
Lon
Protease degradation of Tnp

Figure 1.7. Target immunity of bacteriophage Mu. The MuB protein is an ATP-dependent DNA binding protein; when MuB-ATP is bound to DNA, it stimulates insertion of MuA-bound bacteriophage Mu DNA (red line; green lines are flanking chromosomal DNA that is packaged with the Mu DNA in the phage particle). Dissociation of MuB from DNA occurs in the presence of MuA Tnp-element complexes which stimulate ATPase activity of MuB. This dissociation of MuB-DNA complexes in the presence of MuA Tnp-element complexes result in target immunity, as the presence of the element would prohibit annealing of MuB to nearby loci.

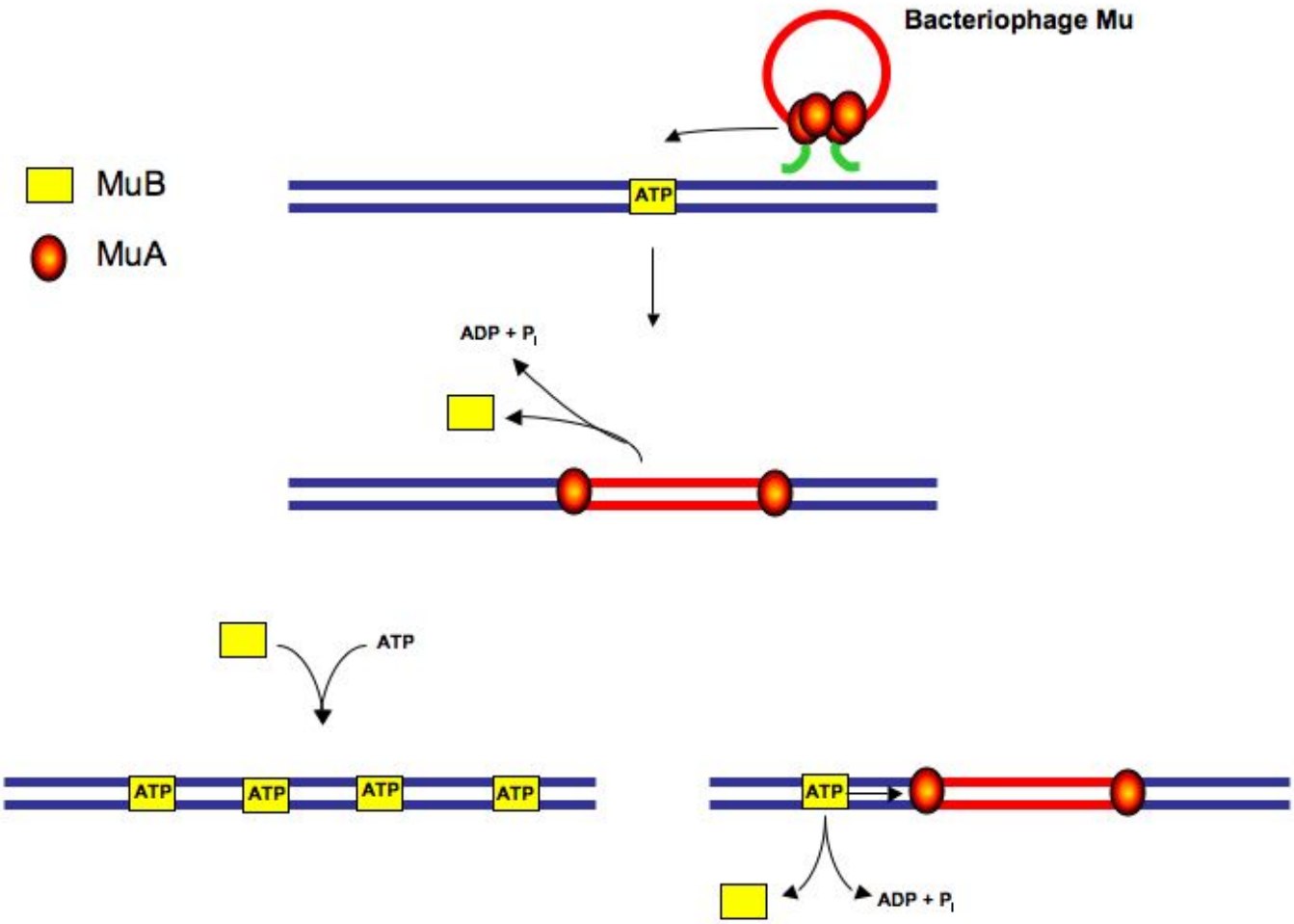
Bacteriophage Mu
MuB
MuA
ATP
ADP + P$_i$
ATP
ATP
ATP
ATP
ATP
ATP
ADP + P$_i$

Figure 1.8. IS*492*-mediated phase varation of EPS in *P. atlantica*. A) The phase variation of peripheral EPS (^{p}EPS) in *P. atlantica* results in two colony morphologies: ^{p}EPS^{-} (crenated) and ^{p}EPS^{+} (mucoid). B) The insertion of IS*492* (red line) into *epsG* (gold line) results in a target site duplication of 5 bp (blue boxes) and a crenated phenotype. Precise excision of IS*492* from *epsG* restores the *epsG* sequence; IS*492* is able to form a circular product following excision in which the left and right ends of the element are bridged by a single copy of the target site duplication. IS*492* insertion and excision are mediated by the MooV Tnp.

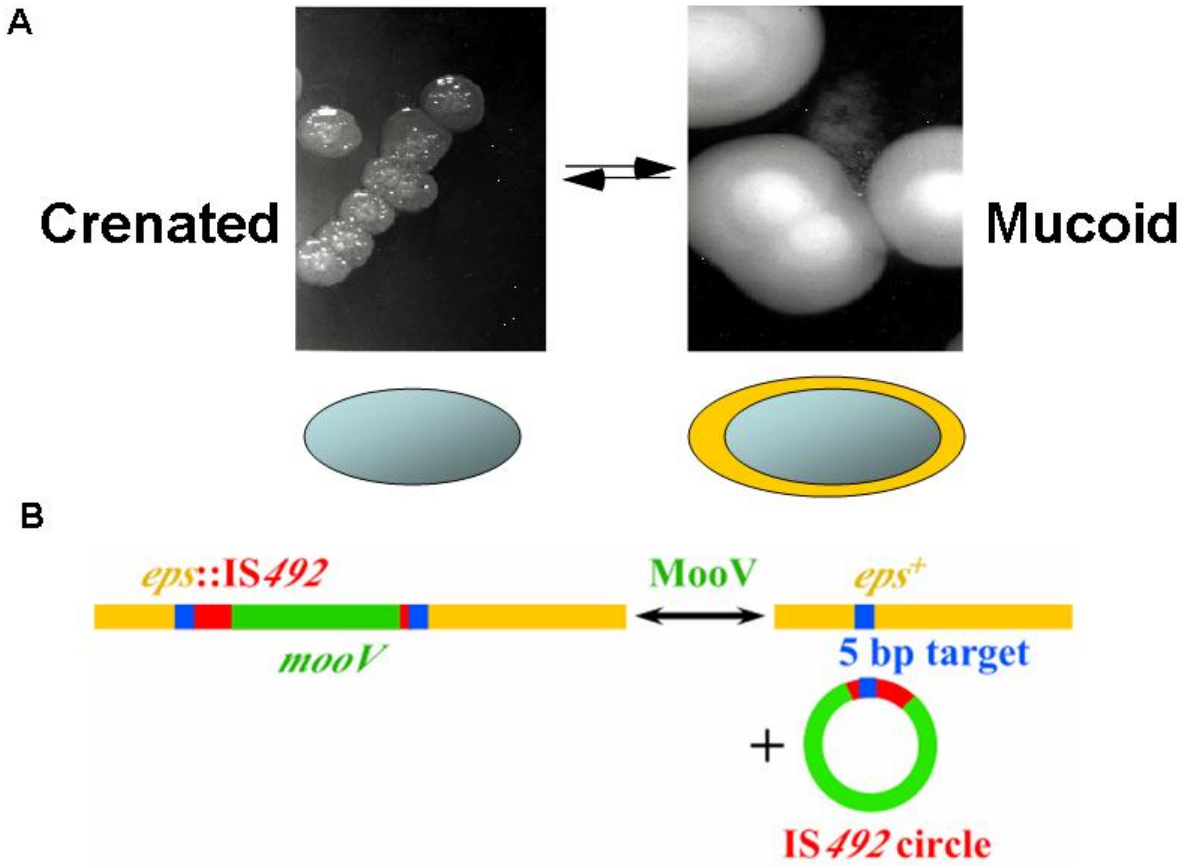
A
Crenated
Mucoid
B
eps::IS492
MooV
eps+
mooV
5 bp target
+
IS492 circle

CHAPTER 2

CHROMOSOMAL CONTEXT DIRECTS IS*492* HIGH FREQUENCY PRECISE EXCISION CONTROLLING EPS PHASE VARIATION IN *PSEUDOALTEROMONAS ATLANTICA*[1]

[1]Higgins, B.P., Robertson, A.E., and Karls, A.C. Submitted to the *Proceedings of the National Academy of Sciences*

ABSTRACT

DNA rearrangements, such as site-specific insertions, deletions and inversions, control gene expression in numerous prokaryotic and eukaryotic systems, ranging from phase variation of virulence factors in bacterial pathogens to generation of immunoglobulin gene diversity in human B-cells. Here, we report that precise excision of the insertion sequence, IS*492*, from one site on the *P. atlantica* chromosome directly correlates with the phase variation of peripheral extracellular polysaccharide (^{p}EPS) production from off (*epsG:*:IS*492*) to on (*epsG*$^{+}$). In a novel application of quantitative PCR technology, we determined that the frequency of this transposase-dependent precise excision is remarkably high, ranging from 10^{-3} to 10^{-2} per cell per generation. High frequency excision resulting in nonmutagenic repair of donor DNA is extremely unusual for a classical transposable element. Interestingly, high frequency precise excision of IS*492* does not occur at four additional insertion sites on the *P. atlantica* chromosome despite identity in the nucleotide sequence of the elements and 5-7 bp flanking DNA. Examination of the genome for features that distinguish the five insertion sites revealed that the *epsG*-associated IS*492* is likely to have high levels of host-initiated transcription through the element; quantitative RT-PCR assays for externally-derived transposase transcripts from each IS*492* copy confirmed this prediction. This positive effect of chromosomal context at *epsG*::IS*492* on excision frequency may reflect a local increase in transposase expression or a role for transcription per se in the excision reaction. Excision assays in *E. coli* support that transcription through IS*492* boosts transposase levels to a critical threshold concentration required for detectable excision.

INTRODUCTION

Transposons are discrete genetic elements that can move to multiple sites in a host genome and generate DNA rearrangements that contribute to genome diversity. These mobile elements utilize different mechanisms for movement, including rolling circle transposition and nonreplicative transposition mediated by tyrosine (Y)- and serine (S)-site-specific recombinases (1-4). However, the majority of the characterized transposons move by a common mechanism involving hydrolysis of phosphodiester bonds at element-host junctions and DNA strand transfer (one-step transesterification) catalyzed by a classical DDE-transposase (Asp, Asp, Glu catalytic motif). While there are various intermediates in the transposition reactions of the classical transposons, resulting in replication or simple insertion of the elements, the chemistries of the DNA cleavage and strand transfer reactions are conserved [reviewed in (5)]. Because the transposon is excised from donor DNA by hydrolysis reactions, precise excision in which the host DNA is restored to the original target sequence is rarely observed. In eukaryotes, nonhomologous end joining host functions can restore the donor sequence (6) and in prokaryotes it has been shown that short flanking direct repeats, facilitated by the terminal inverted repeats of Tn*5* and Tn*10,* can mediate DNA replication-dependent (RecA- and transposase-independent) precise excision events [reviewed in (7)]. However, in addition to resulting in precise excision of mobile elements, these processes are often mutagenic, generating deletions and small insertions.

Insertion sequence (IS)*492* controls peripheral extracellular polysaccharide (^{p}EPS) expression in the marine bacterium *Pseudoalteromonas atlantica* by insertion and precise excision at a single site within a predicted glucosyl-transferase gene (*epsG*) (**Fig. 2.1**) (this work; (8, 9). IS*492* is a member of the unusual IS*110* family of insertion elements that do not

have terminal inverted repeats and encode novel recombinases that mediate transposition by an undetermined mechanism (10). The transposase of IS*492*, MooV, is one of the defining members of the Piv-MooV DNA recombinase family, which includes site-specific invertases (Piv from *Moraxella lacunata* and *M. bovis*) as well as the transposases of the IS*110* family (11). MooV is required for precise excision of IS*492* (9). Although MooV and Piv appear to mediate conservative site-specific excision and inversion, respectively, these recombinases show no identity or similarity to the Y- or S-site-specific recombinases. Instead, the recombinases of the Piv-MooV family have a conserved DEDD motif, which has been shown to be essential for Piv-mediated DNA inversion, and is predicted to have a tertiary structural motif that is common to the DDE transposases and the DEDD-motif Holliday junction resolvases (RuvC-related) (12, 13).

Many of the unusual features of IS*492* and its transposition products suggest a novel transposition mechanism, and here we focus on the precise excision of IS*492*. The frequency of phase variation of ^{p}EPS in *P. atlantica,* based on switching of colony morphology (8), suggests that IS*492* may excise precisely from *epsG* in one of every one hundred cells. Using quantitative PCR (qPCR), we directly assayed precise excision from a single site within *epsG* and determined that the frequency of precise excision approaches 2×10^{-2} per cell per generation, correlating well with the frequency of colony phase variation measured for the same cell populations. This level of precise excision from the chromosome is unprecedented for classical transposable elements (14, 15). Interestingly, this activity is unique to the *eps*-associated copy of IS*492* in that four identical IS*492* copies located at different sites on the *P. atlantica* chromosome do not exhibit high frequency precise excision.

We show that the frequency of IS*492* precise excision is dependent on the chromosomal context of the element in *P. atlantica* and positively correlates with the level of transcription that initiates upstream of the element and passes through the *mooV* gene. Excision assays in *E. coli* show that external transcription through *mooV* stimulates IS*492* excision, but external transcription from the opposing direction does not promote excision of the element. The positive effect of transcription through IS*492* and frequent repair of the donor sequence in excision are unexpected features for a classical insertion sequence and strongly support that IS*492* utilizes a novel mechanism for transposition.

MATERIALS AND METHODS

Bacterial strains, Media, and Growth Conditions. *P. atlantica* T6c (16), DB27 (*hsd1*, Rif^r) and DB27*recA* (DB50), gifts from D. Bartlett (8), were cultured at 25°C under aerobic conditions on Difco 2216 marine medium. *E. coli* DH5α (9) was grown at 37°C on Luria-Bertani (LB) medium (Fisher Biotech).

Plasmid Constructions. The plasmids utilized as control templates in PCR, qPCR and qRT-PCR assays, and as substrates in excision assays in *E. coli* were created by TOPO TA cloning of PCR products from Taq polymerase (Promega) or Pfu polymerase (Stratagene) reactions (primer sequences are listed in **Table 2.2** and plasmid names with corresponding primers and products are listed in **Table 2.3**). Restriction and modification enzymes used in plasmid constructions and characterizations were purchased from New England Biolabs (NEB). All plasmids were sequenced to confirm inserted PCR product (University of Michigan Biomedical Research Core Facilities).

Colony-morphology Assays for ^{p}EPS Phase Variation and qPCR for IS*492* Excision in *P. atlantica*. The following protocol was carried out with six independent *P. atlantica* DB27 *recA*

crenated colonies. One colony was resuspended in 40 µl marine broth, plated on marine agar at HCD and LCD, incubated seven days at 25^{o}C, and 1000 colonies from HCD plates and 100 colonies from LCD plates were each resuspended in 10 ml marine broth. Cells were washed and resuspended in one ml marine broth. Three separate 100 µl aliquots were removed for serial dilutions and platings for enumeration of crenated to mucoid switching within the cell population. Genomic DNA was isolated using standard protocols (17) from an aliquot of each sample that correlated to ~1.5x10^{9} cells. Each genomic sample was digested with NgoMIV (NEB), which does not have a recognition site within the *agr* or *eps* amplified sequences, before determining the DNA concentration (based on absorbance at 260/280 nm; Eppendorf BioPhotometer).

qPCR reactions were performed using 18 replicates from each genomic DNA sample. The forward and reverse primers for the *eps* target site and for *agr* are designated FWEPS/RVEPS and AGARL/AGARR, respectively; the probes for the restored *eps* site and for *agr* are EPSPRB3 (FAM-490 fluorophore on the 5'-end and Black Hole Quencher1 on the 3'end) and AGARPRB (HEX-530 fluorophore on the 5'-end and Black Hole Quencher2 on the 3'end), respectively (see **Fig. 2.2** and **Table 2.2**). Real-time PCR reactions (50 µl) contained: 100 ng digested chromosomal DNA, 1x Taq Polymerase PCR Buffer B (Fisher), 2 U Taq Polymerase, 400 nM each dNTP (Amersham), 6 mM $MgCl_2$, 300 nM of AGARL and AGARR, 500 nM of FWEPS and RVEPS, 5 nM of AGARPRB, and 200 nM of EPSPRB3. To generate a standard curve for quantification of template in the reactions, pBHG126, which encodes both the 107 bp *eps* and 100 bp *agr* sequences to be amplified, was prepared (Eppendorf FastPlasmid MiniPrep Kit), quantitated, and used in a dilution series corresponding to 100 pg to one fg target DNA (4 replicates of each dilution was used for the standard curve in each experiment). Cycling

conditions for standards and experimental reactions were: 50°C for 2 min, 95°C for 3 min, followed by 30 cycles of 95°C for 30 sec and 57°C for 2 min. Standard plots of log starting quantity versus threshold cycles (C_T) were generated with the BioRad iCycler iQ software v3.0 using the data from the pBHG126 dilution series for the amplification of *agr* and *eps*; the starting quantities (SQ) of chromosomes with a restored *eps* site and total chromosomal copies (*agr*) in each genomic sample (HCD1-6 and LCD1-6) were calculated.

P_{PV} was calculated using the fraction of cells switching from crenated to mucoid (X_{PV}): $P_{PV}= 1-(1 - X_{PV})^{1/n}$, where n is the number of generations in the sample population (18). In the determination of P_{EX}, X_{EX} was determined by dividing the total amount of restored *eps* locus (in fg) present in each sample by the total amount of *agr* locus (in fg) present in the same sample. When calculating the number of generations (n), the inoculum was 1000 cells for HCD samples and 100 cells for LCD samples (each colony in the pooled samples started from a single cell). Statistical analyses of the data are described in Supporting Methods and Materials.

Statistical Analyses of P_{PV} and P_{EX} Data. The data from each of the six independent runs of the experiment was considered one block; so the P_{PV} and P_{EX} values from HCD and LCD for each block are the averages from three P_{PV} and 18 P_{EX} values. Kruskall-Wallis one-way analysis of variance was used to separately determine the effect of colony density on P_{PV} and P_{EX}. This test assigns ranks to data in each treatment population (HCD and LCD) and tests for differences between populations. The results showed that density had a significant effect on both P_{PV} and P_{EX}. The relationship between P_{PV} (independent variable x_1) and P_{EX} (dependent variable y) was determined using a simple linear regression analysis: $y=\alpha + ß_1x_1 + \varepsilon$ (where α is the y-intercept, $ß_1$ is the slope, and ε is the random error term). Three models were developed using HCD data

only (r^2 of 0.57; p=0.0809), LCD data only (r^2 of 0.8432; p=0.0097), or all the data combined (r^2 of 0.945 was observed; p<0.0001 [**Fig. 2.3**]). Multiple linear regression analysis was used to investigate whether the correlation between P_{PV} and P_{EX} is independent of colony density. As a qualitative variable (x_2), colony density was assigned the value 0 or 1 for HCD or LCD, respectively, in the model: $y=\alpha + ß_1x_1 + ß_2x_2 + \varepsilon$ (x_1 is P_{PV}); the model was not strengthened (r^2 = 0.943, p<0.0001) compared to the simple linear regression model (r^2 = 0.945, p<0.0001). The same model was obtained regardless of which colony density was set to 0 for x_2. Therefore, P_{PV} alone is the best predictor of P_{EX} regardless of density. All statistical analyses were conducted with SAS software (SAS Institute, Inc.; Cary, NC).

PCR Assays for IS*492* Precise Excision from Different Sites in *P. atlantica*. *P. atlantica* chromosomal DNA from the qPCR assays above (HCD 1, 2 and LCD 1, 2) was used as template for the direct PCR and 6 µl of the products from the direct PCR were used in the nested PCR. The 50 µl reactions contained 600 nM of the paired primers that specifically amplify the individual IS*492* insertion sites (**Table 2.2**), 1x Taq buffer, 3 mM $MgCl_s$, 200 nM dNTPs, and 1 U Taq polymerase. Cycling conditions for all reactions were: 95°C for 5 min, followed by 40 cycles of 95°C for 30 sec, 58°C for 30 sec, and 72°C for 15 sec. Products were electrophoresed on 3% agarose gels.

RNA Isolation and qRT-PCR. Total RNA was isolated from ~$5x10^9$ *P. atlantica* cells using an RNeasy Midi Kit (QIAGEN). Genomic DNA was eliminated by treating each RNA sample with RNase-free DNase I during the isolation procedure and in a subsequent step, which was followed by phenol/chloroform extraction and ethanol precipitation (17). Reverse transcription (RT) was

performed using the First Strand Synthesis Kit (Invitrogen). For each RNA sample, three separate RT reactions were performed: one with ISL270 (for all *mooV*-specific transcripts), another with TRXAR (for the reference gene *trxA*), and the third with both primers but no reverse transcriptase. Each RT reaction contained 2-5 μg of RNA.

qPCR reactions with the resulting cDNA (performed in triplicate for each target transcript from each RNA sample) contained: 1 μl RT-PCR (20 μl reaction), 1x SYBR Green (BioWhittaker Molecular Applications), 1 U *Taq* Polymerase, 3 mM $MgCl_2$, 0.5 μM forward primer for each insertion site (PDB1L, PDB6NL, PDB9L, PDB12L, or EPSL58) and 0.5 μM reverse primer (ISL270). Reactions for the reference gene had 0.5 μM of TRXAL and TRXAR. Cycling conditions were: 3 min at 95°C, 40 cycles: 30 s at 95°C, 30 s at 56°C, and 60 s at 72°C. Two negative controls included in each qPCR run had as template either water or the RT-PCR reaction that had no reverse transcriptase added. Amplification of the correct target was confirmed by melt curve analysis for each qPCR reaction using the BioRad iCycler. The qPCR products were also checked by agarose gel electrophoresis.

The quantity of the cDNA for each targeted transcript was determined as described for the qPCR for IS*492* excision. The standard plot for each target sequence, generated with the corresponding plasmid (pBHG117: *trxA*, pBHG119-123: copies *1-4* and *eps*-associated copy; Supporting Table 3), indicates the PCR efficiency for that reaction (based on the slope) and is used to accurately calculate the unknown target quantity in each reaction since it takes into account the different efficiencies of each qPCR reaction with different primer sets.

Circle junction PCR assays for IS*492* precise excision. Electrocompetent DH5α *E. coli* were transformed with pmooV5.7 or pVoom7.5 and plated on LBAmp, LBAmp with 0.05 mM IPTG,

and LBAmp with 0.02% glucose. Electrocompetent DH5α *E. coli* already containing either pmooV5.7 or pVoom7.5 were transformed with pAG900 and plated under same conditions with the addition of spectinomycin to each plate. Transformations were incubated at 37^{o}C overnight, after which time 3 transformants from each plate were pooled in 40µl TE buffer and boiled for 10 min. The cleared lysate from each sample was then used in a 50µl PCR reaction containing 1x Taq Polymerase Buffer B (Fisher), 2 U Taq Polymerase, 200nM each dNTP, 3mM $MgCl_2$, 600nM CJ250A, 600nM CJ250B. The cycling conditions were: 95^{0}C for 3min, followed by 30 cycles of 95^{0}C for 30 sec, 58^{0}C for 30 sec, 72^{0}C for 30 sec. Ten microliters of each reaction were electrophoresed on a 2% agarose gel and visualized with ethidium bromide.

RESULTS

Precise excision of IS*492* from *epsG* in *P. atlantica* occurs at an unusually high frequency.

To determine the frequency of IS*492* precise excision in *P. atlantica* we developed a real time PCR (qPCR) assay to directly measure the chromosomes in which IS*492* has precisely excised from *eps* relative to the total chromosome copies (**Fig. 2.2A**). In a multiplex qPCR, two dual-labeled fluorogenic probes [Taqman technology; (19)] were used to separately measure amplification of the β-agarase (*agr*) gene and the restored *eps* gene. Quantitation of *agr* reflected total chromosomal DNA as this sequence occurs only once in the *P. atlantica* genome and is unaffected by DNA rearrangements (20). Release of the different 5'-fluorophore (FAM-490 or HEX-530) from each probe resulting from 5'-3' exonuclease activity of Taq polymerase as it extended from the forward primer was monitored by increased fluorescence. The presence of IS*492* within the *eps* locus separates the forward primer and *eps* probe by 1.2 kb (**Fig. 2.2A**). Using a short extension time Taq polymerase does not reach the probe to release FAM-490 (**Fig. 2.2B**). Precise excision of IS*492* moves the primer to within 3 bp of the 5' end of the probe,

which allows Taq polymerase to reach the probe and release FAM-490. The *agr* probe is positioned 2 bp from the forward primer so that the HEX-530 fluorophore is released with every extension reaction. Representative data from one set reactions, including the standards which are dilutions of a known quantity of plasmid DNA encoding the *agr* and *eps* sequences, are shown in **Fig. 2.2C**. The ratio of measured fluorescence of FAM-490 and HEX-530 corresponds to the proportion of chromosomal DNA with a restored *eps* site relative to the total chromosomal DNA (*agr*) in a cell population initiated from crenated colonies and was used to calculate the frequency of precise excision of IS*492* from *epsG*.

It was previously reported that *P. atlantica* DB27 colony switching from crenated ($^{p}EPS^{-}$) to mucoid ($^{p}EPS^{+}$) was variable depending on growth conditions, including colony density on marine agar (8). Therefore we used cells from colonies plated at low colony density (LCD) and high colony density (HCD) on marine agar to obtain a range of frequencies for the correlation of IS*492* excision and colony phase variation. In six independent experiments, a DB27*recA* crenated colony was resuspended in marine broth and dilutions plated to obtain HCD and LCD. After 7 days incubation, the same number of cells were resuspended in marine broth from either HCD or LCD plates and used for colony phase variation assays and for preparation of chromosomal DNA to use in the real time qPCR assays for IS*492* precise excision. The data generated from these assays was used to calculate the frequencies of ^{p}EPS phase variation (P_{PV}) and IS*492* precise excision (P_{EX}) as described in the Materials and Methods. These results indicate that precise excision of IS*492* from *epsG* occurs at frequencies averaging 1.3+/-0.7 x 10^{-3} and 1.1+/-0.5 x 10^{-2} /cell/generation at HCD and LCD, respectively. A plot of the P_{PV} versus P_{EX} from the six independent experiments indicates a direct correlation between ^{p}EPS off-to-on phase variation and IS*492* precise excision (**Fig. 2.3**)**;** using both HCD and LCD data in a simple

linear regression model, a r^2 value of 0.945 was observed ($p<0.0001$). The true connection between these two processes is supported by multiple regression analyses that indicate P_{EX} and P_{PV} are strongly correlated with each other, and this relationship is independent of colony density (Methods and Materials).

IS*492* copies at locations other than the *eps* site on the *P. atlantica* chromosome do not exhibit high frequency precise excision. In light of the surprisingly high frequency precise excision of the *eps*-associated IS*492*, we asked whether other copies of IS*492* located at different sites on the *P. atlantica* chromosome exhibit precise excision. In earlier work we determined that there are at least five copies of IS*492* on the chromosomes of crenated *P. atlantica* cells; inverse PCR revealed the flanking sequence for five elements, which are designated here as copies *1, 2, 3, 4*, and *eps* (9). Using primers that correspond to the unique flanking sequences, each of the five elements were PCR-amplified from chromosomal DNA of crenated cells, cloned, and both strands sequenced. The sequence analysis revealed that all five copies of IS*492* are identical at the nucleotide level; thus all five elements have the potential to excise precisely.

In a PCR-based assay for precise excision of each IS*492* copy, we utilized the *P. atlantica* DB27*recA* chromosomal DNA from the qPCR assays as template since the frequency of excision for the *eps*-associated copy determined for these samples was a convenient reference point. Each reaction utilized a set of inwardly directed primers unique to one chromosomal site. A long extension time was used in this PCR assay so the flanking sequence and the IS*492* element are amplified, and upon excision of IS*492* the restored integration site is amplified (**Fig. 2.4**). The products observed from this direct PCR assay for precise excision suggested that only the *eps*-associated IS*492* excised precisely (**Fig. 2.4**). Nested PCR was utilized to increase the sensitivity

of the assay to detect a precise excision event for copies *1-4*. Amplification with nested PCR primers from the PCR products of the direct PCR consistently yielded precise excision products for copies *3* and *4* and occasionally produced a very small amount of product for copies *1* or *2* (**Fig. 2.4**). The products for copies *1* and *2* were refractory to cloning or sequencing to confirm that precise excision had occurred.

***mooV* transcript levels at *epsG::*IS*492* in *P. atlantica* are significantly higher than at other IS*492* insertion sites**. To relieve regulatory constraints on the movement of IS*492* that may be uniquely present on the *P. atlantica* chromosome, each copy of IS*492* along with 116 to 201 bp of chromosomal flanking sequence was amplified with Pfu polymerase and cloned into the pCR2.1 vector (Invitrogen) and transformed into *E. coli* DH5α. The transformants were then assayed for the repaired donor plasmid that results from precise excision of IS*492* using the same PCR protocol and primers that were utilized in *P. atlantica*. Like the *epsG*-associated IS*492*, which we previously demonstrated excises precisely to form a circular IS*492* product and a repaired donor plasmid in *E. coli* (9), the IS*492* copies *1-4* showed precise excision (**Fig. 2.5**).

These results suggest that it is the chromosomal environment in *P. atlantica* that controls the frequency of precise excision of IS*492*. Therefore, we examined the chromosomal context of each element utilizing the draft genome sequence of *P. atlantica* that we recently obtained through collaboration with the Joint Genome Institute (JGI) and the Department of Energy (GenBank AAKP00000000). We also applied CUPlot, a derivative of FramePlot (21), which considers codon usage of the organism, to identify protein-coding genes on contigs containing the IS*492* elements. The *eps*-associated copy of IS*492* is inserted in a putative glucosyl transferase gene such that *mooV* may be expressed from the *eps* transcript, which may include a

glycosyltransferase gene upstream (**Fig. 2.6A**). These genes are in a cluster of open reading frames (ORFs) with predicted functions that are consistent with EPS production, including a nucleotide sugar epimerase, a UDP-hexose transferase, acyltransferases, a ketal pyruvate transferase, and a polysaccharide export-related protein (22). The other IS*492* insertions are not inserted into identifiable genes and only copies *2* and *4* have ORFs immediately upstream that are in the same orientation as *mooV* (**Fig. 2.6A**). Based on these observations, we performed quantitative Reverse Transcription-PCR (qRT-PCR) to ask whether the level of host-initiated *mooV* transcript at each insertion site corresponds to the level of precise excision of IS*492* from each site in *P. atlantica*.

qRT-PCR reactions were set up with total RNA isolated from crenated colonies under the same conditions used for the real time PCR assay for IS*492* excision (R-HCD1-4 and R-LCD1-4). The RNA was reverse transcribed using a primer outwardly directed from *mooV* and a SYBR green-based quantitative PCR assay was used to measure the amount of cDNA corresponding to host-initiated *mooV* transcripts for each copy (primer locations for each copy are shown in **Fig. 2.6A**). Representative results from the qRT-PCR assay for the host-initiated *mooV* transcripts from the five different chromosomal locations and the *P. atlantica* thioredoxin A gene (*trxA*) transcript, which was the reference gene (23), are shown in **Fig. 2.6B**. The *eps*-associated *mooV* transcript is present at a level 100- to 100,000-fold higher than the level of *mooV* transcript from the IS*492* element at each of the other four sites. Although the absolute amount of *mooV* transcript from each site varied in independent repetitions of this assay at HCD and LCD, the same trend was seen (**Table 2.1**). These results suggest that transcription through IS*492* at the *eps* locus distinguishes it from the other IS*492* loci and may account for the significantly higher frequency of precise excision of the element at the *eps* locus.

Higher levels of IS*492* excision correspond to increased expression of *mooV* from external promoters in *E. coli.* The role of external transcription in the increased precise excision of IS*492* from *epsG* may be to increase the *in cis*-levels of MooV or to physically change the DNA structure, such as increase positive supercoiling in advance of the transcription bubble. To determine how transcription activates IS*492* excision, the element was inserted in both orientations in pCR2.1 with the minimal flanking sequence that is conserved at all the *P. atlantica* insertion sites, CTTGT on the left and CTTGTTA on the right (9). The vector has p*lac* upstream and p*T7* downstream of the multiple cloning site so that transcription can be initiated to impinge on IS*492* from either direction (**Fig. 2.7A**). To assess precise excision of IS*492* from the pmooV5.7 and pVoom7.5 constructs we used a PCR assay to detect the circle junction of the IS*492* circular product of precise excision (9) (**Fig. 2.7A**). Under conditions that stimulate transcription initiation from p*lac* in DH5α (with or without IPTG because the vector is multicopy and does not encode *lacI*^{q}) *mooV* is expressed from pmooV5.7 and the circle junction PCR product from the precisely excised IS*492* is evident (**Fig. 2.7B**). In HMS174(DE3), which has the T7 polymerase gene under control of p*lac* on a λ lysogen, transcription initiates from pT7 and expresses *mooV* from IS*492* in pVoom7.5, resulting in excision (**Fig. 2.7B**). However, in DH5α there is no transcription initiation from pT7 in the absence of T7 polymerase, and no circular IS*492* excision product is detected even though there is still transcription through the element from the opposite direction (p*lac)* and the wild-type copy of IS*492* should be competent for expression of *mooV* from an internal promoter. Providing MooV *in trans* from an expression vector restores excision of IS*492* from pVoom7.5 in DH5α (**Fig. 2.7**). The same

results were obtained when additional flanking sequence was included from the *epsG* or copy *1* insertion sites on the pmooV and pVoom constructs (data not shown).

DISCUSSION

In a novel application of the Taqman technology, the frequency of precise excision of IS*492* was determined and shown by statistical analyses to directly correlate with the high occurrence of ^{p}EPS phase variation (10^{-3}–10^{-2}/cell/generation). This is the highest frequency of nonmutagenic repair of the donor DNA that has been described for any classical transposon or insertion sequence. Another IS element from the IS*110*/IS*492* family (24) and a few IS elements from the IS*3* (25, 26), IS*4* (27), IS*5* (28, 29), and IS*256* (30) families have been reported to excise precisely. The best characterized of these elements are IS*1301* (IS*5* family) and IS*256,* which exhibit reversible insertion that regulates expression of capsular and extracellular polysaccharide in *Neisseria gonorrhoeae* and *Staphyloccus epidermidis,* respectively (28, 30, 31). The frequency of precise excision of these elements has not been determined directly, but based on the phase variation of polysaccharide production it is approximately 10^{-4} /cell/generation for these elements. Both of these elements utilize a DDE-motif transposase. The transposase of IS*256* is required for circle formation by the element (32) but precise excision has not been shown to be dependent on the transposase for either IS*256* or IS*1301*. Precise excision of prokaryotic mobile elements is usually mediated by Y- or S-recombinases, which utilize a covalent recombinase-DNA intermediate to conserve the energy of the phosphodiester bond (reviewed in (5)). MooV is the first prokaryotic DDE- or DEDD-motif transposase demonstrated to be required for precise excision of the transposable element (9).

The DEDD tetrad of the Piv-MooV recombinases is predicted to coordinate divalent metal cations that direct DNA hydrolysis at the element-donor DNA junction and mediate strand

transfer through one-step transesterification (11-13). The proposed mechanism for conservative inversion mediated by Piv, which involves a Holliday junction intermediate (13), may be applied to the precise excision reaction mediated by MooV if the 5 bp direct repeats that flank the inserted element serve as the core cross-over sequences. However, because IS*492* has no terminal inverted repeats, it is difficult to predict how MooV recognizes both ends to set up the appropriate synaptic complex. Biochemical characterization of MooV binding and cleavage of the IS*492* ends is in progress.

To define factors that influence precise excision of IS*492*, we assayed transposition of IS*492* from four different *P. atlantica* chromosomal sites (copies *1-4*) as compared to the *eps* site. Precise excision of IS*492* could not be consistently detected from two of the alternate insertion sites and could be measured at very low levels from the other two sites. Each of the elements at the five chromosomal insertion sites (including the *eps* site) are identical in nucleotide sequence and all have the same 5 and 7 bp sequence immediately flanking the left and right of the element, respectively (9, 13). In addition, copies of IS*492* with the different flanking sequences from the five *P. atlantica* chromosomal sites are competent for precise excision when cloned into pCR2.1 and introduced into *E. coli*. These results are consistent with previous Southern blot analyses of crenated and mucoid phase variants of *P. atlantica* by Bartlett et al. (8), which suggested that insertion of IS*492* into the *eps* site does not result in loss of one of the other copies of IS*492* on the chromosome. Taking all these results into consideration, we examined the context of each IS*492* insertion site on the *P. atlantica* chromosome.

The movement of some mobile elements has been shown to be influenced negatively or positively by DNA sequence-dependent bending, DNA topology, chromosome domain structure, transcription through the element or the target site, and DNA replication [reviewed in (33)]. For

example, local chromosome structure, which is impacted by levels of transcription within a chromosomal domain, influences target site selection by bacteriophage Mu in replicative transposition (34, 35). The organization of genes and the predicted transcription through IS*492* at each insertion site suggested increased expression of *mooV* from the element at the *eps* site. qRT-PCR confirmed that host-initiated transcripts of *mooV* for copies *1-4* were 100- to 100,000-fold lower than for IS*492* at the *eps* insertion site, suggesting a coupling between *mooV* expression and IS*492* transposition. Such coupling could result from an increased localized concentration of MooV at the *eps* locus. Alternatively, transcription through the *eps* locus could facilitate IS*492* transposition from this site. Our results from IS*492* excision assays in *E. coli* indicate that impinging transcription significantly increases expression of *mooV* to a critical level that is required for precise excision of IS*492*; without expression of *mooV* from an external promoter, no precise excision is observed.

Since all the copies of IS*492* are identical, the low level or lack of precise excision product for copies *1-4* does not indicate that these copies are inactive elements. These elements may move by replicative transposition or cut-and-paste transposition with efficient double-strand break repair from a sister chromosome such that the element would be found at both the donor site and the target [for review see (5)]. It is possible that the context of the insertion site determines the mechanism of transposition or controls the level of precise excision through repression or reduced activation of transposition.

Many mobile elements have evolved mechanisms to attenuate impinging transcription from host DNA or inhibit insertion into a transcriptionally active gene to prevent increased expression of transposase and higher levels of transposition that can be lethal to the host [reviewed in (33)]. However, IS*492* precise excision appears to require external transcription

of the transposase. This is consistent with the regulatory role of IS*492* in ^{P}EPS phase variation. An environmental signal turns on transcription of the *eps* operon, which increases *in cis* MooV levels and promotes precise excision of IS*492* to restore a functional *epsG* gene. To protect the host from increased insertion of the element at new sites, the transposase levels required for precise excision of the element may also inhibit reinsertion into the chromosome. This is supported by the results of Southern blot analyses with chromosomal DNA from clonally-derived crenated and mucoid colonies, which show excision of IS*492* from *epsG* does not result in insertion at a new site on the *P. atlantica* chromosome [(8), Chpt. 3].

ACKNOWLEDGEMENTS

The studies of regulation of *P. atlantica* EPS phase variation was supported by NSF grant MCB-0004123 (to ACK). The characterization of IS*492* precise excision was supported by National Institutes of Health grant GM49794 (to ACK). Sequencing and annotation of the *P. atlantica* genome was performed under the auspices of the US Department of Energy's Office of Science, Biological and Environmental Research Program and by the University of California, Lawrence Livermore National Laboratory under Contract No. W-7405-Eng-48, Lawrence Berkeley National Laboratory under contract No. DE-AC03-76SF00098 and Los Alamos National Laboratory under contract No. W-7405-ENG-36.

We thank Tim Hoover and Russ Karls for critical reading of the manuscript and valuable advice, Daniel Promislow and Nina Wurzburger for assistance with the statistical analysis of our data, Mark Schell, Sidney Kushner, and Bijoy Mohanty for productive discussions, and Michael Gatlin, Adam Popkowski, and Peter Caruana for their contributions to plating and counting *P. atlantica* colonies during their undergraduate research experiences.

REFERENCES

1. del Pilar Garcillan-Barcia, M., Bernales, I., Mendiola, M. V. & de la Cruz, F. (2001) *Mol Microbiol* **39,** 494-501.
2. Rudy, C., Taylor, K. L., Hinerfeld, D., Scott, J. R. & Churchward, G. (1997) *Nucleic Acids Res* **25,** 4061-6.
3. Ton-Hoang, B., Guynet, C., Ronning, D. R., Cointin-Marty, B., Dyda, F. & Chandler, M. (2005) *Embo J* **24,** 3325-38.
4. Lyras, D., Adams, V., Lucet, I. & Rood, J. I. (2004) *Mol Microbiol* **51,** 1787-800.
5. Curcio, M. J. & Derbyshire, K. M. (2003) *Nat Rev Mol Cell Biol* **4,** 865-77.
6. Izsvak, Z., Stuwe, E. E., Fiedler, D., Katzer, A., Jeggo, P. A. & Ivics, Z. (2004) *Mol Cell* **13,** 279-90.
7. Lovett, S. T. (2004) *Mol Microbiol* **52,** 1243-53.
8. Bartlett, D. H., Wright, M.E., and Silverman, M. (1988) *Proc Natl Acad Sci U S A* **85,** 3923-3927.
9. Perkins-Balding, D., Duval-Valentin, G. & Glasgow, A. C. (1999) *J Bacteriol* **181,** 4937-48.
10. Chandler, M. a. M., J. (2002) in *Mobile DNA II*, ed. Craig, N. L., Craigie, R., Gellert, M., and Lambowitz, A.M. (ASM Press, Washington, D.C.).
11. Lenich, A. G. & Glasgow, A. C. (1994) *J Bacteriol* **176,** 4160-4.
12. Tobiason, D. M., Buchner, J. M., Thiel, W. H., Gernert, K. M. & Karls, A. C. (2001) *Mol Microbiol* **39,** 641-51.
13. Buchner, J. M., Robertson, A. E., Poynter, D. J., Denniston, S. S. & Karls, A. C. (2005) *J Bacteriol* **187,** 3431-7.

14. Kidwell, M. G. & Lisch, D. R. (2002) in *Mobile DNA II*, ed. Craig, N. L., Craigie, R., Gellert, M., and Lambowitz, A.M. (ASM Press, Washington, D.C.), pp. 59-90.

15. Godoy, V. G. & Fox, M. S. (2000) *Proc Natl Acad Sci U S A* **97,** 7393-8.

16. Corpe, W. A. (1980) in *Adsorption of Microorganisms to Surfaces*, ed. Bitton, G., and Marshall, K.C. (John Wiley and Sons, Inc., New York, N.Y.), pp. 105-144.

17. Ausubel, F. M., Brent, R., Kingston, R. E., Moore, D. D., Seidman, J. G., Smith, J. A. & Struhl, K. (2005) *Current Protocols in Molecular Biology* (John Wiley & Sons, Inc., Hoboken, New Jersey).

18. Gally, D. L., Bogan, J. A., Eisenstein, B. I. & Blomfield, I. C. (1993) *J Bacteriol* **175,** 6186-93.

19. Heid, C. A., Stevens, J., Livak, K. J. & Williams, P. M. (1996) *Genome Res* **6,** 986-94.

20. Belas, R. (1989) *J Bacteriol* **171,** 602-5.

21. Ishikawa, J. & Hotta, K. (1999) *FEMS Microbiol Lett* **174,** 251-3.

22. Becker, B. U., Kosch, K., Parniske, M. & Muller, P. (1998) *Mol Gen Genet* **259,** 161-71.

23. Lim, C. J., Daws, T., Gerami-Nejad, M. & Fuchs, J. A. (2000) *Biochim Biophys Acta* **1491,** 1-6.

24. Partridge, S. R. & Hall, R. M. (2003) *J Bacteriol* **185,** 6371-84.

25. Mullin, D. A., Zies, D. L., Mullin, A. H., Caballera, N. & Ely, B. (1997) *Mol Gen Genet* **254,** 456-63.

26. Kusumoto, M., Nishiya, Y. & Kawamura, Y. (2000) *Appl Environ Microbiol* **66,** 1133-8.

27. Brass, S., Ernst, A. & Boger, P. (1996) *Appl Environ Microbiol* **62,** 1964-8.

28. Hammerschmidt, S., Hilse, R., van Putten, J. P., Gerardy-Schahn, R., Unkmeir, A. & Frosch, M. (1996) *Embo J* **15,** 192-8.

29. Munoz, R., Lopez, R. & Garcia, E. (1998) *J Bacteriol* **180,** 1381-8.

30. Ziebuhr, W., Krimmer, V., Rachid, S., Lossner, I., Gotz, F. & Hacker, J. (1999) *Mol Microbiol* **32,** 345-56.

31. Conlon, K. M., Humphreys, H. & O'Gara, J. P. (2004) *J Bacteriol* **186,** 6208-19.

32. Loessner, I., Dietrich, K., Dittrich, D., Hacker, J. & Ziebuhr, W. (2002) *J Bacteriol* **184,** 4709-14.

33. Nagy, Z. & Chandler, M. (2004) *Res Microbiol* **155,** 387-98.

34. Manna, D., Breier, A. M. & Higgins, N. P. (2004) *Proc Natl Acad Sci U S A* **101,** 9780-5.

35. Manna, D. & Higgins, N. P. (1999) *Mol Microbiol* **32,** 595-606.

Fig. 2.1. ^{p}EPS phase variation in *P. atlantica*. **(A)** IS*492* (white and cross-hatched bar) inserts specifically into a single site in *eps*, resulting in a 5 bp direct repeat of the target sequence (black bar) flanking the element. The transposase, encoded by *mooV* (cross-hatched bar), mediates this insertion and the precise excision of IS*492* that restores *eps* and generates a circular form of the element with one copy of the 5 bp target sequence at the circle junction. **(B)** Phase variation of ^{p}EPS results in colony morphology switching; mucoid (^{p}EPS^{+}) and crenated (^{p}EPS^{-}) colonies is shown.

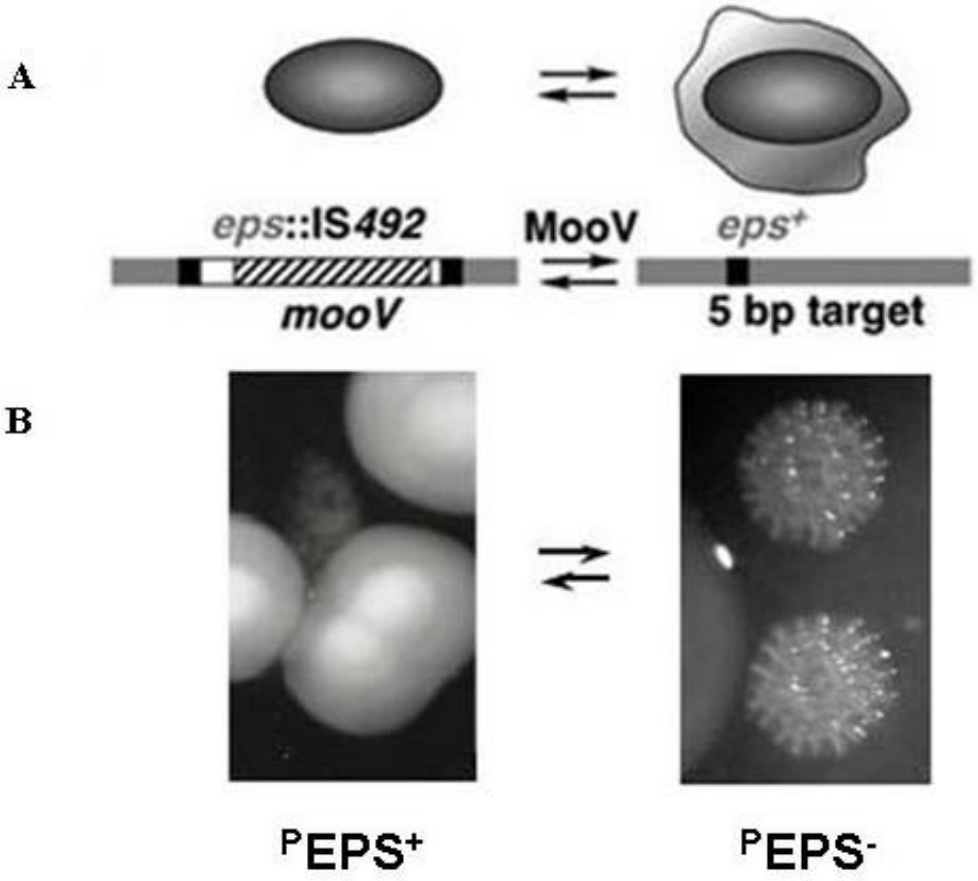
A
eps::IS492
MooV
eps+
mooV
5 bp target
B
PEPS+
PEPS-

Fig. 2.2. Quantitative PCR assay for IS*492* precise excision from *epsG* in *P. atlantica*. (A) qPCR to measure IS*492* excision frequency utilizes two Taqman probes with different fluorophores (circles) and black hole quenchers (diamonds), which are designed to separately measure amplification by the forward and reverse primers (arrows) of the agarase gene (*agr*; wavy lines) and the restored *eps* locus (dark grey line). Release of the fluorophore from the probe by the 5'-3' exonuclease activity of Taq polymerase allows detection of the fluorophore (grey sun) by the BioRad iCycler Real Time PCR System. **(B)** The extension time for detecting the release of the fluorophore from the *eps* probe for intact *eps* but not *eps*::IS*492* was determined empirically. The substrates for the qPCR were pBHG115 (***eps***) and pAG990 (**IS**), which has IS*492,* which is defective for excision (single bp change resulting in *mooV*), inserted in the *eps* sequence. Using a 2 min extension time pBHG115 gave a C_T of 13 and pAG990 gave no signal in 30 cycles. Both substrates gave a C_T of 13 with the 5 min extension time. The PCR products (106 bp and 1,313 bp for ***eps*** and **IS,** respectively) for two extension times are shown here: 2 min- the extension time used for the qPCR assays in *P. atlantica* and 5 min- the shortest extension time at which the fluorophore could be detected from pAG990. Equal amounts of plasmid template were used and the 658 bp PCR product from *bla* on both constructs was used as a template control. The DNA marker (**M**) is a 100 bp ladder (NEB). **(C)** Representative qPCR results are shown for one independent experiment with HCD cells. The curve-fit fluorescence units (**CF RFU**) from the HEX probe (***agr***) and FAM probe (***eps***), adjusted for the signal base line, are plotted versus the PCR **cycle** numbers from the qPCR reactions with chromosomal DNA from HCD cells. The standards are **solid lines** and the 18 DNA samples from HCD cells are lines with **diamond symbols**. The **grey line** is the threshold bar for determining the threshold cycle from these plots. The plot of the standards (**grey circles**) **starting quantity** (in fg) versus

their **threshold cycle** is used to determine the amount of DNA that has the *agr* and repaired *eps* loci in the starting reaction for each unknown (**open squares**). The **correlation coefficient** is the r^2 value for the linear regression analysis of the standards data. The C_T values determined for the unknowns are used to calculate the frequency of IS*492* precise excision in HCD cells (Methods and Materials).

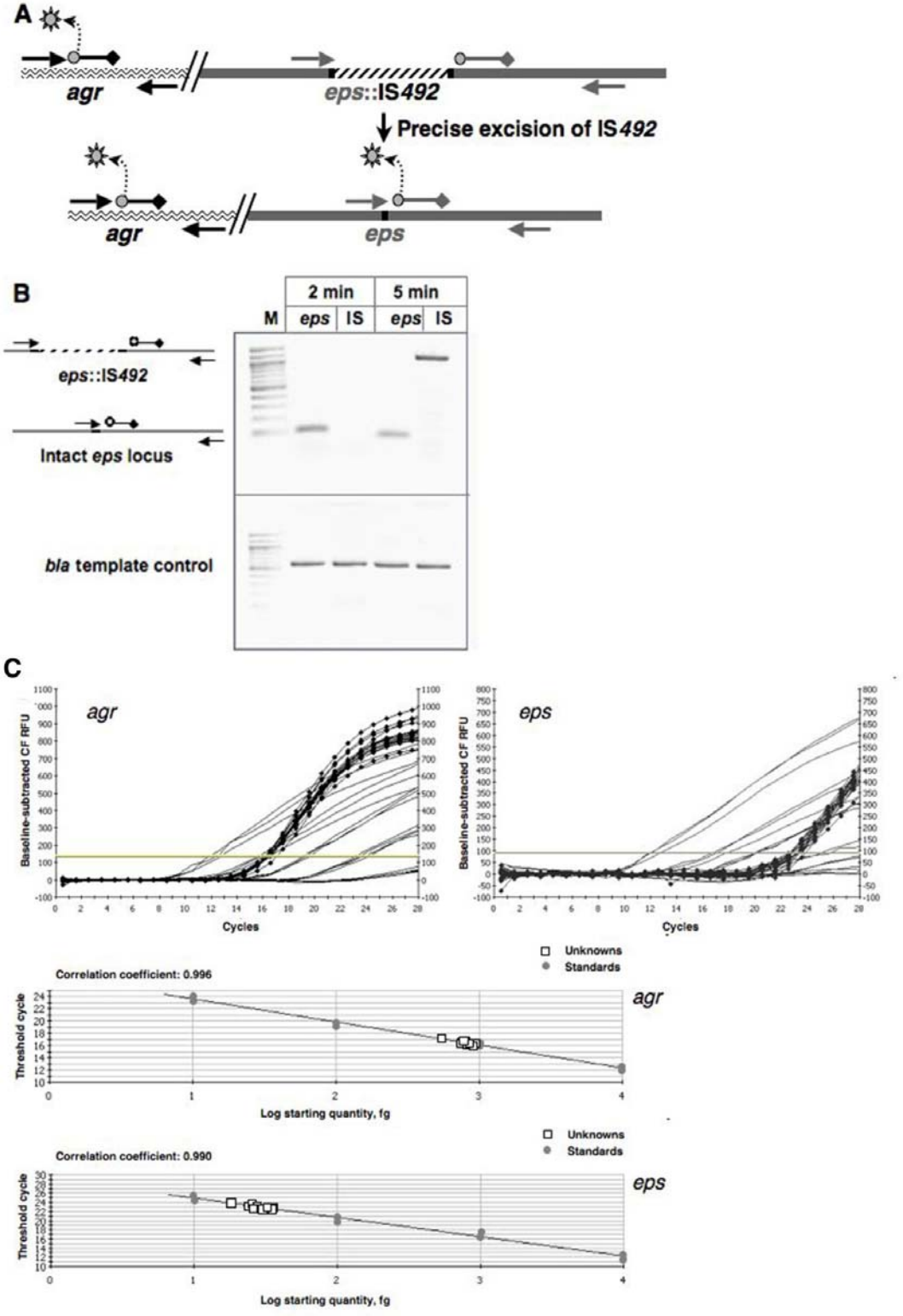
A
agr
eps::IS492
Precise excision of IS492
agr
eps
B
2 min
5 min
M
eps
IS
eps
IS
eps::IS492
Intact eps locus
bla template control
C
agr
eps
Baseline-subtracted CF RFU
Cycles
Unknowns
Standards
Correlation coefficient: 0.996
Threshold cycle
Log starting quantity, fg
agr
Correlation coefficient: 0.990
eps

Fig. 2.3. Correlation of directly measured frequency of IS*492* precise excision with ^{p}EPS phase variation in *P. atlantica*. The frequency of ^{p}EPS phase variation (P_{PV}) mean values are plotted versus the frequency of IS*492* precise excision (P_{EX}) mean values; the data is from six independent experiments. Simple linear regression analysis reveals an r^2 value of 0.945 and slope of 1.08, indicating that there is one precise excision event for each colony morphology phase variation event.

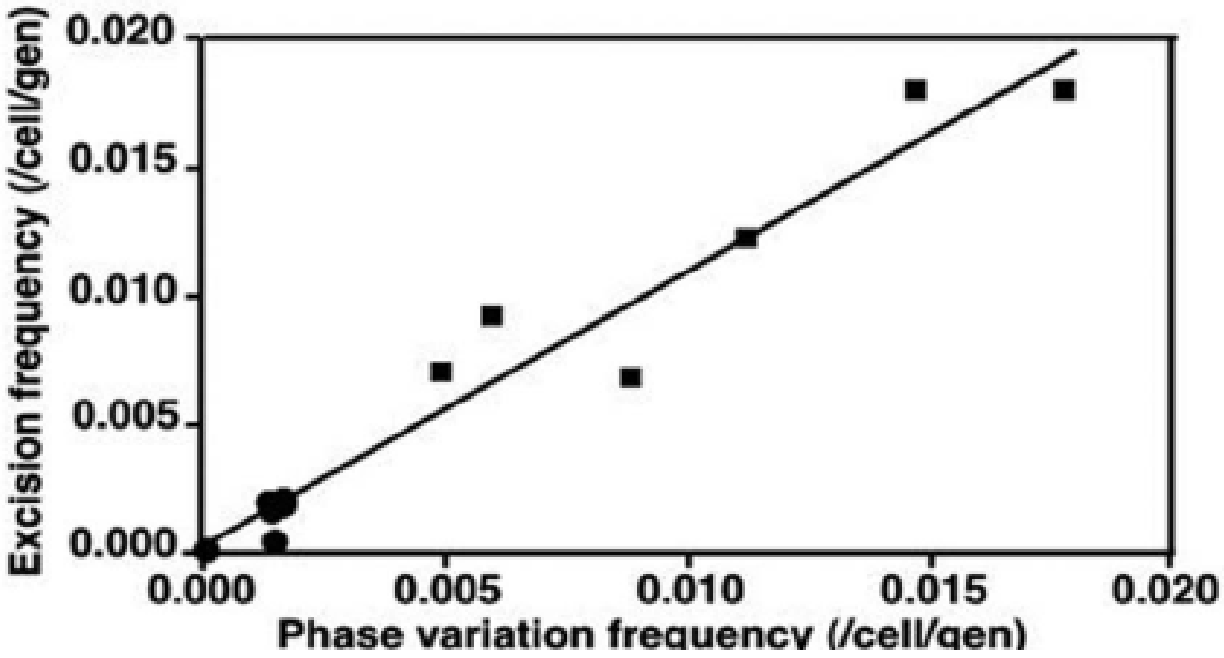
Excision frequency (/cell/gen)
0.020
0.015
0.010
0.005
0.000
0.000
0.005
0.010
0.015
0.020
Phase variation frequency (/cell/gen)

Fig. 2.4. Precise excision of IS*492* from different *P. atlantica* chromosomal locations. PCR products from reactions using forward and reverse primers (**Table 2.2**) that flank IS*492* at each insertion site and chromosomal DNA as template (**Direct PCR**), and from reactions using the PCR products from the Direct PCR assay as template and nested forward and reverse primers that flank the element at each site (**Nested PCR**) were electrophoresed in a 3% agarose gel. The predicted products for precise excision of copies *1-4* from their respective sites were generated and cloned into pCR2.1 (**Table 2.3**) to create the plasmids that were used as template to confirm the activity of the nested primers (**Controls**). The mobilities of the amplified unexcised IS*492* elements with flanking DNA, and of the amplified insertion sites for the precisely excised *eps*-associated element and copies *3* and *4* are indicated. The DNA size marker (**M**) is the Promega 25 bp ladder.

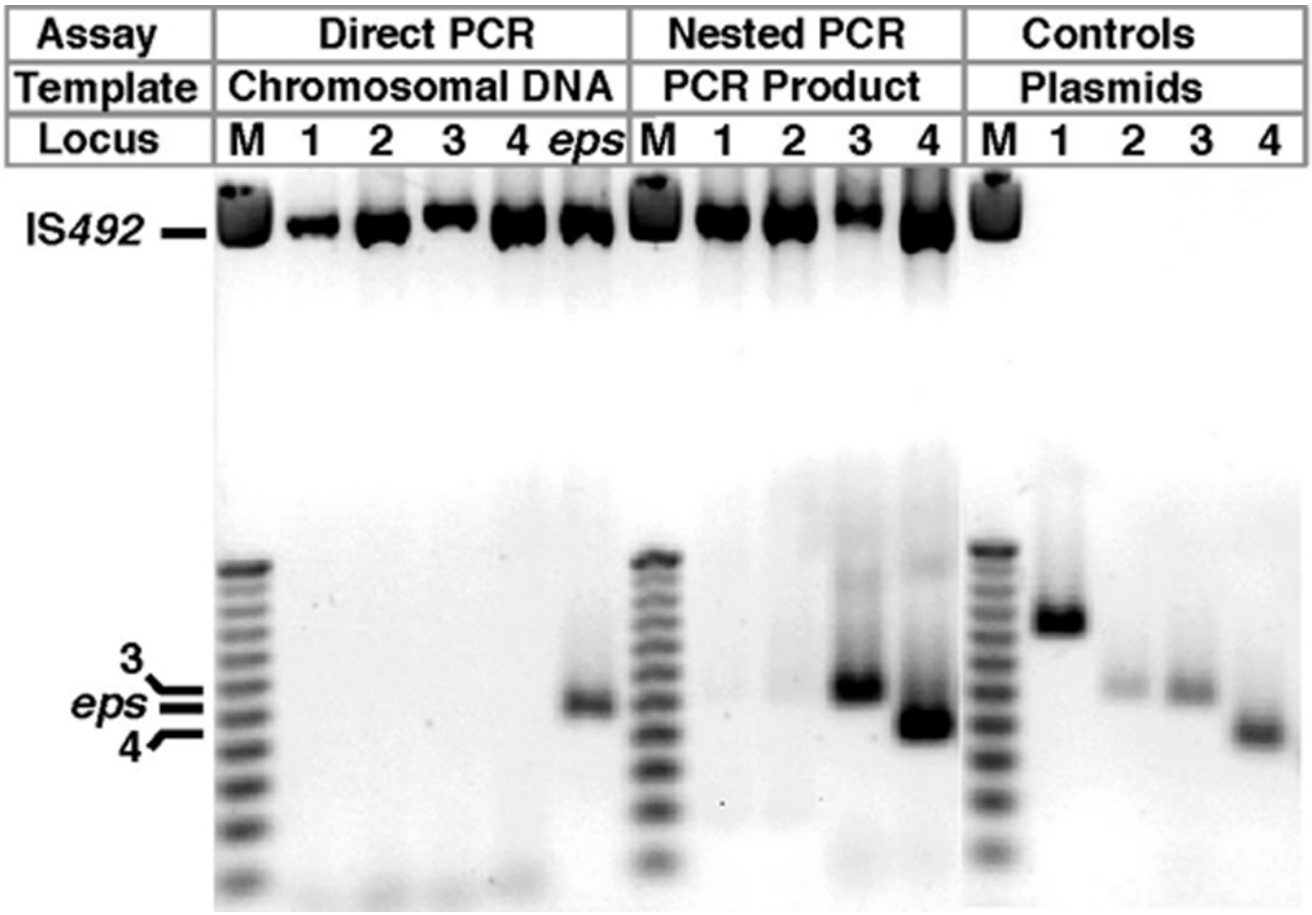
Assay
Direct PCR
Nested PCR
Controls
Template
Chromosomal DNA
PCR Product
Plasmids
Locus
M 1 2 3 4 eps M 1 2 3 4 M 1 2 3 4
IS492
3
eps
4

Fig. 2.5. Precise excision of IS*492* from multi-copy plasmids in *E. coli*. Excision of IS*492* from flanking *P. atlantica* sequence within the cloning site of pCR2.1 was assayed using crude lysates from transformed *E. coli* DH5α and the same primers and reaction conditions as the nested PCR assays in *P. atlantica* (**Fig. 2.4**). The sizes for the PCR products resulting from precise excision of copies *1-4* and the *eps*-associated copy from the plasmids are indicated to the right of the gel image and DNA marker sizes (from the 25 bp ladder; Promega) are designated on the left. The PCR products for the unexcised element are marked as **IS*492*.**

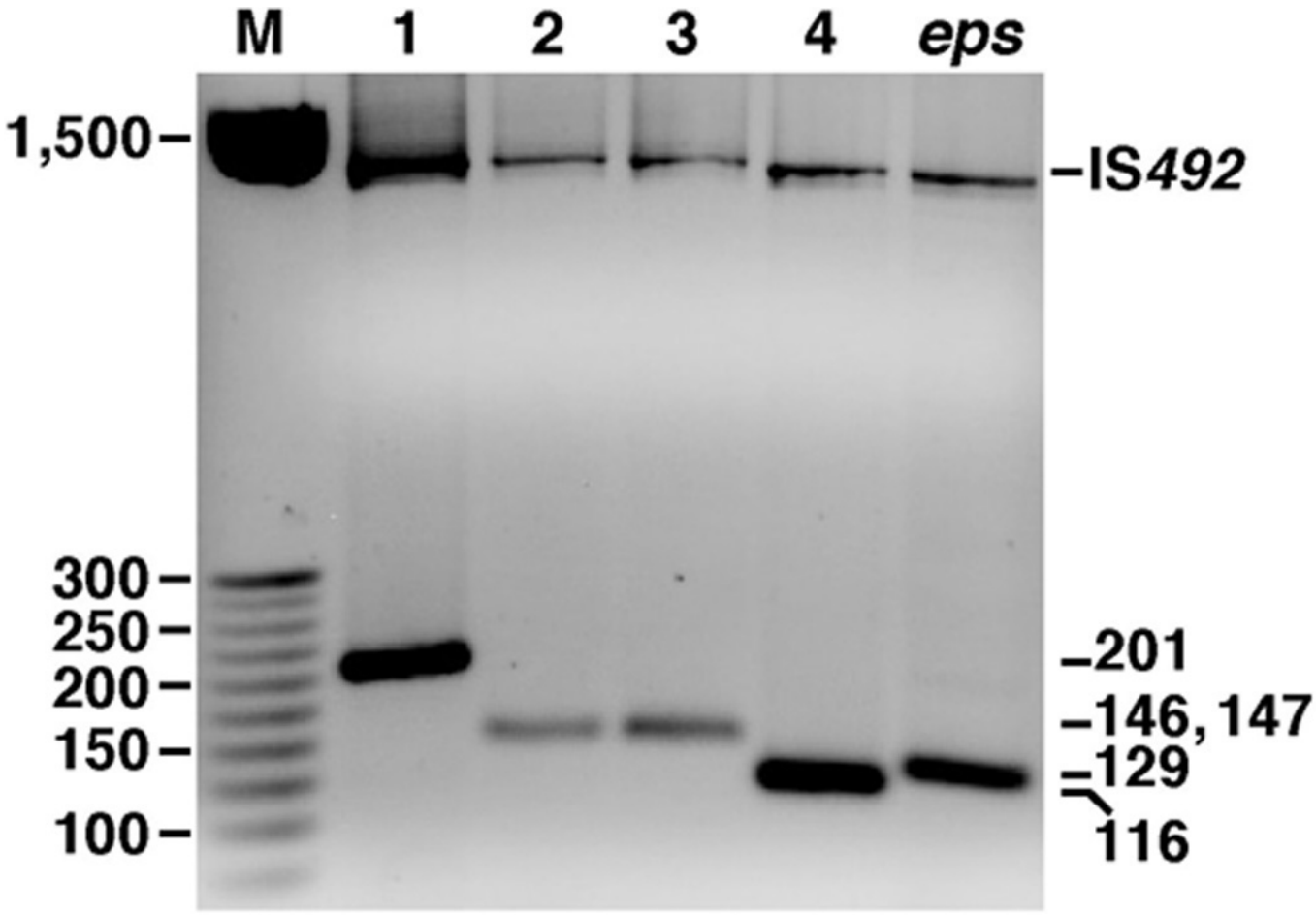
M
1
2
3
4
eps
1,500
300
250
200
150
100
IS492
201
146, 147
129
116

Fig. 2.6. Context of IS*492* insertions in *P. atlantica* genome and representative results of qRT-PCR assay for host-initiated *mooV* transcripts. (**A**) Five insertion sites shown for IS*492* (white box with cross-hatched *mooV*) are found on different contigs in the draft sequence of *P. atlantica* T6c. The 5 bp direct repeats at each insertion site are represented by **black boxes**. The directionality of open reading frames (ORFs) flanking IS*492* insertions and of *mooV* are shown. IS*492* is inserted into a predicted glucosyl transferase gene at the *eps* site; copy *1* is flanked by a gene for a putative oxidoreductase transmembrane protein upstream and a hypothetical gene downstream; copy *2* has a predicted LysR-family regulator gene upstream and a hypothetical gene downstream; copy *3* is preceded and followed by two ORFs with no significant homology to any ORF in the database; and Copy *4* is preceded by a predicted transposase gene from a IS*4*-like element and followed by an integrase-like gene. The position of the RT-PCR primer that is complimentary to *mooV* mRNA sequence is indicated by **leftward arrows**; the positions of the forward primers used in the qRT-PCR reactions with the reverse *mooV* primer for are indicated by **rightward arrows**. (**B**) The curve-fit fluorescence units (**CF RFU**), adjusted for the signal base line, are plotted versus the PCR cycle number from the qRT-PCR reactions with the cDNA generated for host-initiated *mooV* transcripts from each of the five IS*492* copies on the *P. atlantica* chromosome (**filled symbols**) and for the reference *trxA* mRNA (**open squares**). The **Threshold Bar** determines the threshold cycle used to calculate the amount of starting template; the control reactions lacking reverse transcriptase (**open circles**) demonstrate the absence of detectable DNA contamination of the RNA preparations used. The results for RNA from crenated colonies at HCD (R-HCD1) are shown; however independent repetitions of this experiment yielded the same trends for *mooV* transcript levels from the five IS*492* insertion sites (**Table 2.1**).

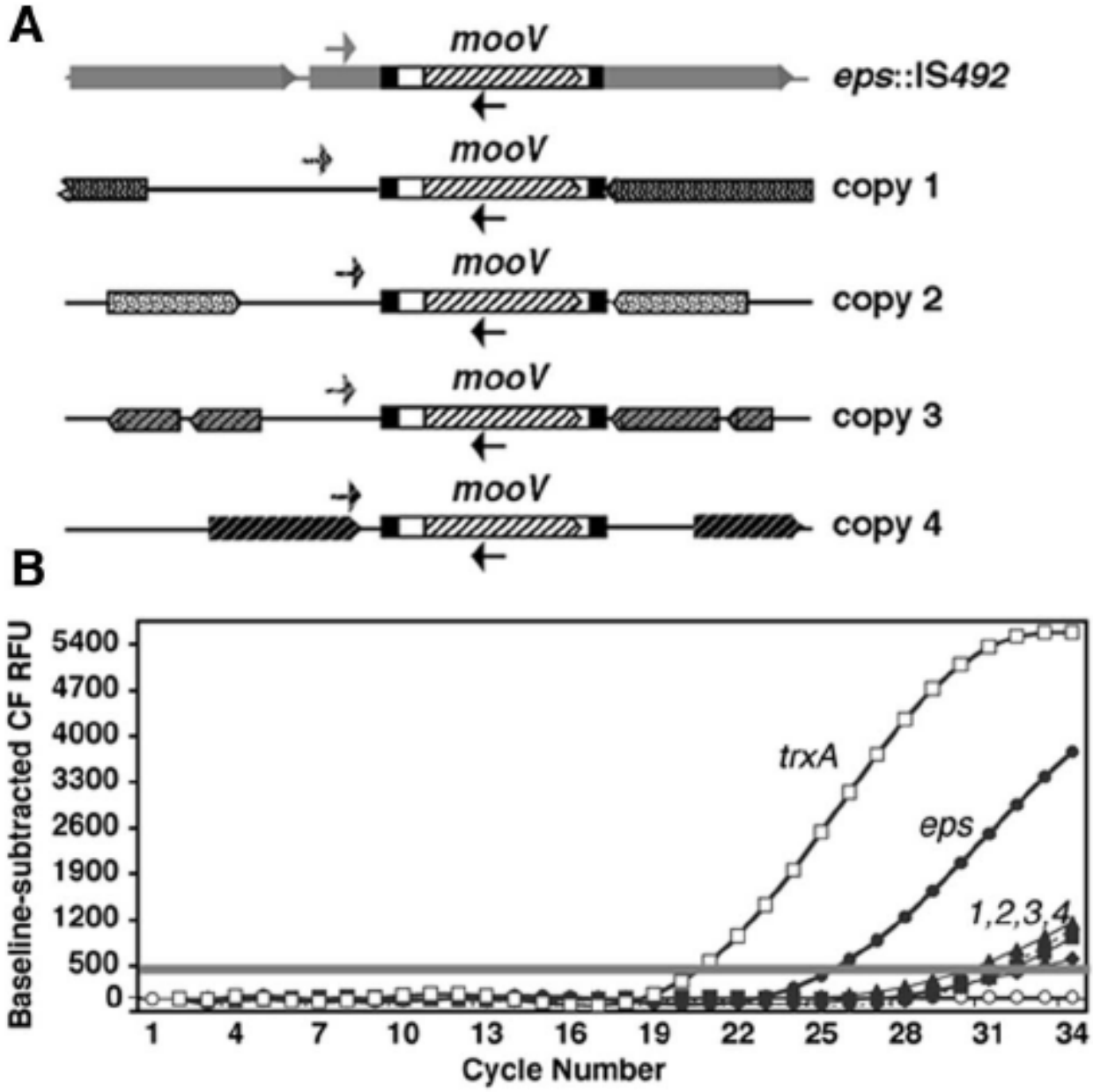
A
mooV
eps::IS492
mooV
copy 1
mooV
copy 2
mooV
copy 3
mooV
copy 4
B
Baseline-subtracted CF RFU
5400
4700
4000
3300
2600
1900
1200
500
0
trxA
eps
1,2,3,4
1
4
7
10
13
16
19
22
25
28
31
34
Cycle Number

Fig 2.7. PCR assay for precise excision of IS*492* under varying external transcription conditions in *E. coli*. (A) It has previously been demonstrated that precise excision of IS*492* is linked to the formation of a circularized IS*492* with the 5 bp flanking sequence joining the ends of the element (9). A PCR assay to detect the circle junction is depicted, with IS492pmooV5.7 and pVoom7.5, which encode IS*492* in two orientations between the plac and pT7 promoters on pCR2.1, are depicted. The products of precise excision and the PCR primers (CJ250A and CJ250B) used in the assay for circle junction formation are shown. **(B) DH5α** or **HMS174(DE3)** were transformed with **pmooV5.7** or **pVoom7.5** (**-**) or with **pAG900** and pmooV5.7 or pVoom7.5 (+) and plated on LBAmp (**0**), LBAmp with 0.05mM IPTG (**I**), and LBAmp with 0.02% glucose (**G**). Cleared lysates were prepared and used in PCR assays with CJ250A and CJ250B primers. The PCR products were electrophoresed on a 2% agarose gel and visualized with ethidium bromide.

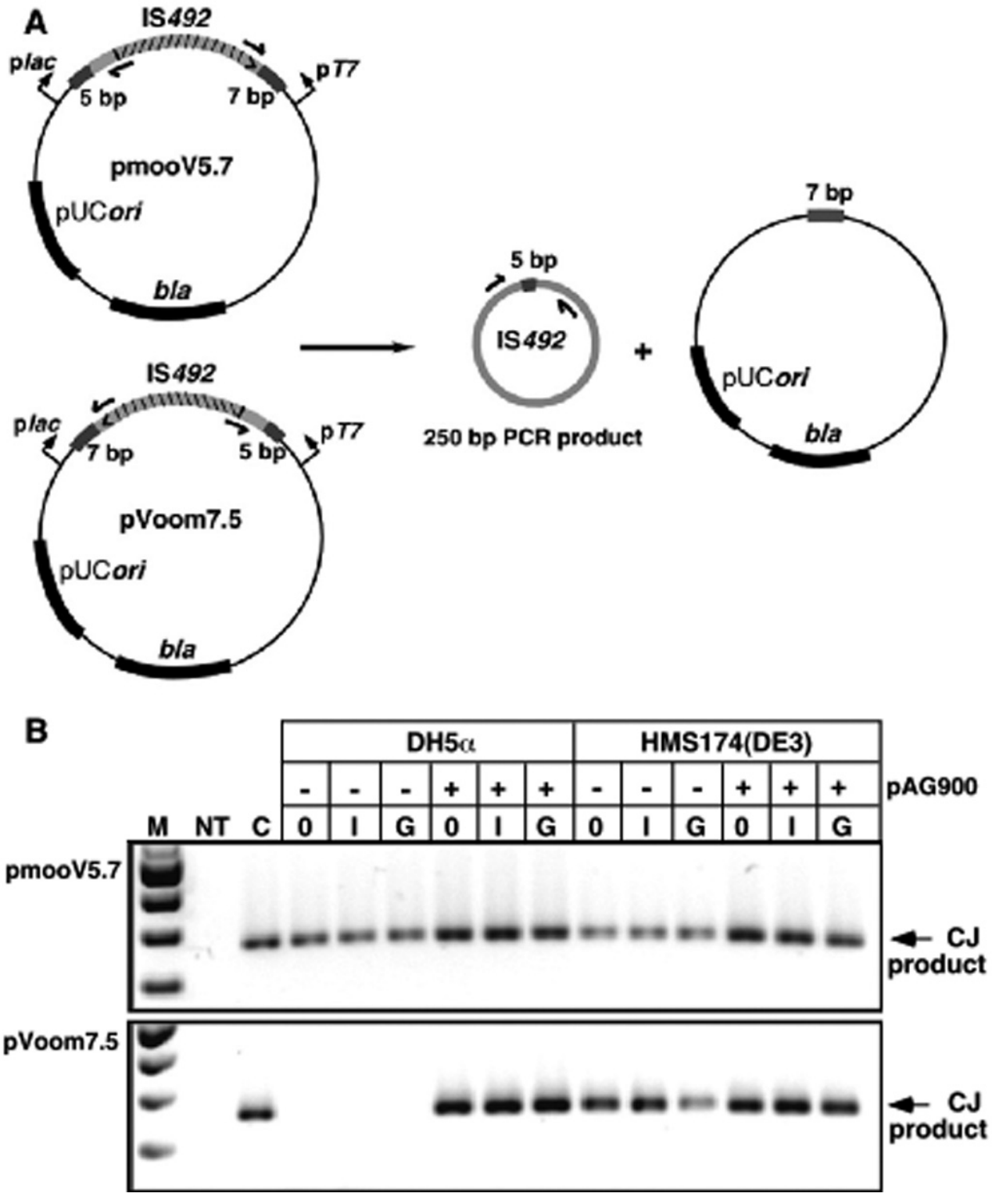
A
IS492
plac
pT7
5 bp
7 bp
pmooV5.7
pUCori
bla
IS492
plac
pT7
7 bp
5 bp
pVoom7.5
pUCori
bla
5 bp
IS492
250 bp PCR product
+
7 bp
pUCori
bla
B
DH5α
HMS174(DE3)
pAG900
M NT C 0 I G 0 I G 0 I G 0 I G
pmooV5.7
CJ product
pVoom7.5
CJ product

Table 2.1. Relative levels of host-initiated *mooV* transcripts for IS*492* copies[1].

Source[2]	copy 1	copy 2	copy 3	copy 4	*eps*-associated
R-LCD1	$7.0x10^{-4}$	$3.2x10^{-3}$	$7.0x10^{-4}$	$4.4x10^{-3}$	1
R-LCD2	$1x10^{-5}$	$2.0x10^{-4}$	$6x10^{-5}$	$5.0x10^{-4}$	1
R-HCD1	$6x10^{-5}$	$4.0x10^{-4}$	$1.0x10^{-4}$	$1.4x10^{-2}$	1
R-HCD2	$2.0x10^{-4}$	$6.0x10^{-4}$	$1.3x10^{-4}$	$1.3x10^{-3}$	1

[1]The amount of cDNA from RT-PCR of the *mooV* transcripts was determined by qPCR and the values were first normalized against the amount of *trxA* cDNA in each sample. The normalized values for the host-initiated *mooV* transcripts from all the IS*492* copies were then divided by the value for the *mooV* transcript from the *eps*-associated IS*492*; these ratios
are given in the table.

[2]Chromosomal RNA isolated from pooled bacteria grown at low (LCD) and high (HCD) colony density

Table 2.2 Oligonucleotides used in PCR, qPCR, and qRT-PCR.

Primer Name*	Sequence (5' to 3')
L58	CGGTACTGTCTTATCATCCTAATCG
R76	CAGGAGGCTCTCTATTGTACAGC
EPSPRB3 (L23PRB)	FAM-TCTATCAAGCTCTCTATTGAGCAAGG-BHQ1
AGARL	AGTATATGATGGAAGAGTTAGAC
AGARR	CATAACCTATGTTGGCTGGG
AGARPRB	HEX-TATTTTGGTCGAGATAACGGTGGC-BHQ2
RN2.BSSHII	TTGGCGCGCTCAATTTCTTCAACAGG
L23.BSSHII	TTGGCGCGCTTGGTGGCATTGAAAAC
PDB6OVRLP	AATAAGCTCTCTAACAAGCTGTTAAAC
PDB6OVRLP2	CTTGTTAGAGAGCTTATTTGC
PDB1OVRLP	ACACGGAATTTAACAAGCGCTTTAAACG
PDB1OVRLP2	CTTGTTAAATTCCGTGTAC
PDB1NL	TATTCATAATTCGACTCTGACC
PDB1NR	TCGAATTAAGCGGTATGTGGC
PDB1R	ACTACTTATATTCAATGAAGTGG
COPY1L (PDB1L)	ATAGAACTTCCTTGTAGGAGC
PDB6NOR	AACATCCTTTTGTTATGGCGC
PDB6NIR	AATTAGAAGGCCGGACGTTTGG
PDB6NL	ATGAGCGAAGCGAACAAAGC
PDB6L	TGTATTTTGTCCTTGTTTAACAG
PDB9NR	ACATTGGGAGATTGGCAACG
PDB9NL	TGAGCTTTTCCAGCCACCG
PDB9R	GGCATTAAGTTCGACACTGC
PDB9L	TCATGCCACCTGACCATCC
PDB12NL	AACGGGCAAAAAATTGTTGGC
PDB12NR	AAATGGGGTACTGGAACTGC
PDB12R	AACTCTTATCGTGATTCCACC
PDB12L	GTTGAACGAAGTGAAAACAGC
FWEPS (L23)	TTTGGTGGCATTGAAAACCTTGT
RVEPS (RN2)	TCAATTTCTTCAACAGGAG
TRXAR	GTTCAAAAACTCTTCTAATTGC
TRXAL	AAAATTATCCAGTTATCGGACG
ISL270	TATCGACACCGACGTTAACG
EPS5	CTTGTATGGATAATAACTCAGG
EPS7	TAACAAGAGACTATGGCGTCA
CJ250A	TTATCGGTCTCTCAACTGAGGAGC
CJ250B	TAAGAAAGTGGCTATTATTGCGTGC

*Parenthetical name is an alternate designation for the oligonucleotide

Table 2.3. Plasmid List.

Plasmid	Primers*	Cloned PCR product in pCR2.1
pBHG100	PDB1L, PDB1R	copy *1*
pBHG104	PDB6NL, PDB6NIR	copy *2*
pBHG107	PDB9L, PDB9R	copy *3*
pBHG109	PDB9L, PDB9R	copy *3* repaired donor
pBHG110	PDB12L, PDB12R	copy *4*
pBHG112	PDB12L, PDB12R	copy *4* repaired donor
pBHG113	EPSL58, EPSR76	*eps* copy
pBHG115	EPSL58, EPSR76	*eps* repaired donor
pBHG116	AGARL, AGARR	agarase control fragment
pBHG117	TRXAL, TRXAR	*trxA* control fragment
pBHG119	PDB1L, ISL270	copy *1* control fragment for RNA
pBHG120	PDB6NL, ISL270	copy *2* control fragment for RNA
pBHG121	PDB9L, ISL270	copy *3* control fragment for RNA
pBHG122	PDB12L, ISL270	copy *4* control fragment for RNA
pBHG123	EPSL58, ISL270	*eps* control fragment for RNA
pBHG124	COPY1L, COPY 1OVRLP COPY1R, COPY1OVRLP2	copy *1* repaired donor generated by overlap PCR**
pBHG125	COPY6NL, COPY6OVRLP COPY6NIR, COPY6OVRLP2	copy *2* repaired donor generated by overlap PCR**
pBHG126	L23.BSSHII, RN2.BSSHII	pBHG116 with *eps* control fragment in BssHI site for qPCR
pmooV5.7	EPS5, EPS7	IS*492* with conserved 5 bp and 7 bp, left and right flanking sequence
pVoom7.5	EPS5, EPS7	IS492 with conserved 5 bp and 7 bp, left and right flanking sequence
pAG990	EPSL58, EPSR76	IS*492* with mutation at nt 268(A→C), site directed mutagenesis; (12)

*oligonucleotides (listed in Table 2.2) used in the amplification of the PCR product;
all PCR products generated from *P. atlantica* chromosomal DNA template
** Overlap PCR was performed as described in reference 23.

CHAPTER 3

THE TRANSPOSITION OF IS492 IS RESPONSIVE TO ENVIRONMENTAL FACTORS[1]

[1] Higgins, B.P., Frank, R., and Karls, A.C. 2006. To be submitted to *Journal of Bacteriology*.

ABSTRACT

The phase variation of peripheral extracellular polysaccharide (^{P}EPS) is controlled by the reversible insertion of IS*492* at *epsG* in the marine organism *Pseudoalteromonas atlantica*. In Chapter 2, we demonstrated that the frequency of IS*492* precise excision (P_{EX}), ~ 10^{-3}-10^{-2}, is the highest reported for a bacterial insertion sequence. The IS*492* P_{EX} also correlated directly to the phase variation frequency (P_{PV}) of ^{P}EPS production in *P. atlantica*. The studies presented herein address the regulation of IS*492* precise excision by environmental factors. Switching from ^{P}EPS^{-} to ^{P}EPS^{+}, as measured by sectoring of colonies on marine agar, is dependent on the plating density, with the highest frequency occurring at low colony density (<1.3 colonies per cm^2). However, colony density-dependence for P_{PV} does not signify cell density dependence; *P. atlantica* grown in liquid medium exhibits the same P_{PV} ($\leq 10^{-4}$) at low and high cell densities. In addition, quorum-sensing molecules (acyl-homoserine lactones) isolated from *P. atlantica* have no affect on the frequency of ^{p}EPS phase variation in solid or liquid medium. The results of P_{PV} and P_{EX} assays on marine medium (solid or liquid) with or without a source for galactose indicate that the presence of this ^{p}EPS building block stimulates IS*492* precise excision. We have previously shown that transcription through IS*492* in the *epsG* gene increases P_{EX}, thus the link between galactose and IS*492* transposition may be that galactose induces expression of the *eps* genes.

INTRODUCTION

Mobile genetic elements are widespread among both prokaryotic and eukaryotic organisms. Greater than 40% of human (1), rice (2, 3), and mouse (4) genomes are composed of transposon-derived sequences. While many of these sequences are no longer active, they represent pastg DNA rearranements that shaped the present genome. The transposition of mobile elements can lead to integration, deletion, inversion, and gene conversion events, all of which can significantly alter an organism's genome arrangement. It was once thought that the potential for such genome plasticity was detrimental to an organism, but this flexibility has evolved to provide benefits to the host. For example, V(D)J (variable (diversity) joining) recombination in humans is mediated by recombinases RAG1/RAG2, which are members of the DDE-motif transposase family (5).

Bacterial transposable elements (TEs) are powerful agents of genetic diversity. In addition to encoding genes to facilitate their own movement, many encode additional functions such as antibiotic resistance genes, the acquisition of which can enhance the fitness of a pathogenic organism. However, the movement of bacterial TEs usually occurs at a very low frequency; in fact, many overlapping regulatory mechanisms have arisen to reduce transposition efficiency presumably to prevent the deleterious effects of frequent transposition. But can IS elements be induced by the host to transpose at a higher frequency to affect change in the chromosome under certain conditions? Recent studies have shown that conditions of host cell stress, such as UV irradiation (6), increased temperature (7), or nutrient starvation (8), can increase the transposition frequency of certain bacterial transposable elements. Rather than being the failure of a host cell to maintain regulatory control over transposition when stressed,

the door has been opened to the possibility that the transposition of certain TEs is an inducible process. For example, transposition of Tn*4652* in *Pseudomonas putida* is controlled by the stationary-phase specific sigma factor σ^S (8). Transposition of the integrative and conjugative element (ICE) ICE*Bs1* has been shown to increase when the SOS response is activated by DNA damaging agents and this increase is dependent upon *recA* (9). Exposure to UV irradiation increases the intermolecular transposition of Tn*10* via a response to induction of the SOS response (6). The DNA rearrangements induced by transposition of TE, including insertion and excision of the element and deletions and inversions of flanking chromosomal DNA [reviewed in (10)], can activate or inactivate gene expression and create new genes, which may give a selective advantage to a cell under the stress conditions.

Phase variation of gene expression allows an organism to respond to changes in the environment, reversibly turning on or off the expression of certain genes involved in the adaptive response. Phase variation in many prokaryotic systems has been found to be controlled by site specific inversion systems and slipped-strand mispairing during DNA replication at polynucleotide repeats [reviewed in (11)]. For example, expression of type 4 pili in the obligate human pathogen *Neisseria gonorrhoeae* phase varies (on and off) by slipped-strand mispairing at homopolymeric nucleotide tracts within *pilC* (12), while the type 1 fimbriae of the uropathogenic *E. coli* phase vary due to site-specific inversion of a chromosomal segment encoding the promoter for the fimbriae gene, *fimA* (13).

Phase variation can also be controlled by TE transposition. The production of polysaccharide intracellular adhesion (PIA) in *Staphylococcus epidermidis* is controlled by the reversible insertion of IS*256* into the *icaA* and *icaC* loci (14). Sialylation of LPS and production of sialic acid capsule in *Neisseria meningitidis* is controlled by the transposition of IS*1301* at the

siaA locus (15). In both cases, transposition of the TE occurs at a low frequency ($\leq 10^{-4}$ per cell per generation), pre-adapting a sub-population of cells for changes in the environment.

The phase variation of peripheral extracellular polysaccharide (^{P}EPS) in the marine bacterium *Pseudoalteromonas atlantica* is controlled by the reversible insertion of IS*492* (16). IS*492* is a member of the IS*110*/IS*492* family of insertion sequences (17). The transposase enzymes of this family are members of the novel Piv/MooV recombinase family, whose members catalyze both site-specific inversion and transposition reactions (18). IS*492* is unique among bacterial IS elements in its target site selection, as it has been found to insert at only one chromosomal site to control phase variation of ^{P}EPS production in *P. atlantica* (see Chapter 4). This site-specific insertion of IS*492* into the *epsG* locus effectively shuts off ^{P}EPS production, resulting in a crenated (C) colony morphology. The precise excision of IS*492* restores the original *epsG* sequence and ^{P}EPS production, resulting in mucoid (M) colony morphology. We have reported previously that the precise excision of IS*492* occurs at a higher frequency than that observed for any other bacterial IS element (see Chapter 2) and this is reflected in the mucoid sectoring of crenated colonies (**Fig. 3.1A**). In this study we provide evidence that IS*492* precise excision, and the resulting ^{P}EPS phase variation, are responsive to changes in environmental conditions. In particular, increased phase variation and IS*492* precise excision are dependent upon colony density on solid medium, but not cell density in liquid medium. Although we found that *P. atlantica* makes at least one quorum-sensing activating acyl-homoserine lactone, phase variation and precise excision were not affected by its presence in solid medium. Increases in on-to-off phase variation and precise excision are observed when *P. atlantica* is incubated under conditions that allow for solid surface contacts and/or provide the sugar building blocks for ^{P}EPS

production. These results are the first demonstration of regulation of IS element transposition in response to environmental conditions.

MATERIAL AND METHODS

Bacterial strains, media, growth conditions, and reagents. *P. atlantica* T6c (19), DB11 (20), DB27 (*hsd1*, Rif^r) and DB27*recA* (DB50), gifts from D. Bartlett (16), ATCC 43667 (*P. atlantica* stock culture American Type Culture Collection) were grown at 25^{o}C under aerobic conditions in Difco 2216 marine broth or on Difco 2216 marine broth solidified with 15 gm/liter agar (Difco) or 20 gm/liter carrageenan (Sigma). *Agrobacterium tumefaciens* indicator strain NT1 (pDCI41E33) (gift of S. Farrand) was grown in AB minimal mannitol liquid medium (ABM) (21) at 28°C. Restriction and modification enzymes used in plasmid constructions and Southern blot analysis were purchased from New England Biolabs (NEB).

Liquid media assays. In experiments testing effects of $CaCl_2$ and galactose, an individual DB27C colony was resuspended in one ml and five µl of the resuspension was used to inoculate five ml marine broth supplemented with 10mM $CaCl_2$, 1% galactose, or 10 mM $CaCl_2$ plus 1% galactose (marine broth contains 12 mM $CaCl_2$). Cultures were incubated at 25^{o}C with gentle agitation for 5 days, after which time aliquots containing ~ 5 x 10^8 cells were washed in marine broth, and used in assays to determine the frequency of ^{p}EPS phase variation (P_{PV}) and frequency of IS*492* precise excision from *epsG* (P_{EX}) as described in Chapter 2.

Solid medium assays with agar or carrageenan. The following protocol was carried out on three independent D27C*recA* crenated colonies. One colony was resuspended in one ml marine broth, plated on marine agar or marine broth plus 2% carrageenan at HCD and LCD, and incubated for seven days at 25^{o}C. One thousand colonies from HCD plates and 100 colonies

from LCD plates were pooled, washed in marine broth, and resuspended in 1 ml marine broth. Three aliquots were removed for serial dilutions and platings for enumeration of crenated to mucoid switching within the cell population for the determination of P_{PV}, as described in Chapter 2. Genomic DNA was isolated from ~ 1 x 10^9 cells, digested with NgoMIV, and used as template in quantitative polymerase chain reactions (qPCR) to determine P_{EX} of IS*492* at *epsG* (see Chapter 2).

Acyl-homoserine lactone extraction, quantitation, and use in ^{p}EPS phase variation assay. Cultures of *P. atlantica* mucoid and crenated cells of DB27*recA* and ATCC43667 were grown to early stationary phase and supernatant was prepared from ~5 x 10^9 cells for analytical and preparative analysis as described in Shaw *et al*. (21) with the exception that the ethyl acetate used for extraction was acidified by addition of glacial acetic acid to 0.01%. Acyl-homoserine lactone (acyl-HSL) molecules from the *P. atlantica* in ethyl acetate extracts were identified and quantitated by comparison to known acyl-HSL molecules (Quorum Sciences, Coralville, IA: Butanoyl-HSL, Octanoyl-HSL, 3-oxo-hexanoyl-HSL, 3-oxo-dodecanoyl-HSL) in an analytical thin-layer chromatography (TLC) assay (21). Briefly, the extracts and standards were separated by TLC on a C_{18} reversed phase silica plate and then overlaid with the *Agrobacterium tumefaciens* indicator strain in ABM agar with 60 μg/ml 5-bromo-4-chloro-3-indolyl-α-D-galactoside (Gold Bio Technology, Inc). The average yield per cell was ~ 5.5 x 10^{-6} nmoles HSL per cell.

Marine agar plates were prepared with ~760 pmol ethyl acetate extract per standard Petri dish or an equivalent volume of the ethyl acetate with 0.01% glacial acetic acid. Overnight cultures from three independent crenated and three independent mucoid *P. atlantica* DB27 colonies were serially diluted and plated in duplicate at HCD and LCD on each set of plates.

Sectoring of colonies was scored for seven days after plating. Phenotypic switching frequency was measured for 1000 and 100 pooled colonies from HCD and LCD plates, respectively, by serial dilution, plating, incubation at 25°C for threer days, and enumeration of crenated and mucoid colonies to calculate P_{PV}.

RESULTS

Variance in *P. atlantica* colony sectoring frequency is dependent on plating density of colonies. Early work on ^{P}EPS phase variation in *P. atlantica* (DB27C*recA*) showed that crenated colonies sector more frequently when plated at low colony density on solid media (Bartlett 1988) (**Fig 3.1A**), but the number of colonies per plate that constituted high and low colony density was not reported. Therefore, to further define this phenomenon we determined the number of colonies per standard Petri dish (100mm diameter) that constitutes high colony density (HCD) versus low colony density (LCD). Ten independent crenated *P. atlantica* DB27C*recA* colonies were each resuspended in marine broth and dilutions were plated on marine agar in standard Petri dishes. The number of crenated colonies with mucoid sectors was scored for each dish after 2, 5, and 7 days incubation at 25°C. Sectoring indicates that during the development of the colony a single cell switched from *eps*$^{-}$ to *eps*$^{+}$ and subsequent divisions of that cell led to a mucoid sector within the colony. Sectoring was highest (67% of colonies) when plates contained less than 100 colonies (**Fig 3.1B**). In contrast, only 7% of the total colonies exhibited sectoring when >1000 colonies were present on a plate. These conditions, 1.3 colonies/cm^2 and 13 colonies/cm^2, are henceforth designated LCD and HCD, respectively. We have used these defined conditions in assays that measured the frequency of ^{P}EPS^{-} to ^{P}EPS^{+} phase variation (P_{PV}) and IS*492* precise excision (P_{EX}) (see Chapter 2). The average P_{PV} at LCD is 7.8-fold higher than the P_{PV} at HCD and the P_{EX} at LCD is 9.6-fold higher than at HCD, correlating well with

the 9.6-fold difference in percent sectoring at the low and high colony densities. It should be noted that a statistically significant 1 to 1 correlation between P_{PV} and P_{EX} has been established (see Chapter 2).

One possible factor that could influence P_{PV} and P_{EX} at LCD versus HCD is the number of generations of cells in the colonies grown at the different densities. The cells in >1000 colonies at LCD or HCD have been enumerated from serial dilution platings and there are an average of 4.3 fewer cell-generations in colonies at HCD as compared to colonies at LCD (data not shown). The generations (n) are calculated from the number of cells in a colony (#): $\# = 2^n$. However, using the number of generations for HCD and LCD samples from six independent P_{PV} and P_{EX} assays (Chapter 2) in a linear regression model, $y= \alpha + \beta_1 x_1 + \epsilon$ (where y is P_{EX} and x_1 equals the number of generations corresponding to each excision frequency), gives a r^2 value of 0.3456 (p=0.444) indicating a weak correlation of the number of generations to P_{EX}. When multiple regression analysis is applied to a model using P_{EX} and number of generations as the x_1 and x_2 values, respectively, $y(P_{PV}) = \alpha + \beta_1 x_1 + \beta_2 x_2 + \epsilon$, the number of generations weakens the model (r^2=0.935) compared to when P_{EX} alone is used as the x variable (r^2=0.945) (Chapter 2), suggesting that the number of generations has no significant role in predicting P_{PV}. It should be noted that cells isolated from HCD plates exhibit increased sectoring when resuspended and subsequently plated at LCD, suggesting the environment is affecting the switch (data not shown).

Colony density-dependent changes in ^{p}EPS phase variation frequency are not regulated by a quorum sensing-related mechanism. The basis for the difference in *P. atlantica* ^{p}EPS phase variation frequencies in colonies at LCD versus HCD is not a simple response to cell density changes, based on the measured P_{PV} for cells grown in marine broth to early-, mid-, and late-log

growth, and at stationary phase. The P_{PV} remains fairly constant at $\leq 10^{-4}$ in liquid medium from low to high cell density [data not shown; (22)].

Although cell density in liquid medium does not affect the frequency of ^{p}EPS phase variation, the effect of colony density on P_{PV} could involve sensing of cell density through a signal molecule produced by *P. atlantica* cells within colonies on solid media. We isolated and characterized a quorum-sensing molecule (acyl-homoserine lactone with a C8 chain length) from the DB27*recA* strain (**Fig. 3.2A**), but there was no effect of this molecule on the frequency of ^{p}EPS phase variation when added to solid medium (**Fig. 3.2B**). It should be noted that the HSL-extraction protocol utilized in this study would not isolate autoinducr 2 (AI-2) molecules produced by many gram negative organisms that are used for interspecies communication (23).

Agar plays a role in the variance of EPS phase variation and IS*492* precise excision frequencies. Contact with a solid surface can alter gene expression in bacteria as first demonstrated for the marine bacterium *Vibrio parahaemolyticus*, which senses contact with a solid surface through its polar flagella and alters expression of genes to facilitate colonization of surfaces versus planktonic growth (24, 25). Since the phase variation of ^{p}EPS is low in marine broth, it is possible that contact with a solid surface starts a signal cascade that turns on expression of genes involved in biofilm formation, including the ^{p}EPS genes whose expression is linked to the precise excision of IS*492* (see Chapter 2).

However a complication with the analysis of EPS phase variation on marine agar is that *P. atlantica* possesses ß-agarase I and II, which are responsible for the breakdown of agar to tetrasaccharides and disaccharides that are taken up into the cell and further broken down by α-neoagarobiose hydrolase into D-galactose and 3,6-anhydro-L-galactose (26, 27). It has been

shown by Uhlinger and White (28) that the addition of galactose to *P. atlantica* T6c cultures in marine broth enhances production of ^{P}EPS. Interestingly, the ^{P}EPS of *P. atlantica* is composed primarily of galactose (57%), glucose (17.4%) and galactouronic acid (6.3%) early in the growth cycle. The expression of the *eps* genes may be linked to the presence of an optimal carbon source for synthesis of ^{p}EPS and, as shown in Chapter 2, the frequency of phase variation and IS*492* precise excision is directly linked to transcription through the *epsG*.

To address whether solid marine agar influenced P_{PV} and P_{EX} through simply the contact of cells and a solid surface we measured P_{PV} and P_{EX} on marine medium solidified with agar or carrageenen. Carrageenan is derived from the red seaweed (agar is extracted from red-purple algae) and differs from agar in the stereoisomer of 3,6-anhydro-α-galactopyranose and has a sulfate group at position 4 of the D-galactopyranose subunit. Carrageenan is not degraded by the *P. atlantica* β-agarases (20). Three independent DB27C colonies were resuspended and plated on marine agar (MA) and marine broth solidified with carrageenen (MB-CARR) at both HCD and LCD. After 7 days incubation the number of sectored colonies on each plate was scored, and 1000 colonies were pooled from HCD plates and 100 colonies were pooled from LCD plates for P_{PV} and P_{EX} assays (Methods and Materials). Briefly, pooled cells were resuspended, plated for bacterial enumeration, and scored for the number of C and M cells that arose to calculate P_{PV}. To determine P_{EX}, genomic DNA from each sample was in used a qPCR reaction designed to measure the amount of intact *epsG* and *agr* loci. Significant decreases in colony sectoring (**Fig. 3.3**), P_{PV} (**Fig. 3.4**), and P_{EX} (**Fig. 3.5**) were observed for cells plated on MB-CARR compared to those from MA at LCD. Smaller decreases were observed for cells plated at HCD. As expected, colonies on MB-CARR did not pit the solid medium, whereas the colonies on MA showed pitting of the agar due to β-agarase activity.

Addition of galactose and $CaCl_2$ alters P_{PV} and P_{EX} frequencies in liquid culture. The carrageenan experiments confirmed that the colony density was not the only factor affecting P_{PV} and P_{EX} on solid medium. Two significant differences between growth conditions for *P. atlantica* on carrageenan versus agar are the absence of breakdown products from agar (galactose) and lower free $CaCl_2$ concentration due to interactions with the sulfate groups on carrageenan. In addition, the addition of $CaCl_2$ to liquid cultures of *Pseudoalteromonas* sp. 1398 significantly increases EPS production (29) and supplementation of marine broth with galactose increases ^{P}EPS production in *P. atlantica* (28). Therefore P_{PV} and P_{EX} were assayed for *P. atlantica* in marine broth supplemented with 10 mM $CaCl_2$ and/or 1% galactose. Increases of 10- and 2.6-fold for P_{PV} and P_{EX}, respectively, were observed for cells grown in the presence of galactose as compared to marine broth alone (**Fig. 3.6**). Cells incubated with additional $CaCl_2$ exhibited decreased P_{PV} and P_{EX} compared to cells in marine broth. Cells grown with both galactose and additional $CaCl_2$ exhibited a smaller increase in P_{PV} and P_{EX} relative to with galactose alone, suggesting the effect of galactose is counteracted in some way by the presence of a relatively high concentration of $CaCl_2$.

DISCUSSION

We report here that the transposition of IS*492* at the *epsG* locus of *P. atlantica* is responsive to environmental signals. The frequency of ^{P}EPS^{-} to ^{P}EPS^{+} phenotypic switching (P_{PV}), which correlates with IS*492* precise excision from *epsG* (Chapter 2), increases 10-fold for *P. atlantica* cells plated at LCD compared to HCD. However, when *P. atlantica* is cultured in marine broth, P_{PV} remains low from early log through the stationary phase of growth. This is

consistent with solid medium assays which demonstrate that the number of generations is not responsible for this high frequency phase variation. The lack of high frequency phase variation in liquid medium suggests that solid surface contacts are required as an environmental stimulus.

The expression of genes used by *Vibrio parahaemolyticus* for swarming motility on solid surfaces is controlled by the organism's environment, as conditions which inhibit the rotation of the polar flagellum induce genes required for swarming motility, effectively allowing this marine organism to adapt its environment (24, 25). Cells plated on marine broth solidified with carrageenan exhibited a decrease in P_{PV} and P_{EX} at both HCD and LCD (**Figs. 3.4 and 3.5**), indicating that solid surface contacts alone are not sufficient to initiate phase variation. The results do, however, suggest a role for the nutrients available to *P. atlantica*. In particular, the presence of agar in the media was required to observe high P_{PV} and P_{EX}. The β-agarase enzyme of *P. atlantica* is able to break down agar into simple sugars, which can then be taken up by the cells and used in the production of ^{P}EPS. If this hypothesis is true, then supplementing liquid medium with a sugar utilized by *P. atlantica* in ^{P}EPS production should result in increased P_{PV} and P_{EX}. Previous studies have, in fact, demonstrated that the addition of galactose to *P. atlantica* cultures in liquid medium caused an increase in ^{P}EPS production (28). Does this increase in ^{P}EPS correlate to an increase in P_{PV} and P_{EX}? Our work establishes a link between this environmental stimulus and the transposition of IS*492* by demonstrating that the addition of galactose to liquid media causes a 10- and 2.6-fold increase in P_{PV} and P_{EX}, respectively. These results indicate that P_{PV} and P_{EX} increase under conditions that are favorable for ^{P}EPS production. While ^{P}EPS is an integral component in *P. atlantica* biofilms, its production most likely occurs after cells have attached to a solid surface. This hypothesis stems from the observation that ^{P}EPS^{-} cells adhere to glass test tubes at the air/broth interface in static cultures

while the $^{P}EPS^{+}$ cells clump at the bottom. We suggest, therefore, that the $^{P}EPS^{-}$ to $^{P}EPS^{+}$ phase variation on solid media is time dependent (**Fig. 3.1B**) because the cells need time to accumulate the products produced by the breakdown of agar by the β-agarase enzyme. The increased P_{PV} and P_{EX} are observed only at LCD on solid medium because the cells have access to more agar compared to cells at HCD.

Quorum sensing systems allow bacteria in a population to communicate with each other through the use of signaling molecules. While there are many different signaling molecules utilized, most are a variation of an acyl-homoserine lactone (acyl-HSL) or furanone backbone. The phenomenon of quorum sensing was first discovered in the marine bacterium *Vibrio fischerii* and was found to control the expression of genes responsible for bioluminescence, which plays a critical role in the bacterium's symbiotic relationship with its squid host (30). The regulation of virulence factor expression and the formation of biofilms have also been attributed to acyl-HSL molecules (31). The high frequency phase variation of individual cells in a colony on solid media suggests that the $^{P}EPS^{-} \rightarrow {}^{P}EPS^{+}$ switch is mediated by cell-to-cell signaling. We isolated and characterized an octanoyl acyl-HSL molecule produced by *P. atlantica*. Experiments in which the isolated acyl-HSL was added to liquid and solid medium demonstrated that this acyl-HSL had no influence on P_{PV} (**Fig. 3.2**). These results do not, however, rule out quorum sensing completely, as signaling molecules not identified in this study (such as AI-2 molecules) may be involved. In addition, it is possible that the concentration of extract added to each plate is not sufficient to elicit a response. While the concentration added to each plate is above the values observed for several other organisms, we do not know the physiologically relevant concentration in *P. atlantica*.

The work presented here suggests that the availability of certain nutrients is responsible for the increase in P_{PV} and P_{EX} in *P. atlantica*. The increased P_{EX} under these conditions indicates that the transposition of IS*492* is responsive to environmental stimuli. This type of response is unique among bacterial IS elements, and it defies the belief that transposition of IS elements that control phase variation is simply a low frequency, random event.

REFERENCES

1. Lander, E. S., Linton, L. M., Birren, B., Nusbaum, C., Zody, M. C., Baldwin, J., Devon, K., Dewar, K., Doyle, M., FitzHugh, W., Funke, R., Gage, D., Harris, K., Heaford, A., Howland, J., Kann, L., Lehoczky, J., LeVine, R., McEwan, P., McKernan, K., Meldrim, J., Mesirov, J. P., Miranda, C., Morris, W., Naylor, J., Raymond, C., Rosetti, M., Santos, R., Sheridan, A., Sougnez, C., Stange-Thomann, N., Stojanovic, N., Subramanian, A., Wyman, D., Rogers, J., Sulston, J., Ainscough, R., Beck, S., Bentley, D., Burton, J., Clee, C., Carter, N., Coulson, A., Deadman, R., Deloukas, P., Dunham, A., Dunham, I., Durbin, R., French, L., Grafham, D., Gregory, S., Hubbard, T., Humphray, S., Hunt, A., Jones, M., Lloyd, C., McMurray, A., Matthews, L., Mercer, S., Milne, S., Mullikin, J. C., Mungall, A., Plumb, R., Ross, M., Shownkeen, R., Sims, S., Waterston, R. H., Wilson, R. K., Hillier, L. W., McPherson, J. D., Marra, M. A., Mardis, E. R., Fulton, L. A., Chinwalla, A. T., Pepin, K. H., Gish, W. R., Chissoe, S. L., Wendl, M. C., Delehaunty, K. D., Miner, T. L., Delehaunty, A., Kramer, J. B., Cook, L. L., Fulton, R. S., Johnson, D. L., Minx, P. J., Clifton, S. W., Hawkins, T., Branscomb, E., Predki, P., Richardson, P., Wenning, S., Slezak, T., Doggett, N., Cheng, J. F., Olsen, A., Lucas, S., Elkin, C., Uberbacher, E., Frazier, M., et al. (2001) *Nature* **409,** 860-921.
2. Goff, S. A., Ricke, D., Lan, T. H., Presting, G., Wang, R., Dunn, M., Glazebrook, J., Sessions, A., Oeller, P., Varma, H., Hadley, D., Hutchison, D., Martin, C., Katagiri, F., Lange, B. M., Moughamer, T., Xia, Y., Budworth, P., Zhong, J., Miguel, T., Paszkowski, U., Zhang, S., Colbert, M., Sun, W. L., Chen, L., Cooper, B., Park, S., Wood, T. C., Mao, L., Quail, P., Wing, R., Dean, R., Yu, Y., Zharkikh, A., Shen, R., Sahasrabudhe, S.,

Thomas, A., Cannings, R., Gutin, A., Pruss, D., Reid, J., Tavtigian, S., Mitchell, J., Eldredge, G., Scholl, T., Miller, R. M., Bhatnagar, S., Adey, N., Rubano, T., Tusneem, N., Robinson, R., Feldhaus, J., Macalma, T., Oliphant, A. & Briggs, S. (2002) *Science* **296,** 92-100.

3. Yu, J., Hu, S., Wang, J., Wong, G. K., Li, S., Liu, B., Deng, Y., Dai, L., Zhou, Y., Zhang, X., Cao, M., Liu, J., Sun, J., Tang, J., Chen, Y., Huang, X., Lin, W., Ye, C., Tong, W., Cong, L., Geng, J., Han, Y., Li, L., Li, W., Hu, G., Huang, X., Li, W., Li, J., Liu, Z., Li, L., Liu, J., Qi, Q., Liu, J., Li, L., Li, T., Wang, X., Lu, H., Wu, T., Zhu, M., Ni, P., Han, H., Dong, W., Ren, X., Feng, X., Cui, P., Li, X., Wang, H., Xu, X., Zhai, W., Xu, Z., Zhang, J., He, S., Zhang, J., Xu, J., Zhang, K., Zheng, X., Dong, J., Zeng, W., Tao, L., Ye, J., Tan, J., Ren, X., Chen, X., He, J., Liu, D., Tian, W., Tian, C., Xia, H., Bao, Q., Li, G., Gao, H., Cao, T., Wang, J., Zhao, W., Li, P., Chen, W., Wang, X., Zhang, Y., Hu, J., Wang, J., Liu, S., Yang, J., Zhang, G., Xiong, Y., Li, Z., Mao, L., Zhou, C., Zhu, Z., Chen, R., Hao, B., Zheng, W., Chen, S., Guo, W., Li, G., Liu, S., Tao, M., Wang, J., Zhu, L., Yuan, L. & Yang, H. (2002) *Science* **296,** 79-92.

4. Waterston, R. H., Lindblad-Toh, K., Birney, E., Rogers, J., Abril, J. F., Agarwal, P., Agarwala, R., Ainscough, R., Alexandersson, M., An, P., Antonarakis, S. E., Attwood, J., Baertsch, R., Bailey, J., Barlow, K., Beck, S., Berry, E., Birren, B., Bloom, T., Bork, P., Botcherby, M., Bray, N., Brent, M. R., Brown, D. G., Brown, S. D., Bult, C., Burton, J., Butler, J., Campbell, R. D., Carninci, P., Cawley, S., Chiaromonte, F., Chinwalla, A. T., Church, D. M., Clamp, M., Clee, C., Collins, F. S., Cook, L. L., Copley, R. R., Coulson, A., Couronne, O., Cuff, J., Curwen, V., Cutts, T., Daly, M., David, R., Davies, J., Delehaunty, K. D., Deri, J., Dermitzakis, E. T., Dewey, C., Dickens, N. J., Diekhans, M.,

Dodge, S., Dubchak, I., Dunn, D. M., Eddy, S. R., Elnitski, L., Emes, R. D., Eswara, P., Eyras, E., Felsenfeld, A., Fewell, G. A., Flicek, P., Foley, K., Frankel, W. N., Fulton, L. A., Fulton, R. S., Furey, T. S., Gage, D., Gibbs, R. A., Glusman, G., Gnerre, S., Goldman, N., Goodstadt, L., Grafham, D., Graves, T. A., Green, E. D., Gregory, S., Guigo, R., Guyer, M., Hardison, R. C., Haussler, D., Hayashizaki, Y., Hillier, L. W., Hinrichs, A., Hlavina, W., Holzer, T., Hsu, F., Hua, A., Hubbard, T., Hunt, A., Jackson, I., Jaffe, D. B., Johnson, L. S., Jones, M., Jones, T. A., Joy, A., Kamal, M., Karlsson, E. K., et al. (2002) *Nature* **420,** 520-62.

5. Agrawal, A., Eastman, Q. M. & Schatz, D. G. (1998) *Nature* **394,** 744-51.
6. Aleshkin, G. I., Kadzhaev, K. V. & Markov, A. P. (1998) *Mutat Res* **401,** 179-91.
7. Ohtsubo, Y., Genka, H., Komatsu, H., Nagata, Y. & Tsuda, M. (2005) *Appl Environ Microbiol* **71,** 1822-8.
8. Ilves, H., Horak, R. & Kivisaar, M. (2001) *J Bacteriol* **183,** 5445-8.
9. Auchtung, J. M., Lee, C. A., Monson, R. E., Lehman, A. P. & Grossman, A. D. (2005) *Proc Natl Acad Sci U S A* **102,** 12554-9.
10. Curcio, M. J. & Derbyshire, K. M. (2003) *Nat Rev Mol Cell Biol* **4,** 865-77.
11. Henderson, I. R., Owen, P. & Nataro, J. P. (1999) *Mol Microbiol* **33,** 919-32.
12. Jonsson, A. B., Nyberg, G. & Normark, S. (1991) *Embo J* **10,** 477-88.
13. Abraham, J. M., Freitag, C. S., Clements, J. R. & Eisenstein, B. I. (1985) *Proc Natl Acad Sci U S A* **82,** 5724-7.
14. Ziebuhr, W., Krimmer, V., Rachid, S., Lossner, I., Gotz, F. & Hacker, J. (1999) *Mol Microbiol* **32,** 345-56.

15. Hammerschmidt, S., Hilse, R., van Putten, J. P., Gerardy-Schahn, R., Unkmeir, A. & Frosch, M. (1996) *Embo J* **15,** 192-8.

16. Bartlett, D. H., Wright, M. E. & Silverman, M. (1988) *Proceedings of the National Academy of Sciences of the United States of America* **85,** 3923-3927.

17. Mahillon, J. & Chandler, M. (1998) *Microbiol Mol Biol Rev* **62,** 725-74.

18. Lenich, A. G. & Glasgow, A. C. (1994) *J Bacteriol* **176,** 4160-4.

19. Corpe, W. A. (1980) in *Adsorption of Microorganisms to Surfaces*, eds. Bitton, G. & Marshall, K. C. (John Wiley and Sons, Inc., New York, N.Y.), pp. 105-144.

20. Belas, R., Bartlett, D. & Silverman, M. (1988) *Appl Environ Microbiol* **54,** 30-37.

21. Shaw, P. D., Ping, G., Daly, S. L., Cha, C., Cronan, J. E., Jr., Rinehart, K. L. & Farrand, S. K. (1997) *Proc Natl Acad Sci U S A* **94,** 6036-41.

22. Bartlett, D. H., Wright, M.E., and Silverman, M. (1988) *Proc Natl Acad Sci U S A* **85,** 3923-3927.

23. Bassler, B. L., E.P. Greenberg, and Stevens, A.M. (1997) *Journal of Bacteriology* **179,** 4043-4045.

24. McCarter, L., Hilmen, M. & Silverman, M. (1988) *Cell* **54,** 345-51.

25. McCarter, J. S. a. L. L. (2006) *Journal of Bacteriology* **188,** 2625-2635.

26. Day, D. F. & Yaphe, W. (1975) *Can J Microbiol* **21,** 1512-8.

27. Morrice, L. M., McLean, M. W., Long, W. F. & Williamson, F. B. (1983) *Eur J Biochem* **137,** 149-54.

28. Uhlinger, D. J. & White, D. C. (1983) *Appl Environ Microbiol* **45,** 64-70.

29. Patrauchan, M. A., Sarkisova, S., Sauer, K. & Franklin, M. J. (2005) *Microbiology* **151,** 2885-97.

30. Nealson, K. H., Platt, T. & Hastings, J. W. (1970) *J Bacteriol* **104,** 313-22.

31. Gambello, M. J. & Iglewski, B. H. (1991) *J Bacteriol* **173,** 3000-9.

Figure 3.1. Sectoring of *P. atlantica* colonies on solid medium. A) Phase variation of ^{p}EPS results in colony morphology switching; mucoid ($^{p}EPS^{+}$) sectoring of crenated ($^{p}EPS^{-}$) colonies is shown. B) Crenated colonies were resuspended in marine broth and plated at dilutions to achieve ~100 colonies per standard (100 x 15 mm) Petri dish (LCD) and ~1,000 colonies per dish (HCD). The percent of total colonies per plate (mean value +/- standard deviation from 10 replicas) that exhibit sectoring at HCD (black bar) and at LCD (grey bar) is indicated for 2, 5, and 7 days of incubation at 25^{o}C.

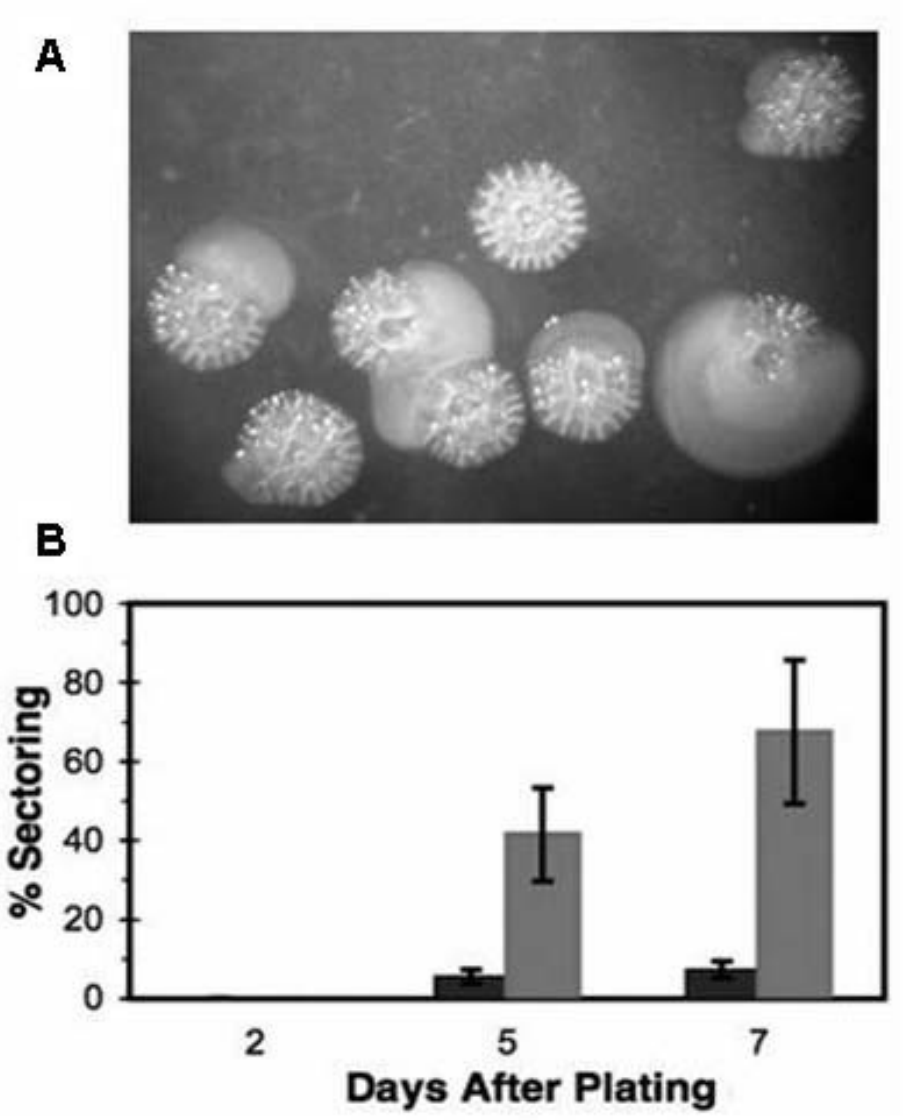
A
B
100
80
60
40
20
0
% Sectoring
2
5
7
Days After Plating

Figure 3.2. Acyl-homoserine lactones from *P. atlantica* and ^{P}EPS phase variation on solid medium. A) Thin layer chromatography of acyl-homoserine lactones (acyl-HSL) produced by *P. atlantica*. Samples were chromatographed on C18 reversed-phase thin-layer plates, developed with methanol/water (60:40, vol:vol), and the spots were visualized by seeding a soft-agar overlay containing X-Gal with the *A. tumefaciens* reporter strain enocding *lacZ* fused to a gene that is controlled by autoinduction (21). Acyl-HSL autoinducer standards were included for estimating the carbon chain size and substitutions. 1: 3-oxo-dodecanoyl-HSL standard (52 pmol); 2: 3-oxo-hexanoyl-HSL standard (3pmol); 3: a mixture of the standards from 1 and 2; 4-5: 1 and 2 µl acyl-HSL extract from DB27C; 6-7: 5 and 6 µl from 1 month old acyl-HSL extract from DB27C; 8-9: 4 and 6 µl from fresh acyl-HSL extract from *P. atlantica* ATCC 43667; 10: octanoyl-HSL standard (38 pmol). B) Three independent colonies of DB27C*recA* (crenated) and DB27M*recA* (mucoid) *P. atlantica* were resuspended and plated at LCD and HCD onto marine agar plus ethyl acetate with 0.01% glacial acetic acid (EAGA) used in the extraction of acyl-HSL and marine agar plus 780 pmol acyl-HSL extract from *P. atlantica* DB27C (Extract). The percent of total colonies exhibiting sectoring on day 7 are indicated (mean +/- standard error). Data for the crenated to mucoid phase variation is presented; no crenated colonies arose from platings of cells from mucoid colonies.

A

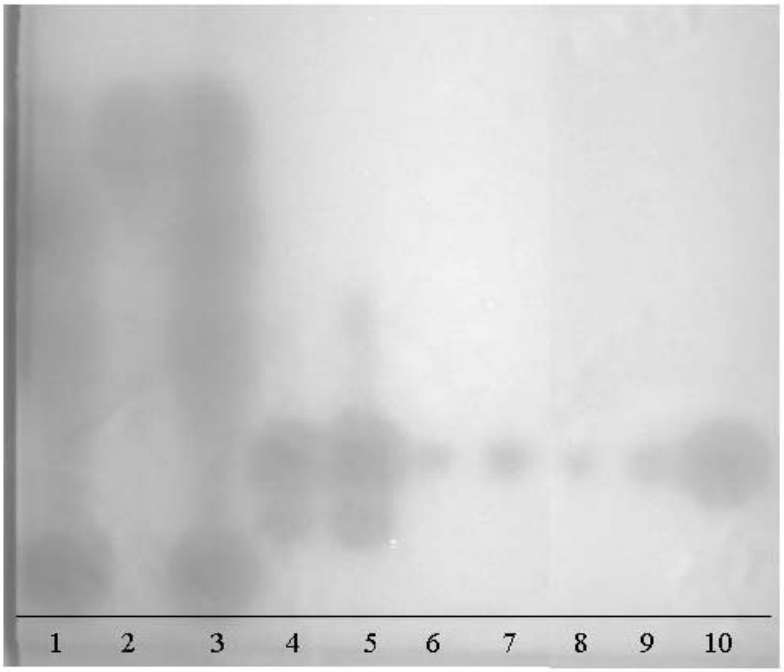
1
2
3
4
5
6
7
8
9
10

B

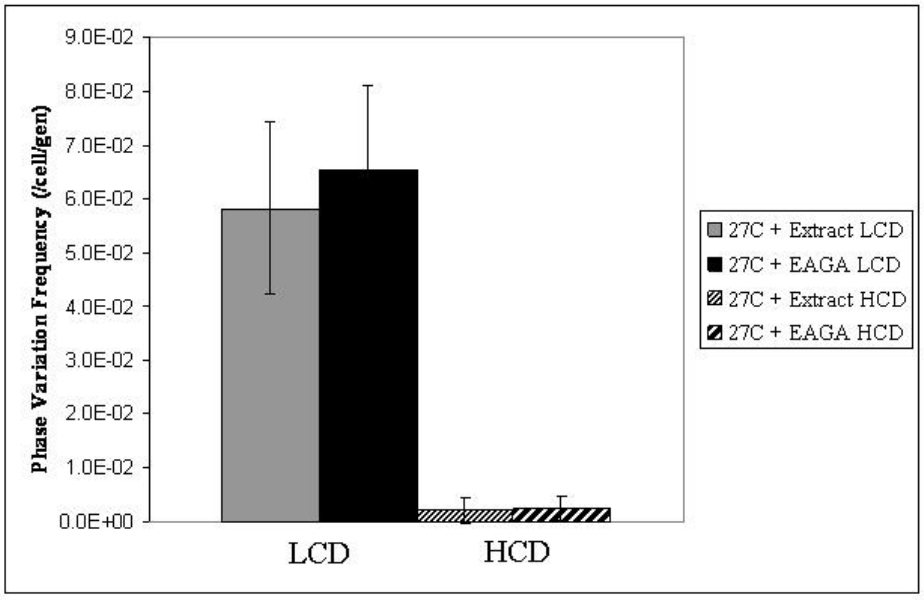
9.0E-02
8.0E-02
7.0E-02
6.0E-02
5.0E-02
4.0E-02
3.0E-02
2.0E-02
1.0E-02
0.0E+00
Phase Variation Frequency (/cell/gen)
LCD
HCD
27C + Extract LCD
27C + EAGA LCD
27C + Extract HCD
27C + EAGA HCD

Figure 3.3. Effect of carrageenan on $^{P}EPS^{+}$ sectoring of $^{P}EPS^{-}$ cells on solid medium. Three independent colonies of DB27C*recA P. atlantica* were resuspended and plated at LCD and HCD onto marine agar (MA) and marine broth plus 2% carrageenan (CARR). The percent of total colonies exhibiting sectoring on day 7 after incubation are indicated (mean +/- standard error) for samples plated at LCD and HCD onto marine agar (black) and marine broth plus carrageenan (grey). It should be noted that the HCD plates contained >3000 colonies/plate, which most likely accounts for the decrease sectoring compared to figure 3.1, where the plates contained between 1058 and 1328 colonies/plate.

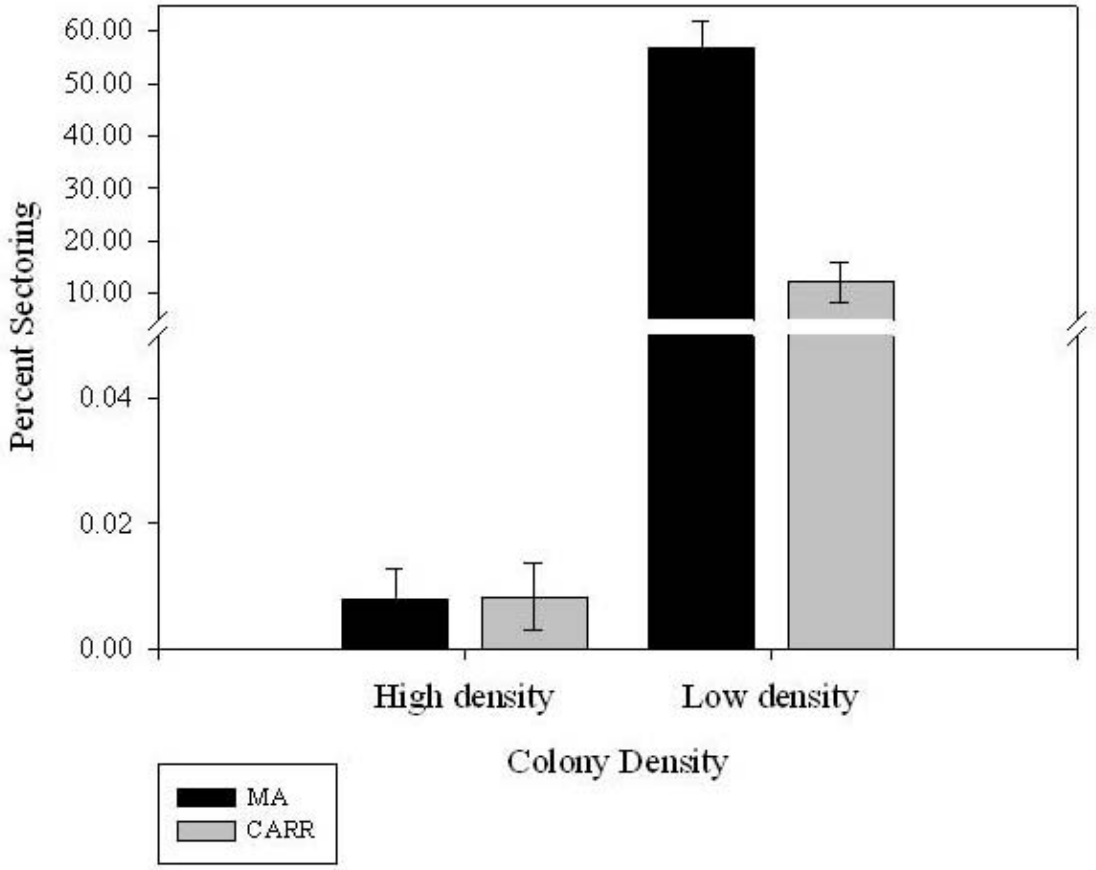
60.00
50.00
40.00
30.00
20.00
10.00
0.04
0.02
0.00
Percent Sectoring
High density
Low density
Colony Density
MA
CARR

Figure 3.4. Effect of carrageenan on phase variation of ^{P}EPS^{-} cells on solid medium. Three independent colonies of DB27C*recA P. atlantica* were resuspended and plated at LCD and HCD onto marine agar (MA) and marine broth plus 2% carrageenan (CARR). The phase variation frequencies of DB27C*recA* colonies plated at LCD and HCD onto marine agar (black) and marine broth plus carrageenan (grey) are indicated (mean +/- standard error).

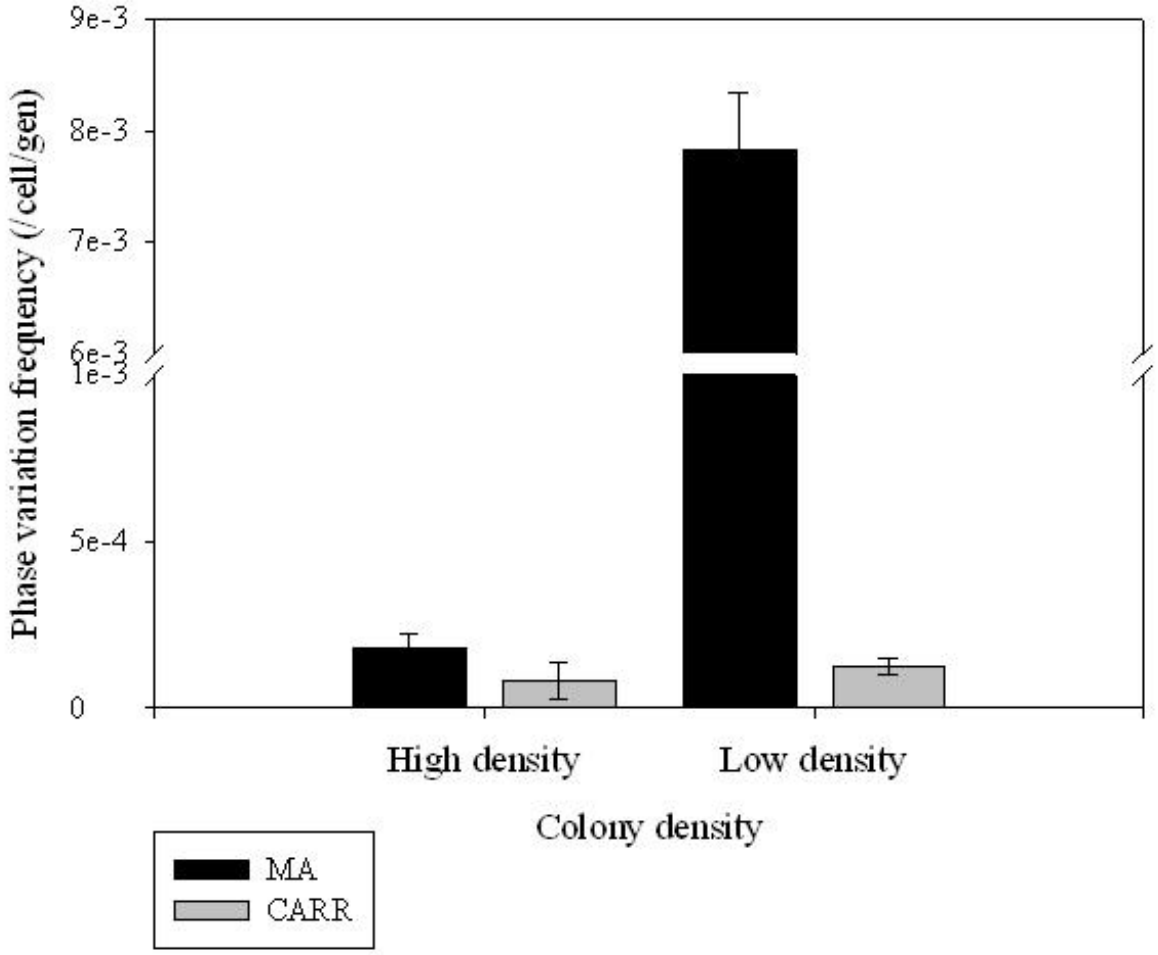
9e-3
8e-3
7e-3
6e-3
1e-3
5e-4
0
Phase variation frequency (/cell/gen)
High density
Low density
Colony density
MA
CARR

Figure 3.5. Effect of carrageenan on the precise excision frequency of IS*492* from *epsG* on solid medium. Three independent colonies of DB27C*recA P. atlantica* were resuspended and plated at LCD and HCD onto marine agar (MA) and marine broth plus 2% carrageenan (CARR). The P_{EX} of DB27C*recA* colonies plated at LCD and HCD onto marine agar (black) and marine broth plus carrageenan (grey) are indicated (mean +/- standard error).

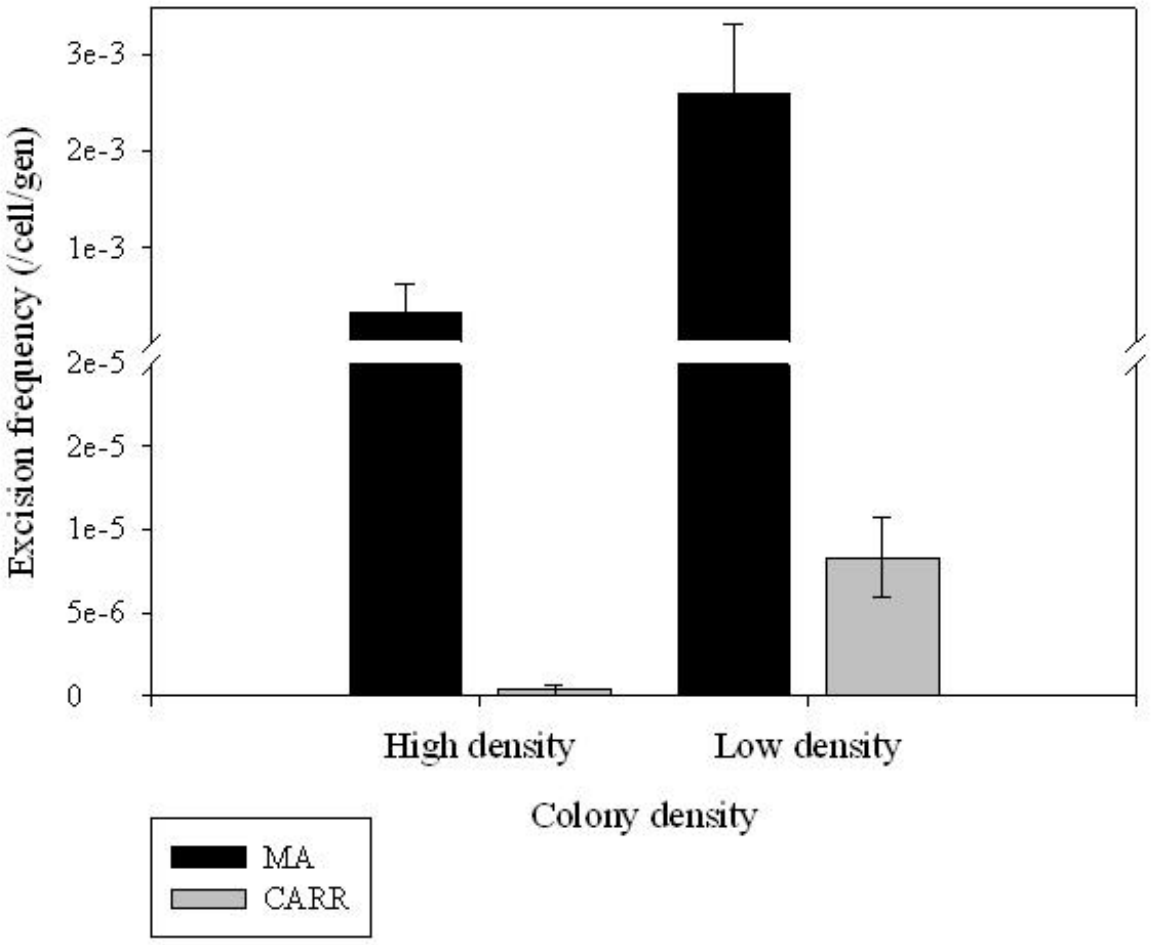
Excision frequency (/cell/gen)
3e-3
2e-3
1e-3
2e-5
2e-5
1e-5
5e-6
0
High density
Low density
Colony density
MA
CARR

Figure 3.6. Galactose and $CaCl_2$ alter the ^{P}EPS phase variation and IS*492* precise excision frequencies in liquid medium. DB27C*recA P. atlantica* cells were incubated for five days in marine broth (grey), marine broth with 22 mM $CaCl_2$ (black), marine broth with 1% galactose (tight hatch), and marine broth plus $CaCl_2$ and galactose (broad hatch). Aliquots were removed from each sample after five days and assayed for $^{p}EPS^{-}$ to $^{p}EPS^{+}$ phase variation (A) and P_{EX} (B). Error bars represent standard error.

A

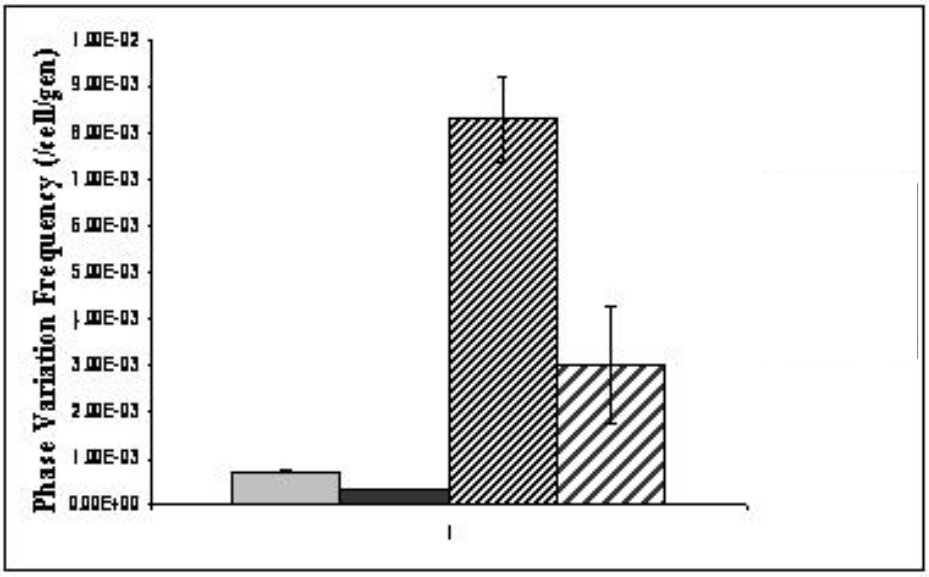
Phase Variation Frequency (/cell/gen)

B

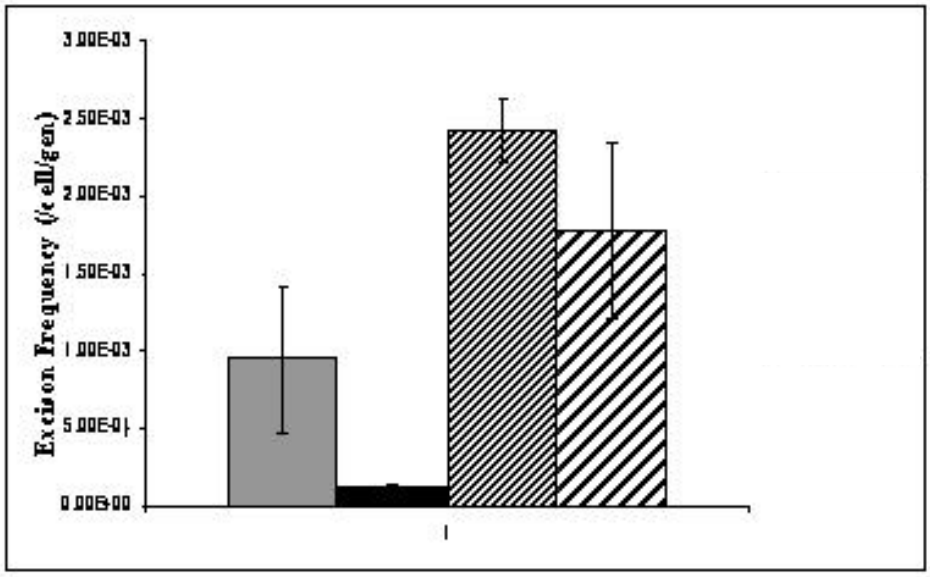
Excision Frequency (/cell/gen)

CHAPTER 4

CHARACTERIZATION OF IS*492* INSERTION AT THE *epsG* LOCUS IN PSEUDOALTEROMONAS ATLANTICA[1]

[1]Higgins, B.P., Frank, R., Cottrell, A., Caruana, P., and Karls, A.C. 2006. To be submitted to the *Journal of Bacteriology*.

ABSTRACT

The movement of transposable elements (TE) throughout a genome can have lethal consequences if an essential gene is interrupted by an insertion event. The insertion specificity of bacterial IS elements varies widely, from those that target consensus sequence motifs to those that appear to select their target site in a random fashion. The work described here indicates that insertion of IS*492* in *Pseudoalteromonas atlantica* is site- and orientation-specific.. Using a novel qPCR assay, the insertion frequency of IS*492* into the *epsG* locus, resulting in the disruption of peripheral extracellular polysaccharide (^{P}EPS) synthesis, was found to be $2.7x10^{-7}$/cell/gen. This marks the first measurement of an insertion frequency for any TE.

INTRODUCTION

IS*492* is a member of the unique IS*110*/*492* family of bacterial IS elements (1, 2). Members of this family often lack 1) lack terminal inverted repeats (TIR) and 2) target site duplications. Transposases (Tnp) of this family belong to a novel family of DNA recombinases, the Piv/Moov family, whose members are able to carry out both site-specific recombination and transposition (1). Recombinases of this family do not share any of the conserved amino acid motifs of the characterized recombinase (Y,S) or Tnp (Y, Y2, S, RT, DDE) families (3). The Tnp of IS*492*, MooV (mover of IS*492* in oceanic variants), shares significant amino acid homology with Piv (pilin inversion), a site-specific invertase responsible for antigenic pilin variation in *Moraxella lacunata* (1).

The transposition of IS*492* at the *eps* (extracellular polysaccharide synthesis) locus controls the phase variation of peripheral extracellular polysaccharide (^{P}EPS) in the gram-negative marine bacterium *Pseudolateromonas atlantica* (4). Excision of IS*492* from *epsG* occurs at a high frequency and correlates directly to the resulting phenotypic switch from ^{P}EPS^{-} (crenated colony morphology, C) to ^{P}EPS^{+} (mucoid colony morphology, M) (Chapter 2). The insertion of IS*492* targets a very small region of *epsG* and generates a 5 bp target site duplication. In addition, each of the six identified copies of IS*492* on the *P. atlantica* chromosome are flanked by the same 5 and 7 bp on the left and right side, respectively, suggesting a common target site is utilized by each.

Target specificity among bacterial IS elements is rarely observed. Several IS elements target small regions of the chromosome which then become known as hotspots. Examples

include IS*256*, which preferentially inserts into a one kb region of the *icaC* region of *Staphylococcus epidermidis* (5), and IS*4321*, which targets the TIR of Tn*21* family transposons (6). Several members of the IS*110*/*492* family exhibit similar target site preferences. IS*621* targets repetitive extragenic palindromic (REP) sequences on the *E. coli* chromosome (7). IS*110* preferentially inserts at the same site on the temperate phage ΦC31 from the *Streptomyces coelicolor* genome (8). IS*117*, normally found as a 2.5 kb mini-circle, preferentially targets one site on the *S. lividans* chromosome, but is found at additional sites which do not resemble the preferred target site (9-11).

The MooV Tnp shares significant amino acid homology with a site-specific invertase and lacks the common catalytic DDE motif found in a majority of identified bacterial IS elements. These observations, in addition to previous studies by Bartlett et al. (4), suggest that IS*492* may target sequences for insertion to an extent previously unobserved for bacterial IS elements. We therefore characterized the insertion of IS*492* the *eps* locus. Using a real-time PCR based assay, we determined the insertion frequency of IS*492* into the *eps* locus to be 2.7×10^{-7}/cell/generation. Characterization of 60 independent insertion events revealed that insertion in this region is site-specific. In addition, each identified non-*eps* associated copy of IS*492* is flanked by the same immediate sequence on the left and right ends, suggesting that those copies target the same sequence as that found at *eps*. This type of target specificity has never been reported before for a bacterial IS element.

MATERIALS AND METHODS

Bacterial strains, media, growth conditions, and reagents. *P. atlantica* T6c (12), DB27 (*hsd1*, Rifr) and DB27*recA* (DB50), gifts from D. Bartlett (4), were cultured at 25°C under aerobic conditions on Difco 2216 marine medium. *E. coli* DH5α (13) was grown at 37°C on Luria-

Bertani (LB) medium (Fisherbiotech). Restriction and modification enzymes used in plasmid constructions and Southern blot analysis were purchased from New England Biolabs (NEB). All sequencing was performed by the University of Michigan Biomedical Research Core Facilities.

Plasmids and plasmid construction. The sequences of all oligonucleotides utilized in this work are listed in Table 4.1. Plasmids used this work are listed in Table 4.2

Isolation of EPS$^+$ to EPS$^-$phase variants. M→C variants were obtained from wild type and *recA P. atlantica* (DB27) in the following manner: one M colony was used to inoculate 5 ml MB and incubated at 25^{o}C for 18 hrs at 220 rpm. After 18hrs incubation, a sterile cotton swab was used to remove ring from glass tube at air-broth interface. The same swab was then streaked onto a MA plate and used to inoculate another 5 ml MB. This procedure was repeated until C colonies appeared on the restreak of the cotton swab. C colonies were then restreaked for isolation. In addition, one M colony present in the same restreak was restreaked for isolation and marked "sibling." Once isolated colonies were visible, colony PCR was performed according to (13) using primers (CJ250B and RVEPS) to amplify element-*eps* junction. PCR products were purified using the QIAquick PCR purification Kit (Qiagen) and sequenced using the CJ250B primer.

Southern blotting. *P. atlantica* chromosomal DNA was transferred to Magnagraph nylon membranes (GE Osmonics, Minnetonka, MN) with alkaline buffer according to the standard techniques described in Ausubel et al (14). DNA was crosslinked to the membrane using a BioRad GS Gene Linker. Hybridization and detection steps were performed using DIG High Prime DNA Labeling and Detection Starter Kit I (Roche Applied Science, Indianapolis, IN). Hybridization was performed at 68^{o}C, followed by one low stringency wash in 2X SSC-0.1%

SDS for 10 min, one wash in 0.5X SSC-0.1% SDS for 10 min, and 2 washes in 0.1X SSC for 10 min each (all washes performed at 68^{o}C).

The DNA probe used for detection of IS*492* was prepared using primers EPSL0 and MOOVR, which amplify the first 744-bp of IS*492*. The left side of IS*492* was used to generate the probe to minimize hybridization with partial/truncated copies of IS*492* on the *P. atlantica* chromosome, all of which are missing a significant portion of the left end. The probe fragment was generated from *P. atlantica* genomic DNA with Pfu polymerase using the following cycling conditions: 95^{o}C for 3 min, followed by 30 cycles of 95^{o}C for 30 sec, 57^{o}C for 30 sec, and 72^{o}C for 2 min.

Colony morphology assay to obtain EPS^{+} to EPS^{-} phase variation frequency and qPCR to determine the insertion frequency at *epsG*. The following protocol was carried out with 3 independent *P. atlantica* DB27M*recA* colonies. One colony was resuspended in 40 µl marine broth, plated onto marine broth, and incubated seven days at 25^{o}C. One hundred colonies from each plate were pooled, washed once in one ml marine broth, and resuspended in one ml marine broth. One aliquot of 100 µl was removed for serial dilutions and platings for enumeration of mucoid to crenated switching within the cell population. Genomic DNA was isolated using standard protocols (14) from an aliquot of the sample correlating to ~7x10^{9} cells. Each genomic sample was digested with NgoMIV, which does not have a recognition site within the *agr* or IS*492*::*epsG* sequences amplified, before determining the DNA concentration (based on absorbance at 260/280 nm; Eppendorf BioPhotomoter).

qPCR reactions were performed using six replicates from each genomic DNA sample. The forward and reverse primers for the IS*492*::*eps* target site and for *agr* are designated EPSPRIMER3/RVEPS and AGARL/AGARR, respectively; the probes for the IS*492*::*epsG* site

and for *agr* are EPSPRB3 (FAM-490 fluorophore on the 5'-end and Black Hole Quencher 1 on the 3'-end) and AGARPRB (HEX-530 fluorophore on the 5'-end and Black Hole Quencher 2 on the 3'-end), respectively (**Fig. 4.1**). Real-time PCR reactions (50 µl) contained: 100 ng digested chromosomal DNA, 1x Taq Polymerase PCR Buffer B (Fisher), 2 U Taq Polymerase, 400 nM each dNTP (Amersham), 6 mM MgCl2, 300 nM of AGARL and AGARR, 500 nM of FWMV and RVEPS, 5 nM of AGARPRB, and 200 nM of EPSPRB3.

To generate a standard curve for quantification of template in the reactions, a standard plot was generated for each target using pAG957 (IS*492*Δ*moov*::*cat*) and pBHG116 (*agr*). Plasmid pAG957 contains IS*492::epsG* with 357 bp of *mooV* replaced with the chloramphencil acetyltransferase (*cat*) gene (13). Plasmid DNA was isolated, quantitated, and used in a dilution series corresponding to 100 pg to 1 fg target DNA (4 replicates of each dilution was used for the standard curve in each experiment). Cycling conditions for standards and experimental reactions were: 50^{o}C for 2min, 95^{o}C for 3 min, followed by 30 cycles of 95^{o}C for 30 sec and 57^{o}C for 2 min. Standard plots of log starting quantity versus threshold cycles (C_T) were generated with the BioRad iCycler iQ software v3.0 using the data from the dilution series corresponding to the amplification of *agr* and IS*492*::*epsG*; the starting quantities (SQ) of chromosomes with an IS*492* insertion at *eps* and total chromosomal copies (*agr*) in each genomic sample were calculated.

The frequency of IS*492* insertion at *eps* (P_{INS}) was calculated using the formula: $P_{INS}=1-1(1-X_{INS})^{1/n}$, where n is the number of generations in the sample population (15). X_{INS} was determined by dividing the total amount of IS*492*::*eps* DNA (in fg) present in each sample by the total amount of *agr* locus (in fg) present in the same sample. When calculating the number of generations (n), the inoculum was 100 cells (each colony in the pooled samples started from a

single cell). No C→M phase variation frequency ($P_{PV'}$) was obtained due to lack of C colonies on plates after serial dilutions of pooled samples.

RESULTS

The IS*492*::*epsG* junction is identical in $^{P}EPS^{+}\rightarrow{}^{P}EPS^{-}$ phase variants. The analysis ^{P}EPS regulation in *P. atlantica* by Bartlett et al. (4) led to the discovery that ^{P}EPS phase variation was controlled by the insertion sequence IS*492*. Southern blot analysis of $^{P}EPS^{+}\rightarrow{}^{P}EPS^{-}$ phase variants suggested that the insertion of IS*492* targeted a very specific region of a locus essential for ^{P}EPS production (4), which was later determined to be a glycosyltransferase (*epsG*) in the *eps* regulon (16). In order to characterize the insertion of IS*492* at *epsG* more precisely, isolation of additional $^{P}EPS^{+}\rightarrow{}^{P}EPS^{-}$ variants was undertaken. Using the enrichment protocol outlined in the **Materials and Methods**, $^{P}EPS^{+}\rightarrow{}^{P}EPS^{-}$ phase variants were isolated from wild-type and *recA* DB27M cells. Once isolated, the *epsG* locus of each variant was examined for the presence of IS*492* via PCR (**Fig. 4.1**). Using an outwardly directed IS*492*-specific primer (CJ250B) and *epsG*-specific reverse primer, the 3' end of the IS*492*::*epsG* junction was amplified and sequenced. To date we have isolated 60 $^{P}EPS^{+}\rightarrow{}^{P}EPS^{-}$ phase variants, and in all cases where insertion was observed, the IS*492*::*epsG* junction was identical. In addition, all insertions were observed in the same orientation, suggesting an orientation bias which places the *mooV* and *epsG* transcripts in the same orientation (**Fig. 4.1**). To detect insertion in the opposite orientation of that depicted in **Figure 4.1**, PCR reactions utilizing primers CJ250B and L58 were performed. No products were obtained from these PCR reactions.

Insertion of IS*492* at the *epsG* locus is a low frequency event. The results of Chapter 2 supported the original observation by Bartlett et al. (4) that the $^{P}EPS^{-}\rightarrow{}^{P}EPS^{+}$ phase variation

correlated to the precise excision of IS*492* from *epsG*. While both the $^{P}EPS^{-}\rightarrow{}^{P}EPS^{+}$ phase variation frequency (P_{PV}) and IS*492* precise excision frequency (P_{EX}) were found to be high for a bacterial IS element, little is known about the frequency of IS*492* insertion at *epsG*. While Bartlett et al suggested that the $^{P}EPS^{+}\rightarrow{}^{P}EPS^{-}$ phase variation frequency ($P_{PV'}$) is below $1x10^{-5}$ (4), very few isolates were screened. In addition, it is not known if the $P_{PV'}$ correlates to the frequency of IS*492* insertion (P_{INS}) at *epsG*. Experiments were designed to measure $P_{PV'}$ and P_{INS} and determine if there is a correlation between them.

To measure $P_{PV'}$ and P_{INS}, DB27M cells were plated on marine agar and incubated at 25^{o}C for 7 days, after which time 100 colonies were pooled and assayed for P_{INS} and $P_{PV'}$. P_{INS} was determined by using genomic DNA from each sample in qPCR reaction designed to measure both the amount of IS*492*::*epsG* DNA and agarase locus DNA (**Fig. 4.1**). The 5' end of the dual-labeled Taqman probe, EPSPRB3, is four bp downstream of the 5'-CTTGT-3' sequence targeted by IS*492*. The forward primer used, EPSPRIMER3, anneals to the last 23 bases of IS*492*. When insertion occurs the forward primer and probe are brought together in close proximity, resulting in the Taq-mediated cleavage of the 5'fluorophore from EPSPRB3. The liberated fluorophore is now able to give off a signal (fluorescence) uninhibited by the 3' quencher. No signal is detected when *epsG* is intact, as cj250B is IS*492* specific and EPSPRB3 and RVEPS are *epsG* specific. Signal detected in each sample from the agarase locus is a measurement of the total DNA in each sample. The amount of these two loci in each sample is quantitated and a frequency of insertion is calculated using the formula $P_{INS} = 1-(1-X)^{(1/n)}$, where X is the ratio of IS*492::epsG* DNA to agarase DNA present in that sample. The P_{INS} was determined to be $2.7x10^{-7}$/cell/generation. Platings of the same cells used in the determination of P_{INS} gave no $^{P}EPS^{+}\rightarrow{}^{P}EPS^{-}$ phase variants

after incubation. In light of the low value for P_{INS}, our inability to determine a value for $P_{PV'}$ is not surprising, as it is likely beyond the limit of detection.

^{P}EPS^{+}→^{P}EPS^{-} phase variation is the result of insertion at *epsG*. Our inability to detect $P_{PV'}$suggests that insertion events are very infrequent (as evidenced by P_{INS}). To determine if the ^{P}EPS^{+}→^{P}EPS^{-} switch was the result of IS*492* insertion at *epsG*, additional variants were isolated using the enrichment protocol of Bartlett et al. (4). In addition to a C variant, genomic DNA was isolated from the variant's parental mucoid and a mucoid sibling. Each grouping of these three represents one family. PCR analysis of genomic DNA from each family member using copy-specific primers confirmed that ^{P}EPS^{+}→^{P}EPS^{-} is due to the insertion of IS*492*. Analysis of the siblings allows for a direct comparison of all IS*492* copies detected by the IS*492* probe. The number of non-*epsG* associated IS*492* copies remains constant regardless of whether insertion has occurred or not (**Fig. 4.2**). In addition, the relative arrangement of the non-*epsG* copies remains consistent as well. Thirty complete families were confirmed by PCR.

DISCUSSION

The regulation of transposition is essential for maintaining the integrity of a host genome. Many transposable elements (TE) regulate their own transposition at the level of transposase (Tnp) transcription and translation. Target site preference was not believed to be a regulatory mechanism utilized by TEs, as their insertion appeared to occur in a random fashion. Recent studies, however, suggest that TEs exhibit a target site preference to ensure that integreation is not deleterious to the host. The highest specificity observed for TEs is exemplified by Tn*7*, which preferentially inserts at one site (*att*Tn*7*) in the *E. coli* chromosome. Other TEs appear to recognize particular sequence motifs, such as palindromic sequences (7, 17, 18). Studies with

the eukaryotic TEs P element and Sleeping Beauty suggest nucleotide sequence is not the feature targeted by the Tnp, but instead the local DNA topology is the characteristic recognized by the transposition machinery (19, 20). In these scenarios, characteristics such as DNA bendability and protein-induced deformability play an important role in target site selection. This hypothesis represents an attractive model for target site preference, as it accounts for the fact that no consensus target sequence can be defined for many of the identified TEs. Instead of the nucleotide sequence being recognized by the transposition machinery, the structural features of the insertion site are recognized. This type of recognition allows for flexibility in what nucleotide sequence is targeted for each insertion event, as multiple arrangements of nucleotides are able to take on similar DNA structures.

The site-specific insertion of Tn*7* is facilitated by an element-encoded protein, TnsD, which specifically binds *att*Tn*7* and recruits the TnsABC transposition machinery (21). In contrast, bacterial IS elements encode only enough information to facilitate their own movement. While some elements encode a second open reading frame in addition to their Tnp, as in the case of IS*911* (22), the target site selection of these elements is not nearly as extensive as that of Tn*7*. This does not mean, though, that IS element insertion is random. As mentioned above, recent studies suggest that transposition machinery seek out areas that are easily accessible. This type of intermediate specificity allows for IS elements to be more discriminate in their target selection, such as the targeting of repetitive extragenic palindromic (REP) sequences. Elements such as IS*911* (23) and IS*30* (24) have been shown to target sequences with homology to their own ends. While strict nucleotide sequence requirements have been identified for a bacterial IS element, insertion hotspots have been found for several elements. IS*256* inserts at different regions of the *icaC* locus in *S. epidermidis* (5) and IS*6110* inserts preferentially into a single site

in the *plcD* locus of *Mycobacterium tuberculosis* (25). The regional specificity of these hotspots is essential for these elements, as it allows for the phase variation of gene expression. In the case of IS*256*, the ability of the host to form biofilms is lost when insertion occurs at the *icaC* locus. The insertion of IS*6110* at *plcD* disrupts the expression of phospholipase C, and important virulence factor of *M. tuberculosis*.

The insertion specificity of IS*492* is very unique among bacterial IS elements. All five characterized copies of the element on the genome, which are active and for circle junction formation and precise excision in *E. coli*, are flanked by the same 5 and 7 bp sequences on the left and right, respectively. While one of the non-*epsG* copies is the likely donor for the *epsG* insertion (via replicative transposition), only the *epsG* associated copy exhibits high frequency precise excision. This inactivity on behalf of the non-*epsG* copies is due at least in part to the chromosomal context of each target site, as only the copy inserting into the highly transcribed region (*epsG*) is able to excise precisely at a high frequency. Coupled with the fact that one of the non-*epsG* copies must be the donor for *epsG* insertion, the low insertion frequency at *epsG* further supports the idea that these non-*epsG* elements have very low transposition frequencies. By targeting regions not highly transcribed, IS*492* provides a self-imposed limit on its transposition.

We propose that site-specific insertion into *epsG* reflects an evolutionary adaptation benefiting both element and host. By inserting into *epsG*, IS*492* provides an effective means for ^{P}EPS phase variation. In this context, IS*492* acts as a regulator; when no ^{P}EPS is produced, transcription through *epsG* is low and IS*492* does not excise. This ensures that no ^{P}EPS, which is energetically costly, is produced when ^{P}EPS expression is turned off. When *P. atlantica* encounters conditions in which ^{P}EPS production is desirable, transcription through

epsG increases and causes the precise excision of IS*492*. Based on the results of Chapter 2, not all cells experience this precise excision event, and therefore not all switch to $^{P}EPS^{+}$. This allows for a small sub-population of cells to remain $^{P}EPS^{-}$, thereby ensuring a heterogeneous population with respect to $^{P}EPS^{\cdot}$ This type of heterogeneity is advantageous in the marine environment, where conditions can change rapidly.

The similarity of the MooV Tnp with the site-specific invertases of the novel Piv/MooV family of recombinases implies the utilization of a unique transposition mechanism. The sequence and orientation specific insertion of IS*492* are reminiscent of a site-specific recombination reaction. This type of specificity has not been observed in bacterial IS elements before, and we propose that this specificity plays a key role in the ability of *P. atlantica* to survive in the dynamic aquatic environment. We report here the first measurement of an insertion frequency for a bacterial IS element at the molecular level. This system could easily be adapted to other transposition systems, resulting in a significant increase in our understanding of regulatory mechanisms controlling transposition.

REFERENCES

1. Lenich, A. G. & Glasgow, A. C. (1994) *J Bacteriol* **176,** 4160-4.
2. Mahillon, J. & Chandler, M. (1998) *Microbiol Mol Biol Rev* **62,** 725-74.
3. Curcio, M. J. & Derbyshire, K. M. (2003) *Nat Rev Mol Cell Biol* **4,** 865-77.
4. Bartlett, D. H., Wright, M. E. & Silverman, M. (1988) *Proceedings of the National Academy of Sciences of the United States of America* **85,** 3923-3927.
5. Ziebuhr, W., Krimmer, V., Rachid, S., Lossner, I., Gotz, F. & Hacker, J. (1999) *Mol Microbiol* **32,** 345-56.
6. Thorsted, P. B., Macartney, D. P., Akhtar, P., Haines, A. S., Ali, N., Davidson, P., Stafford, T., Pocklington, M. J., Pansegrau, W., Wilkins, B. M., Lanka, E. & Thomas, C. M. (1998) *J Mol Biol* **282,** 969-90.
7. Choi, S., Ohta, S. & Ohtsubo, E. (2003) *J Bacteriol* **185,** 4891-900.
8. Chater, K. F., Bruton, C. J., Foster, S. G. & Tobek, I. (1985) *Mol Gen Genet* **200,** 235-9.
9. Smokvina, T., Henderson, D. J., Melton, R. E., Brolle, D. F., Kieser, T. & Hopwood, D. A. (1994) *Mol Microbiol* **12,** 459-68.
10. Smokvina, T. & Hopwood, D. A. (1993) *Mol Gen Genet* **239,** 90-6.
11. Henderson, D. J., Brolle, D. F., Kieser, T., Melton, R. E. & Hopwood, D. A. (1990) *Mol Gen Genet* **224,** 65-71.
12. Corpe, W. A. (1980) in *Adsorption of Microorganisms to Surfaces*, eds. Bitton, G. & Marshall, K. C. (John Wiley and Sons, Inc., New York, N.Y.), pp. 105-144.
13. Perkins-Balding, D., Duval-Valentin, G. & Glasgow, A. C. (1999) *J Bacteriol* **181,** 4937-48.
14. Ausubel, F. M., R. Brent, R. Kingston, D. Moore, J. Seidman, J. Smith, and K. Struhl (1993) (Wiley, New York, N.Y.).
15. Gally, D. L., Bogan, J. A., Eisenstein, B. I. & Blomfield, I. C. (1993) *J Bacteriol* **175,** 6186-93.
16. Copeland, A., Lucas,S., Lapidus,A., Barry,K., Detter,J.C., Glavina, del Rio, T., Hammon,N., Israni,S., Dalin,E., Tice,H., Pitluck,S.,, Saunders, E., Brettin,T., Bruce,D., Han,C., Tapia,R., Gilna,P.,, Schmutz, J., Larimer,F., Land,M., Hauser,L., Kyrpides,N., Kim,E., & Karls, A. C., Bartlett,D., Higgins,B.P. and Richardson,P. (2006) (NC_008228.
17. Ramos-Gonzalez, M. I., Campos, M. J., Ramos, J. L. & Espinosa-Urgel, M. (2006) *J Bacteriol* **188,** 37-44.
18. Calcutt, M. J., Lavrrar, J. L. & Wise, K. S. (1999) *J Bacteriol* **181,** 7597-607.
19. Liao, G. C., Rehm, E. J. & Rubin, G. M. (2000) *Proc Natl Acad Sci U S A* **97,** 3347-51.
20. Vigdal, T. J., Kaufman, C. D., Izsvak, Z., Voytas, D. F. & Ivics, Z. (2002) *J Mol Biol* **323,** 441-52.
21. Peters, J. E. & Craig, N. L. (2001) *Nat Rev Mol Cell Biol* **2,** 806-14.
22. Loot, C., Turlan, C., Rousseau, P., Ton-Hoang, B. & Chandler, M. (2002) *Embo J* **21,** 4172-82.
23. Normand, C., Duval-Valentin, G., Haren, L. & Chandler, M. (2001) *J Mol Biol* **308,** 853-71.
24. Olasz, F., Fischer, T., Szabo, M., Nagy, Z. & Kiss, J. (2003) *J Mol Biol* **334,** 967-78.
25. Viana-Niero, C., Rodriguez, C. A., Bigi, F., Zanini, M. S., Ferreira-Neto, J. S., Cataldi, A. & Leao, S. C. (2006) *J Med Microbiol* **55,** 451-7.

Figure 4.1. Diagram of PCR assays used to characterize IS*492* insertion at *epsG*. An *epsG* locus (grey line) with an IS*492* (hatched line) insertion, and the resulting 5 bp duplication (black boxes*)* is shown. The primers used to characterize the insertion of IS*492* at *epsG* are depicted as arrows. Solid grey arrows anneal to the *epsG* flanking sequence; hatched arrows anneal to IS*492* sequence. The Taqman probe used to determine P_{INS} is depicted as an arrow with a star at its left end. Arrow at left end of IS*492* depicts internal *mooV* promoter and direction of *mooV* transcript.

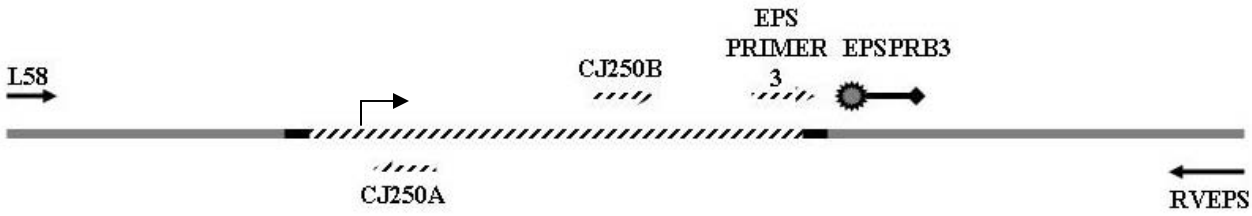
EPS
PRIMER
3
EPSPRB3
L58
CJ250B
CJ250A
RVEPS

Figure 4.2. Southern blot analysis of ^{P}EPS^{+}→^{P}EPS^{-} phase variants. Genomic DNA was isolated from 3 DB27M*recA* isolates (M) and their corresponding crenated variants (C) obtained after enrichment. After restriction digest with EcoRI, genomic DNA was probed with a 744 bp IS*492*-specific probe. The red arrow denotes the band associated with an IS*492* insertion at *epsG*.

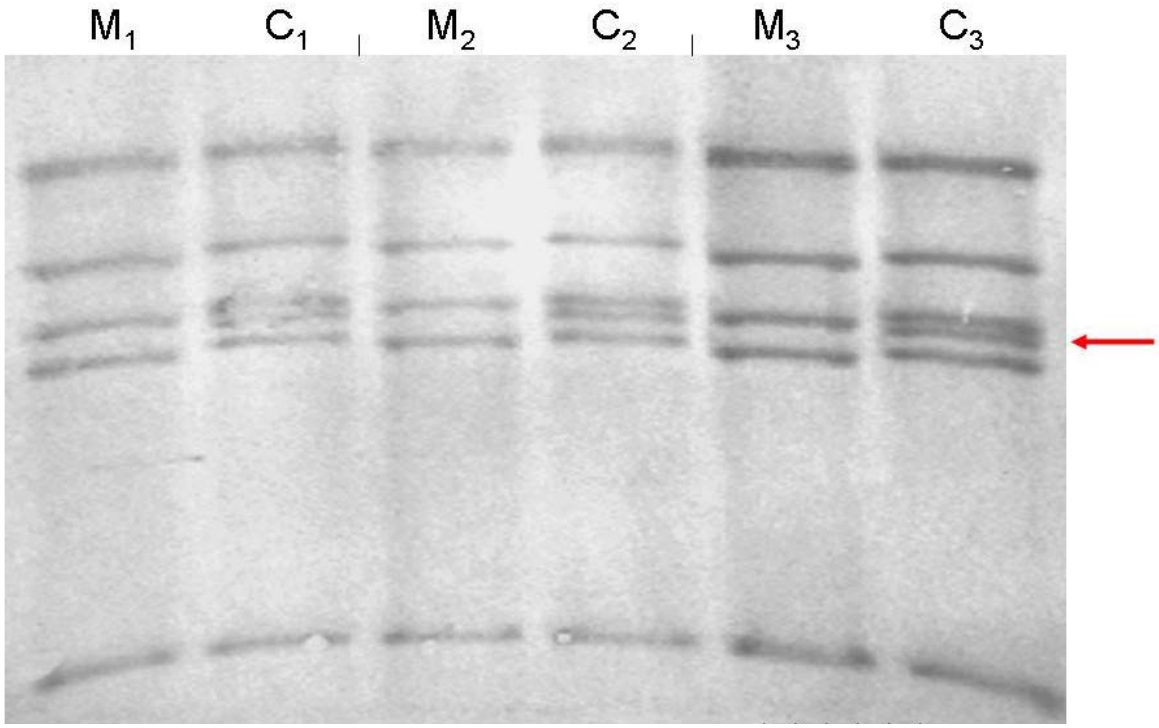
M1
C1
M2
C2
M3
C3

Table 4.1 Oligonucleotides used in PCR and qPCR

Primer Name*	Sequence (5' to 3')
EPSPRIMER3	AGGATGATAAGACAGTACCGATAGTTCTTGT
EPSPRB3 (L23PRB)	FAM-TCTATCAAGCTCTCTATTGAGCAAGG-BHQ1
AGARL	AGTATATGATGGAAGAGTTAGAC
AGARR	CATAACCTATGTTGGCTGGG
AGARPRB	HEX-TATTTTGGTCGAGATAACGGTGGC-BHQ2
RVEPS (RN2)	TCAATTTCTTCAACAGGAG
CJ250A	TTATCGGTCTCTCAACTGAGGAGC
CJ250B	TAAGAAAGTGGCTATTATTGCGTGC
MOOVR	ATGCGATTACGATTCTAGCCTGC
EPSL0	ATGGATTATATACCTGCATGACATGC
L58	CGGTACTGTCTTATCATCCTAATCG
R76	CAGGAGGCTCTCTATTGTACAGC

*Parenthetical name is an alternate designation for the oligonucleotide

Table 4.2 Plasmid List.

Plasmid	Primers*	Cloned PCR product in pCR2.1
pAG957	EPSL58, EPSR76	IS*492*Δ*mooV*::*cat* (13)
pBHG116	AGARL, AGARR	agarase control fragment

*oligonucleotides used in the amplification of the PCR product;
all PCR products generated from *P. atlantica* chromosomal DNA template

CHAPTER 5

SUMMARY AND DISCUSSION

DNA recombination events are an important tool for generating genetic diversity. Transposition is a form of specialized DNA recombination that involves the movement of an autonomous mobile genetic element from one loci to another that can result in deletion, inversion, and gene conversion (1). Because most of the transposition systems studied to date exhibit little specificity for homology at their target sites, this form of recombination is an especially powerful evolutionary tool.

The classification of characterized transposable elements (TE) is currently based on the enzyme that mediates movement of the element, the transposase (Tnp) (see Chapter 1). Tnps that are grouped together share essential amino acid motifs and/or transposition intermediates. The Tnp of IS*492*, MooV, is a member of the Piv/MooV family of recombinases. Members of this family do not share the common amino acid motifs of similarity well characterized site-specific recombinases or transposases (2). In addition, members of the Piv/MooV family catalyze both site-specific inversion and transposition reactions. Conservation of amino acid motifs in this family of recombinases that can catalyze both types of specialized recombination reactions suggests that a novel mechanism is being utilized (2).

IS*492* is responsible for controlling the ^{P}EPS phase variation (PV) in *P. atlantica* through reversible insertion into the *epsG* locus (3). This work characterizes five functional copies of IS*492* on the *P. atlantica* chromosome (Chapter 2). IS*492* is an unusual IS element because its movement shares similarities with transposition and site-specific recombination reactions. All five characterized full-sequence copies of IS*492* are flanked by the same 5 (5'CTTGT-3') and 7

(5'CTTGTTA-3') base pairs on the left and right, respectively (4). This 7 bp sequence occurs 783 times on the *P. atlantica* chromosome (personal communication, Jan Mzarek). Southern blot analysis (Chapter 4) and determination of the genomic sequence (5) indicate that IS*492* resides in only six loci. Such specificity would be expected in a site-specific recombination system, but not for a bacterial IS element. In addition, Perkins-Balding et al. (4) demonstrated that these 5 and 7 bp were required for the MooV-dependent precise excision (PE) and circle formation of IS*492* in *E. coli*, suggesting that these 5 and 7 bp play a role analogous to the core sequences of site-specific recombination systems (4). The lack of terminal inverted repeats on the element and the similarities between MooV and the site-specific invertase Piv suggest that IS*492* is a unique element that can offer valuable new insight into the field of DNA recombination.

The goal of this work was to study the regulation of IS*492* transposition in *P. atlantica*. While the mechanistic aspects of IS*492* transposition are intriguing, the control of this transposition is also unusual for a bacterial IS element. The PE of IS*492* from the *epsG* locus in *P. atlantica* occurs at a frequency higher than previously reported for any bacterial IS element (Chapter 2) and strongly correlates to the EPS^- to EPS^+ phase variation exhibited by *P. atlantica*.

A unique feature of IS*492* transposition is the apparent utilization of two different mechanisms for excision from a donor site. While PE is observed easily at the *epsG* locus, nested PCR is required to see PE for two of the non-*epsG* associated copies; no PE is observed for the remaining two copies (Chapter 2). Cloning of each copy into an *E. coli* plasmid vector demonstrated that each copy is an active element capable of circle formation and precise excision in *E. coli* (Chapter 2). Our work in Chapter 2 suggests that the chromosomal context of IS*492* directs the high frequency precise excision. Externally generated *mooV* transcripts were found

100- to 1000-fold more frequently at the *epsG* locus compared to the other four sites. Studies in *E. coli* with IS*492* present on a multicopy plasmid vector demonstrate that circle formation is only observed when transcription of *mooV* is generated externally from a strong promoter.

The role of the environmental signals in regulation is explored in Chapter 3. The high frequency phase variation and precise excision observed in Chapter 2 were significantly different for samples from high colony density (HCD) versus low colony density (LCD); cells at LCD exhibited an 8- and 9-fold increase in phase variation and precise excision, respectively, compared cells plated at HCD. Multiple linear regression analysis demonstrated that this difference is not due to the difference in the number of generations seen at LCD versus HCD. No change in phase variation was observed in liquid medium over three stages of growth, leading to the hypothesis that that the increase in phase variation and precise excision required solid surface contacts. However, experiments with an alternative gelling agent (carrageenan) demonstrated that this increase in phase variation and precise excision frequencies required more than just a solid surface contact. To determine the physical aspects in marine agar that could alter the phase variation and precise excision frequencies in liquid medium, crenated cells were incubated under a variety of conditions which have been shown to increase biofilm production in *Pseudoalteromonas* species. EPS has been shown to be an essential component of biofim formation, so the rationale was that any condition enhancing biofilm production may increase the phase variation and precise excision frequencies. The addition of galactose to liquid medium increase the phase variation and precise excision frequencies significantly (11-and 2-fold, respectively) relative to marine broth alone. This appears to confirm that the high frequency phase variation and precise excision frequencies are not solely dependent on solid surface contacts, as they can be duplicated in liquid medium under certain conditions.

In Chapter 4, the role of target site preference in the regulation of IS*492* transposition is addressed. Previous Southern blot analysis of $^{P}EPS^{+}$ (M) to $^{P}EPS^{-}$ (C) variants suggested that the non-*eps* copies of IS*492* do not change their position on the chromosome. To determine if the insertion of IS*492* at *epsG* is site specific, a series of M→C variants was isolated by screening the phenotypic switch that accompanies an insertion event into *eps*G. These M→C variants were analyzed using PCR, and in cases where insertion was observed, insertion targeted the same sequence each time. Southern blot analysis of variants and their mucoid siblings suggest that the non-*epsG* copies of IS*492* occupy only one site each (in addition to *epsG*, depending on whether that copy is the donor) on the *P. atlantica* chromosome.

The isolation of M→C variants required an enrichment process adapted from (3) involving several rounds of subculturing. This suggests that insertion into the *epsG* locus occurs at a very low frequency compared to the high frequency of precise excision observed in Chapter 2. A qPCR system similar to that employed in Chapter 2 was developed to determine the frequency of IS*492* insertion at the *epsG* locus. Whereas traditional methods (serial dilutions, screening colony phenotypes) failed to detect an insertion event, qPCR determined the insertion frequency at *epsG* to be ~$2.6x10^{-7}$/cell/generation. This low frequency explains why attempts to determine an M→C phase variation frequency were unsuccessful. In addition, this method allows for the determination of a true insertion frequency, as it does not rely on any phenotypic changes in its calculations (any number of mutations in *epsG* could render a cell $^{P}EPS^{-}$, which would give a false positive for insertion upon screening colony morphologies). This marks the first true measurement of IS element insertion frequency at the molecular level.

While this work has made important steps towards understanding the regulation of IS*492* transposition, there are still many questions that remain unanswered. First, does IS*492* employ a *cis*-acting preference mechanism similar to that utilized by IS*903* (**Fig. 1.6)** (6)? This could explain why increased *mooV* transcript levels at the *epsG* locus correlate to increased phase variation and precise excision frequencies. Additionally, this would account for the results in *E. coli* demonstrating that circle junction formation, which occurs after a precise excision event, is observed only when IS*492* is placed downstream of a strong promoter. Further experiments will be directed at placing a strong inducible promoter upstream of each non-*epsG* associated IS*492* copy in *P. atlantica*. Once accomplished, the qPCR system developed in this work could easily be adapted to measure the excision frequency at each locus. In addition, primer extension studies that search for an RNA transcript analogous to the pOUT transcript of IS*10* (7) should be performed, as the presence of a pOUT in IS*492* could also explain the requirement for an increase in *mooV* transcription levels (**Fig. 1.4)**.

The mechanism by which IS*492* transposes into the *epsG* locus is yet to be determined. Southern blot analysis suggest that a replicative mechanism is utilized, but a coupling of cut and paste transposition and chromosome replication would result in the same end products as those seen in a replicative event. Using allelic exchange, future experiments will mark each copy of IS*492* in order to determine if one or all of the non-*epsG* associated copies of IS*492* an act as the donor to the *epsG* locus.

The target site preference of IS*492* is very unusual among bacterial IS elements. To further characterize this specificity, a *cat* marked IS*492* element will be placed onto a suicide vector carrying the wild-type *mooV* sequence and conjugated into *P. atlantica*. Analysis of the insertion sites will reveal the true nature of the specificity and determine if IS*492*, like its fellow

IS*110*/IS*492* family member IS*117*, will target secondary sites if the preferred site(s) are not available (8). Attempts on my part at creating this suicide vector were unsuccessful.

One issue not addressed in this work but central to understanding the regulation of IS*492* is the role of the circularized element. The formation of a strong promoter by IS*492* was demonstrated by Perkins-Balding et al (4), but it is not known if this circle is an intermediate in transposition (as in the case of IS*911* (9)) or a transpositional end product that is diluted out and degraded. It is hypothesized that the formation of a circle, and the resulting P_{JUNC} promoter (**Fig. 1.5**), increases the likelihood of element re-insertion by increasing the levels of *cis*-Tnp. Excision of IS*492* from *epsG*, however, does not appear to result in insertion at another locus in *P. atlantica*. Work by Karls lab member Adrienne Cottrell suggests that the junction of the left and right ends of IS*492* are active substrates for MooV in *E. coli*, but further experiments are needed to determine its role definitively.

The regulation of phase variation and precise excision on solid medium is poorly understood. Evidence thus far suggests that a signal or signaling molecule is present on solid medium that triggers and increase in phase variation. It is possible that the agarase gene is involved in this regulation, but studies with an agarase mutant are needed to determine its role. In addition, assays similar to those used to identify and characterize signaling molecules produced by *Myxococcus xanthus* will be conducted in an attempt to identify conditions under which a positive or negatively regulating signaling molecule is produced (10). This work establishes that colony density alone is not responsible for the increase in phase variation and precise excision, but the significant difference in these values at HCD versus LCD suggests the presence or absence of a signaling molecule/environmental factor under one of these conditions.

This work developed novel techniques to study the transposition of a bacterial IS element. These techniques can be readily applied to a number of systems, allowing for a more thorough characterization of transposition in each case. The transposition of IS*492* likely utilizes novel aspects in its mechanism and is of great interest, as it may provide a bridge between enzymes that catalyze site-specific recombination and transposition. In addition, characterization of IS*492* transposition may shed light on poorly understood recombination systems which do not fit into any of the traditional classifications.

REFERENCES

1. Curcio, M. J. & Derbyshire, K. M. (2003) *Nat Rev Mol Cell Biol* **4,** 865-77.
2. Lenich, A. G. & Glasgow, A. C. (1994) *J Bacteriol* **176,** 4160-4.
3. Bartlett, D. H., Wright, M. E. & Silverman, M. (1988) *Proceedings of the National Academy of Sciences of the United States of America* **85,** 3923-3927.
4. Perkins-Balding, D., Duval-Valentin, G. & Glasgow, A. C. (1999) *J Bacteriol* **181,** 4937-48.
5. Copeland, A., Lucas,S., Lapidus,A., Barry,K., Detter,J.C., Glavina, del Rio, T., Hammon,N., Israni,S., Dalin,E., Tice,H., Pitluck,S.,, Saunders, E., Brettin,T., Bruce,D., Han,C., Tapia,R., Gilna,P.,, Schmutz, J., Larimer,F., Land,M., Hauser,L., Kyrpides,N., Kim,E., & Karls, A. C., Bartlett,D., Higgins,B.P. and Richardson,P. (2006) Accession number NC_008228.
6. Derbyshire, K. M. & Grindley, N. D. F. (1996) *Molecular Microbiology* **21,** 1261-1272.
7. Davis, M. A., Simons, R. W. & Kleckner, N. (1985) *Cell* **43,** 379-87.
8. Henderson, D. J., Brolle, D. F., Kieser, T., Melton, R. E. & Hopwood, D. A. (1990) *Mol Gen Genet* **224,** 65-71.
9. Ton-Hoang, B., Polard, P. & Chandler, M. (1998) *Embo J* **17,** 1169-81.
10. Lev, M. (1954) *Nature* **173,** 501.